

Computation of geometric partial differential equations and mean curvature flow

Klaus Deckelnick, Gerhard Dziuk and Charles M. Elliott

Acta Numerica / Volume 14 / May 2005, pp 139 - 232
DOI: 10.1017/S0962492904000224, Published online: 19 April 2005

Link to this article: http://journals.cambridge.org/abstract_S0962492904000224

How to cite this article:

Klaus Deckelnick, Gerhard Dziuk and Charles M. Elliott (2005). Computation of geometric partial differential equations and mean curvature flow. *Acta Numerica*, 14, pp 139-232 doi:10.1017/S0962492904000224

Request Permissions : [Click here](#)

Computation of geometric partial differential equations and mean curvature flow

Klaus Deckelnick

*Institut für Analysis und Numerik,
Otto-von-Guericke-Universität Magdeburg, Universitätsplatz 2,
D-39106 Magdeburg, Germany*
E-mail: Klaus.Deckelnick@Mathematik.Uni-Magdeburg.de

Gerhard Dziuk

*Abteilung für Angewandte Mathematik,
Albert-Ludwigs-Universität Freiburg i. Br., Hermann-Herder-Straße 10,
D-79104 Freiburg i. Br., Germany*
E-mail: gerd.dziuk@mathematik.uni-freiburg.de

Charles M. Elliott

*Department of Mathematics,
University of Sussex, Mantell Building,
Falmer, Brighton, BN1 9RF, UK*
E-mail: C.M.Elliott@sussex.ac.uk

This review concerns the computation of curvature-dependent interface motion governed by geometric partial differential equations. The canonical problem of mean curvature flow is that of finding a surface which evolves so that, at every point on the surface, the normal velocity is given by the mean curvature. In recent years the interest in geometric PDEs involving curvature has burgeoned. Examples of applications are, amongst others, the motion of grain boundaries in alloys, phase transitions and image processing. The methods of analysis, discretization and numerical analysis depend on how the surface is represented. The simplest approach is when the surface is a graph over a base domain. This is an example of a *sharp interface* approach which, in the general *parametric approach*, involves seeking a parametrization of the surface over a base surface, such as a sphere. On the other hand an interface can be represented implicitly as a level surface of a function, and this idea gives rise to the so-called *level set method*. Another implicit approach is the *phase field method*, which approximates the interface by a zero level set of a

phase field satisfying a PDE depending on a new parameter. Each approach has its own advantages and disadvantages. In the article we describe the mathematical formulations of these approaches and their discretizations. Algorithms are set out for each approach, convergence results are given and are supported by computational results and numerous graphical figures. Besides mean curvature flow, the topics of anisotropy and the higher order geometric PDEs for Willmore flow and surface diffusion are covered.

CONTENTS

1	Introduction	140
2	Some geometric analysis	150
3	Definition and elementary properties of mean curvature flow	155
4	Parametric mean curvature flow	157
5	Mean curvature flow of graphs	166
6	Mean curvature flow of level sets	174
7	Phase field approach to mean curvature flow	181
8	Anisotropic mean curvature flow	189
9	Fourth order flows	208
	Appendix	223
	References	225

1. Introduction

A geometric evolution equation defines the motion of a hypersurface by prescribing the normal velocity of the surface in terms of geometric quantities. As well as being of striking mathematical interest, geometric evolution problems occur in a wide variety of scientific and technological applications. A traditional source of problems is materials science, where the understanding of the strength and properties of materials requires the mathematical modelling of the morphology of microstructure. Evolving surfaces might be grain boundaries, which separate differing orientations of the same crystalline phase, or solid–liquid interfaces exhibiting dendritic structures in under-cooled solidification. On the other hand newer applications are associated with image processing. For example, in order to identify a dark shape in a light background in a two-dimensional image a so-called snake contour is evolved so that it wraps around the shape.

In this article we survey numerical methods for the evolution of surfaces whose normal velocity is strongly dependent on the mean curvature of the surface. The objective is to find a family $\{\Gamma(t)\}_{t \in [0,T]}$ of closed compact and orientable hypersurfaces in \mathbb{R}^{n+1} whose evolution is defined by specifying the velocity V of $\Gamma(t)$ in the normal direction ν . An example of a general

geometric evolution equation is

$$V = f(x, \nu, H) \quad \text{on } \Gamma(t), \quad (1.1)$$

where f depends on the application and the x dependence might arise from evaluating on the surface $\Gamma(t)$ field variables which satisfy their own system of nonlinear partial differential equations in \mathbb{R}^{n+1} away from the surface. It is important to note that, in order to specify the evolution of the surface, it is sufficient to define the normal velocity.

The prototype problem is *motion by mean curvature*, for which

$$V = -H \quad \text{on } \Gamma(t), \quad (1.2)$$

where H is the sum of the n principal curvatures of $\Gamma(t)$. We call H the mean curvature rather than the arithmetic mean of the principal curvatures. Our sign convention is that H is positive for spheres, with ν being the outward normal. It is well known that, starting from an initial surface Γ_0 , this equation is a gradient flow for the area functional,

$$E(\Gamma) = \int_{\Gamma} 1 \, dA. \quad (1.3)$$

In applications the area functional is an *interfacial energy* with a constant energy density 1. Equation (1.2) may be viewed as an analogue for surfaces of the parabolic heat equation

$$u_t - \Delta u = 0.$$

On the other hand, another geometric equation is

$$V = \Delta_{\Gamma(t)} H \quad \text{on } \Gamma(t), \quad (1.4)$$

where $\Delta_{\Gamma(t)}$ is the Laplace–Beltrami or surface Laplacian operator on $\Gamma(t)$. This can be viewed as an analogue of the spatially fourth order parabolic equation

$$u_t + \Delta^2 u = 0.$$

1.1. Approaches

In order to solve a surface evolution equation analytically or numerically, we need a description of $\Gamma(t)$. Each choice of description leads to a particular nonlinear partial differential equation defining the evolution. Thus the computational method depends strongly on the way we choose to describe the surface. For this article we shall focus on four possible approaches.

Parametric approach. The hypersurfaces $\Gamma(t)$ are given as

$$\Gamma(t) = X(\cdot, t)(M),$$

where M is a suitable reference manifold (fixing the topological type of $\Gamma(t)$) and $X : M \times [0, T] \rightarrow \mathbb{R}^{n+1}$ has to be determined. Here $X(p, t)$, for $p \in M$, is

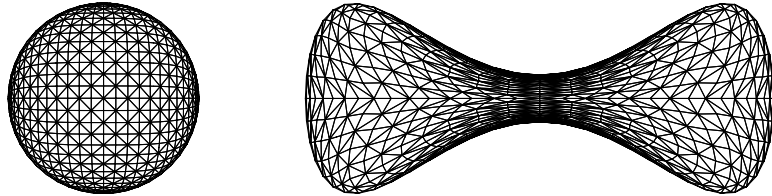


Figure 1.1. A dumbbell-shaped two-dimensional surface parametrized over the unit sphere.

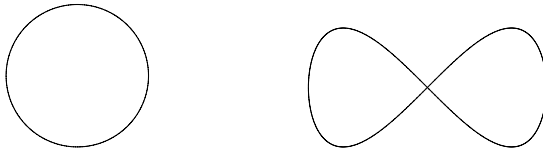


Figure 1.2. A lemniscate, parametrized over the unit circle.

the position vector at time t of a point on $\Gamma(t)$. If we are interested in closed curves in the plane then M can be the unit circle S^1 , whereas if $\Gamma(t)$ is a two-dimensional surface then M could be the unit sphere S^2 (see Figures 1.1 and 1.2). Geometrical quantities are easily expressed as derivatives of the parametrization so that evolution laws such as (1.2) may be translated into nonlinear parabolic systems of PDEs for the vector X . With this approach there is no notion of the surface being the boundary of an open set and having an inside and outside, so *self-intersection* is perfectly natural for smooth parametrizations and is not necessarily associated with singularities. For example in the plane a figure of eight curve can be smoothly mapped onto the unit circle one to one (Figure 1.2). At the crossing point the curve has two smoothly evaluated normals and curvatures which depend on the parametrization. A parametrized curve evolving by mean curvature can evolve smoothly from this configuration.

Graphs. We assume that $\Gamma(t)$ can be written in the form

$$\Gamma(t) = \{(x, u(x, t)) \mid x \in \Omega\},$$

where $\Omega \subset \mathbb{R}^n$ and the height function $u : \Omega \times [0, T] \rightarrow \mathbb{R}$ has to be found. We shall see that the law (1.2) leads to a nonlinear parabolic PDE for u . Clearly, the assumption that $\Gamma(t)$ is a graph is rather restrictive; however, techniques developed for this case have turned out to be very useful in understanding more general situations. Since the height is a smooth function we can view $\Gamma(t)$ as dividing $\Omega \times \mathbb{R}$ into two sets, namely the regions above and below the graph.

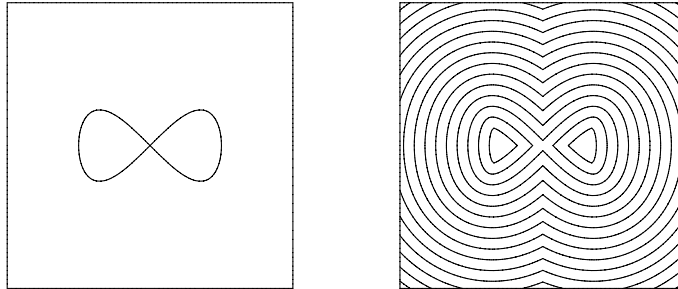


Figure 1.3. Level lines of a level set function (right) for the figure of eight curve (left).

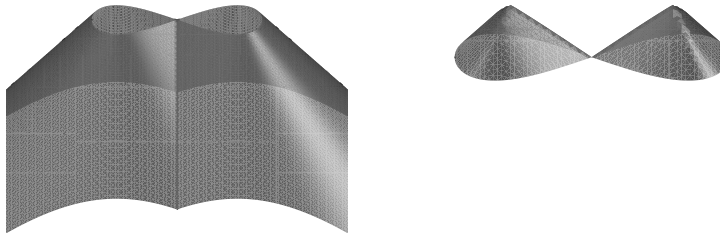


Figure 1.4. Graph of a level set function for the figure of eight curve, cut at the zero level. Negative part left and positive part (graphically enlarged) right.

Level set method. We look for $\Gamma(t)$ as the zero level set of an auxiliary function $u : \mathbb{R}^{n+1} \times [0, \infty) \rightarrow \mathbb{R}$, that is,

$$\Gamma(t) = \{x \in \mathbb{R}^{n+1} \mid u(x, t) = 0\}.$$

The law (1.2) now translates into a nonlinear, degenerate and singular PDE for u . Clearly intrinsic to this approach is the notion of $\Gamma(t)$ being a dividing surface between the two regions where the level set function is positive and negative. Thus we have the notion of inside and outside. In order to describe a figure of eight by a level set function it is necessary to have the level set function positive and negative, as shown in Figures 1.3 and 1.4.

Phase field approach. The phase field approach is based on an approximation of the sharp interface by a diffuse interface

$$\Gamma_\epsilon(t) = \{x \in \mathbb{R}^{n+1} \mid -1 + C\epsilon \leq u_\epsilon(x, t) \leq 1 - C\epsilon\}$$

of width $O(\epsilon)$, across which the phase field function u_ϵ has a transition from approximately one bulk negative value -1 to approximately a second positive bulk value $+1$. The zero level set of the phase field function approximates the surface. Just as in the level set method there is the notion

of a material interface separating an inside and outside and in the basic implementation interface self-intersection and topological change are handled automatically. The bulk values of the phase field function correspond to the minima of a homogeneous energy function with two equal double wells. Interfacial energy is assigned to the diffuse interface via the gradient of the phase field function. For motion by mean curvature the evolution is defined as a semilinear parabolic equation of reaction–diffusion or Ginzburg–Landau type. Frequently in applications mathematical models are derived which, from the beginning, involve diffuse interfaces and phase field functions.

Comments

Conceptually the graph formulation is the simplest and most efficient. It involves solving a scalar nonlinear parabolic equation in n space dimensions and directly computes the surface. However, there are many circumstances where the surface is not a graph. Furthermore, even if the initial surface is a graph it is possible that over the course of the evolution that property might be lost, despite the surface evolving smoothly. This would lead to gradient blow-up of the solution of the graph equation. There is the possibility that the solution of a numerical discretization exists globally and appears to be stable even though there is no solution to the continuous equation.

The parametric approach is also direct. It is conceptually more advanced than the graph approach and one has to solve for an n -dimensional surface a system of $n + 1$ parabolic equations. If the surface is a graph then the parametric approach is less efficient than solving for the height of the surface. On the other hand it is more widely applicable. In the case of a closed curve one can use periodic boundary conditions on the unit interval in order to solve over the circle. A closed two-dimensional surface can be approximated by a polyhedral surface. A parametrized surface does not ‘see’ an inside or outside. From the point of view of differential geometry this may not be an issue. However, when the surface separates two phases, or two materials, or two colours, there are significant issues. For example, consider using two colours in Figure 1.2 in order to define the curve as the interface between the coloured regions. Black may be used to colour the inside of both loops and white to colour the rest of the plane, but if black is used inside just one loop then the other loop is lost. Thus, in order to use the parametric approach with this initial condition, one either thinks of a parametrization which traverses the curve without a crossing, but with a single self-intersection, or regards them as being two separate closed curves which touch at one point. These choices lead to differing evolutions for mean curvature flow.

Contrary to the parametric approach, the level set method has the capability of tracking topological changes (like pinching-off or merging) of $\Gamma(t)$ in an automatic way. In the basic implementation of the method topological

change is nothing special and is observed in post-processing the computational output. This is because, in principle, zero level sets of continuous functions can exhibit these features. However, from the mathematical point of view there are issues of existence of solutions of the degenerate partial differential equations that the level set approach generates. In the case of motion by mean curvature there is the notion of a *viscosity* solution which yields a unique evolution from any continuous function. The example of the lemniscate discussed in the context of the parametric approach introduces a new idea in the level set approach of *fattening* of the interface. The level set for this example develops an interior whose boundary yields both of the described solutions. Self-intersection, merger and pinch-off can all be simulated by this approach. This advantage, however, needs to be offset against the fact that the problem now becomes $(n + 1)$ -dimensional in space.

The phase field approach can also handle topological change, self-intersection, merger and pinch-off without doing anything special. It is the one approach which in its conception involves an approximation. The fact that it involves a new parameter ϵ is both an advantage and a disadvantage. The parabolic equations are in principle easy to solve but possess a certain computational *stiffness* due to the thickness of the diffuse interface. However, in many applications phase field models arise naturally and the ϵ parameter allows us to resolve singularities in a way which may be viewed as being physically motivated. From both the mathematical and physical points of view it is widely applicable in a rational way, whereas the use of the level set method is frequently *ad hoc*.

In general, the choice of one or the other approach will depend on whether one expects topological changes in the flow.

1.2. Applications

In what follows we list some problems in which a law of the form (1.1) or generalizations of it arise.

Grain boundary motion

Grain boundaries in alloys are interfaces which separate bulk crystalline regions of the same phase but with differing orientations. Associated with the grain boundary is a surface energy which gives rise to a thermodynamic restoring force. For a constant surface energy density this is simply the surface tension force proportional to the mean curvature and the resulting evolution law is just (1.2). Frequently there is also a driving force causing motion of the grain boundary.

Surface growth

The growth of thin films on substrates is technologically important. For example, epitaxy is a method for growing single crystals by the deposition

of atoms and molecules onto a growing film surface. There are numerous physical mechanisms operating at differing time and length scales which affect the growth process. A simple model would have a driving force representing the deposition flux of atoms onto the surface which might be in the normal direction or in a fixed vertical direction parallel to a beam of arriving atoms.

Image processing

One of the most important problems in image processing is to automatically detect contours of objects. We essentially follow the exposition of Aubert and Kornprobst (2002). Suppose that $M \subset \mathbb{R}^{n+1}$ ($n = 1$ or 2) is a given object and let $I(x) = \chi_{\Omega \setminus M}(x)$ be the characteristic function of $\Omega \setminus M$. The function

$$g(x) = \frac{1}{1 + |\nabla I_\sigma(x)|^2},$$

where I_σ is a mollification of I , will be small near the contour of M . It is therefore natural to look for minimizers of the functional

$$J(\Gamma) = \int_{\Gamma} g(x) \, dA$$

where Γ is a curve in \mathbb{R}^2 or a surface in \mathbb{R}^3 . The corresponding L^2 -gradient flow leads to the following evolution law: find curves/surfaces ('moving 'snakes') $\Gamma(t)$ such that

$$V = -\nabla \cdot (g \nu) = -g H - \nabla g \cdot \nu \quad \text{on } \Gamma(t).$$

Here, t plays the role of an artificial time; clearly this law fits into the framework (1.1).

Stefan problem for undercooled solidification

Consider a container $\Omega \subset \mathbb{R}^{n+1}$ ($n = 1$ or 2) filled with an undercooled liquid. Solidification of the liquid follows the nucleation of initial solid seed with characteristic diameter larger than the critical radius. The seed will then grow into the liquid. A mathematical model for this situation is the Stefan problem with kinetic undercooling, in which the solid–liquid interface is described by a curve/surface $\Gamma(t)$ and has to be determined together with the temperature distribution. Here the interior of $\Gamma(t)$ is the solid region $\Omega_S(t)$ and the exterior is the liquid region $\Omega_L(t)$. Using a suitable non-dimensionalization the problem then reads: for a given initial phase boundary Γ_0 and initial temperature distribution $\Theta_0 = \Theta_0(x)$ ($x \in \bar{\Omega}$), find the non-dimensional temperature $\Theta = \Theta(x, t)$ and the phase boundary $\Gamma(t)$ ($t > 0$), such that the heat equation is satisfied in the bulk, that is,

$$\Theta_t - \Delta \Theta = 0 \quad \text{in } \Omega \setminus \Gamma(t),$$

together with the initial value $\Theta(\cdot, 0) = \Theta_0$ in $\overline{\Omega}$. On the moving boundary the following two conditions are satisfied:

$$V = -\frac{1}{\varepsilon_l} \left[\frac{\partial \Theta}{\partial \nu} \right] \quad \text{on } \Gamma(t), \quad (1.5)$$

$$\Theta + \varepsilon_V \beta(\nu) V + \sigma H_\gamma = 0 \quad \text{on } \Gamma(t). \quad (1.6)$$

Here, $[\partial \Theta / \partial \nu]$ denotes the jump in the normal derivative of the temperature field across the interface and ε_l is the constant measuring the latent heat of solidification. Equation (1.6) is the Gibbs–Thomson law; ε_V, σ are non-dimensional positive constants measuring the strength of the kinetic undercooling and surface tension which depress the temperature on the solid–liquid interface from the scaled equilibrium zero melting temperature. Furthermore, H_γ is an anisotropic mean curvature associated with a surface energy density, $\gamma(\nu)$, depending on the orientation of the normal. There may also be anisotropy, $\beta(\nu)$, in the kinetic undercooling. Note that (1.6) can be rewritten as

$$\frac{\varepsilon_V}{\sigma} \beta(\nu) V = -H_\gamma - \frac{1}{\sigma} \Theta \quad \text{on } \Gamma(t).$$

If we consider Θ as being given, this equation again fits into our general framework (1.1) provided we allow for a coefficient in front of V and a generalized notion of mean curvature.

Figure 1.5 from Schmidt (1996) shows a simulation in which the free boundary was described by the parametric approach resulting in a sharp interface model. One can see the free boundary forming a dendrite. For

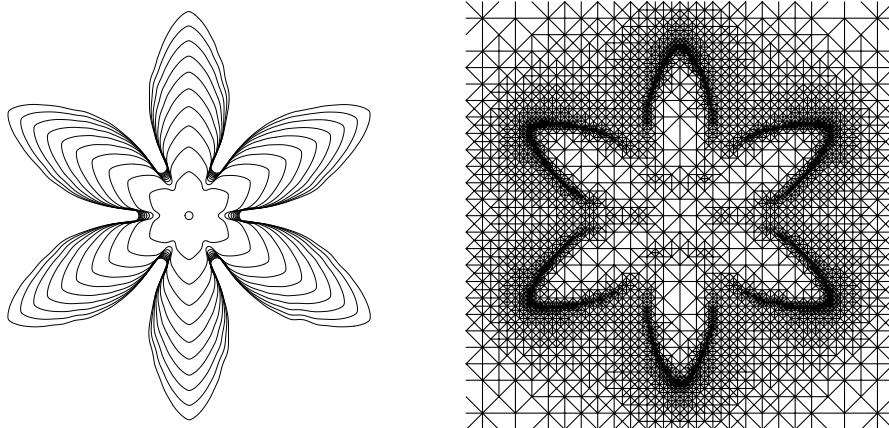


Figure 1.5. Evolution of a dendrite with sixfold anisotropy.
Time-steps of the free boundary (left) and adapted grid for
the temperature at one time-step (right).

results concerning three-dimensional dendrites and more information about the algorithm we refer to Schmidt (1996).

Figure 1.6 from Fried (1999) illustrates a possible effect of using a level set method for the free boundary in this problem. Dendrites may seem to merge. But if a smaller time-step is used the dendrites stay apart. For more information about a level set algorithm for dendritic growth we refer to Fried (1999, 2004).

Surface diffusion and Willmore flow

The following laws do not fit into (1.1), but we list them as examples of important geometric evolution equations in which the normal velocity depends on higher derivatives of mean curvature.

The surface diffusion equation

$$V = \Delta_\Gamma H \quad (1.7)$$

models the diffusion of mass within the bounding surface of a solid body. At the atomistic level atoms on the surface move along the surface owing to a driving force consisting of a chemical potential difference. For a surface with constant surface energy density the appropriate chemical potential in this setting is the mean curvature H . This leads to the flux law

$$\rho V = -\operatorname{div}_\Gamma \mathbf{j},$$

where ρ is the mass density and \mathbf{j} is the mass flux in the surface, with the constitutive flux law (Herring 1951, Mullins 1957)

$$\mathbf{j} = -D \nabla_\Gamma H.$$

Here, D is the diffusion constant. From these equations we obtain the law (1.7) after an appropriate non-dimensionalization. In order to model the

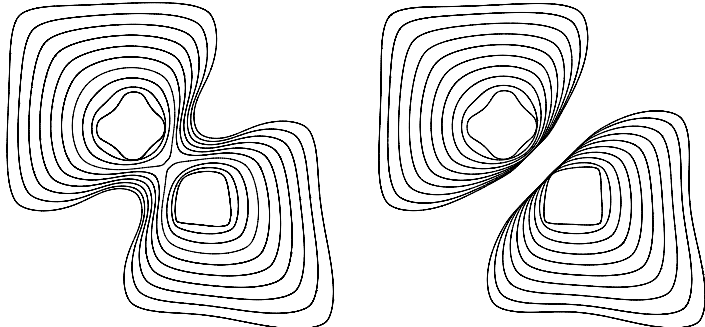


Figure 1.6. A possible effect of the use of a level set method. Growing dendrites: merging (left) for large time-step size and staying apart (right) for smaller time-step size.

underlying structure of the solid body bounded by Γ , anisotropic surface diffusion is important, that is,

$$V = \Delta_\Gamma H_\gamma, \quad (1.8)$$

with H_γ denoting the anisotropic mean curvature of the surface Γ as it is introduced in (8.15).

A similar evolution law is Willmore flow,

$$V = \Delta_\Gamma H + H|\nabla_\Gamma \nu|^2 - \frac{1}{2}H^3 \quad \text{on } \Gamma(t), \quad (1.9)$$

which arises as the L^2 -gradient flow for the classical bending energy $E(\Gamma) = \frac{1}{2} \int_\Gamma H^2 dA$. Apart from applications in mechanics and membrane physics this flow has recently been used for surface restoration and inpainting.

1.3. Outline of article

This article is organized as follows. In Section 2 we present some useful geometric analysis, in particular the notion of mean curvature. The basic mean curvature flow is defined in Section 3 and some elementary properties are described. The next four sections consider in turn basic approaches for numerical approximation. In Section 4 we consider the parametric approach. We start with the classical curve shortening flow and present a semidiscrete numerical scheme as well as error estimates. Next, we show how to apply the above ideas to the approximation of higher-dimensional surfaces. A crucial point is to construct numerical schemes which reflect the intrinsic nature of the flow. Section 5 is concerned with graphs. We prove an error bound for a semidiscrete finite element scheme thereby showing the virtue of working with geometric quantities. A fully discrete scheme along with stability issues is discussed afterwards. In Section 6 we introduce the level set equation as a way of handling topological changes. We briefly discuss the framework of viscosity solutions which allows a satisfactory existence and uniqueness theory. For numerical purposes it is convenient to regularize the level set equation. We collect some properties of the regularized problem and clarify its formal similarity to the graph setting. The approximation of mean curvature flow by phase field methods is considered in Section 7. Even before numerical discretization there is the notion of approximation of a sharp interface by a diffuse interface of width $O(\epsilon)$. The phase field approach depends on the notion of a diffuse interfacial energy composed of quadratic gradient and homogeneous free energy terms involving a phase field function. The choice of double well energy potential is discussed. We recall some analytical results as well as a convergence analysis for a discretization in space by linear finite elements. We finish this section by discussing the discretization in time together with the question of stability. In Section 8 we introduce the concept of the anisotropy γ together with its relevant

properties and subsequently generalize the ideas of the previous sections to this setting. Finally, Section 9 is concerned with fourth order flows: we present discretization techniques for both surface diffusion and Willmore flow.

For the convenience of the reader we have included a long list of references, which are related to the subject of these notes, but not all of which are cited in the text.

2. Some geometric analysis

The aim of this section is to collect some useful definitions and results from differential geometry. We refer to Gilbarg and Trudinger (1998) and Giga (2002) for a more detailed exposition of this material.

2.1. Hypersurfaces

A subset $\Gamma \subset \mathbb{R}^{n+1}$ is called a C^2 -hypersurface if for each point $x_0 \in \Gamma$ there exists an open set $U \subset \mathbb{R}^{n+1}$ containing x_0 and a function $u \in C^2(U)$ such that

$$U \cap \Gamma = \{x \in U \mid u(x) = 0\}, \quad \text{and} \quad \nabla u(x) \neq 0 \quad \text{for all } x \in U \cap \Gamma. \quad (2.1)$$

The tangent space $T_x \Gamma$ is then the n -dimensional linear subspace of \mathbb{R}^{n+1} that is orthogonal to $\nabla u(x)$. It is independent of the particular choice of function u which is used to describe Γ . A C^2 -hypersurface $\Gamma \subset \mathbb{R}^{n+1}$ is called orientable if there exists a vectorfield $\nu \in C^1(\Gamma, \mathbb{R}^{n+1})$ (*i.e.*, $\nu \in C^1$ in an open neighbourhood of Γ) such that $\nu(x) \perp T_x \Gamma$ and $|\nu(x)| = 1$ for all $x \in \Gamma$. In what follows, we shall assume that $\Gamma \subset \mathbb{R}^{n+1}$ is an oriented C^2 -hypersurface.

We define the tangential gradient of a function f , which is differentiable in an open neighbourhood of Γ by

$$\nabla_\Gamma f(x) = \nabla f(x) - \nabla f(x) \cdot \nu(x) \nu(x), \quad x \in \Gamma.$$

Here ∇ denotes the usual gradient in \mathbb{R}^{n+1} . Note also that $\nabla_\Gamma f(x)$ is the orthogonal projection of $\nabla f(x)$ onto $T_x \Gamma$. It is straightforward to show that $\nabla_\Gamma f$ only depends on the values of f on Γ . We use the notation

$$\nabla_\Gamma f(x) = (\underline{D}_1 f(x), \dots, \underline{D}_{n+1} f(x)) \quad (2.2)$$

for the $n + 1$ components of the tangential gradient. Obviously

$$\nabla_\Gamma f(x) \cdot \nu(x) = 0, \quad x \in \Gamma.$$

If f is twice differentiable in an open neighbourhood of Γ , then we define

the *Laplace–Beltrami operator* of f as

$$\Delta_\Gamma f(x) = \nabla_\Gamma \cdot \nabla_\Gamma f(x) = \sum_{i=1}^{n+1} \underline{D}_i \underline{D}_i f(x), \quad x \in \Gamma. \quad (2.3)$$

2.2. Oriented distance function

A useful level set representation of a hypersurface can be obtained with the help of the distance function. Let Γ be as above and assume in addition that Γ is compact. The Jordan–Brouwer decomposition theorem then implies that there exists an open bounded set $\Omega \subset \mathbb{R}^{n+1}$ such that $\Gamma = \partial\Omega$. We assume that the unit normal field to Γ points away from Ω and define the oriented (signed) distance function d by

$$d(x) = \begin{cases} \text{dist}(x, \Gamma), & x \in \mathbb{R}^{n+1} \setminus \bar{\Omega} \\ 0, & x \in \Gamma \\ -\text{dist}(x, \Gamma), & x \in \Omega. \end{cases}$$

It is well known that d is globally Lipschitz-continuous and that there exists $\delta > 0$ such that

$$d \in C^2(\Gamma_\delta), \quad \text{where } \Gamma_\delta = \{x \in \mathbb{R}^{n+1} \mid |d(x)| < \delta\}. \quad (2.4)$$

Every point $x \in \Gamma_\delta$ can be uniquely written as

$$x = a(x) + d(x)\nu(a(x)), \quad x \in \Gamma_\delta, \quad (2.5)$$

where $a(x) \in \Gamma$. Furthermore, $\nabla d(x) = \nu(a(x))$, $x \in \Gamma_\delta$, which implies in particular that

$$|\nabla d(x)| \equiv 1 \quad \text{in } \Gamma_\delta. \quad (2.6)$$

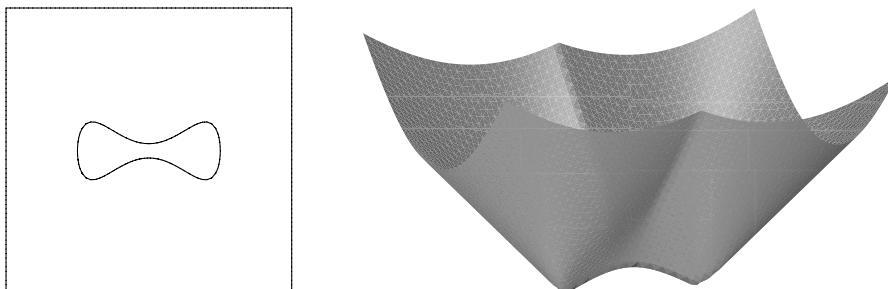


Figure 2.1. Graph (right) of the oriented distance function for the curve (left).

2.3. Mean curvature

Let us next turn to the notion of mean curvature. By assumption, ν is C^1 in a neighbourhood of Γ so that we may introduce the matrix

$$H_{jk}(x) = \underline{D}_j \nu_k(x), \quad j, k = 1, \dots, n+1, x \in \Gamma. \quad (2.7)$$

It is not difficult to show that $(H_{jk}(x))$ is symmetric. Furthermore,

$$\sum_{k=1}^{n+1} H_{jk}(x) \nu_k(x) = \sum_{k=1}^{n+1} \underline{D}_j \nu_k(x) \nu_k(x) = \frac{1}{2} \underline{D}_j |\nu|^2(x) = 0,$$

since $|\nu| = 1$ on Γ . Thus, $(H_{jk}(x))$ has one eigenvalue which is equal to zero with corresponding eigenvector $\nu(x)$. The remaining n eigenvalues $\kappa_1(x), \dots, \kappa_n(x)$ are called the principal curvatures of Γ at the point x . We now define the mean curvature of Γ at x as the trace of the matrix $(H_{jk}(x))$, that is,

$$H(x) = \sum_{j=1}^{n+1} H_{jj}(x) = \sum_{j=1}^n \kappa_j(x). \quad (2.8)$$

Note that (2.8) differs from the more common definition $H = \frac{1}{n} \sum_{j=1}^{n+1} H_{jj}$. From (2.7) we derive the following expression for mean curvature,

$$H(x) = \nabla_\Gamma \cdot \nu(x), \quad x \in \Gamma, \quad (2.9)$$

where $\nabla_\Gamma \cdot f = \sum_{j=1}^{n+1} \underline{D}_j f_j$ denotes the tangential divergence of a vectorfield f . In particular we see that $H > 0$ if $\Gamma = S^n$ and the unit normal field is chosen to point away from S^n , i.e., $\nu(x) = x$.

While the sign of H depends on the choice of the normal ν , the mean curvature vector $H\nu$ is an invariant. A useful formula for this quantity can be obtained by choosing $f(x) = x_j$, $j \in \{1, \dots, n+1\}$ in (2.3) and observing that $\underline{D}_i x_j = \delta_{ij} - \nu_j \nu_i$. We then deduce with the help of (2.9) that

$$\Delta_\Gamma x_j = - \sum_{i=1}^{n+1} \underline{D}_i (\nu_j \nu_i) = -(\nabla_\Gamma \cdot \nu) \nu_j - \nabla_\Gamma \nu_j \cdot \nu = -H \nu_j,$$

so that

$$-\Delta_\Gamma x = H\nu \quad \text{on } \Gamma. \quad (2.10)$$

Let us next fix a point $\bar{x} \in \Gamma$ and calculate $H(\bar{x})$ for various representations of the surface Γ near \bar{x} .

Level set representation. Suppose that Γ is given as in (2.1) near \bar{x} . Clearly, we then have

$$\nu(x) = \pm \frac{\nabla u(x)}{|\nabla u(x)|}$$

for $x \in U \cap \Gamma$. If the plus sign applies we obtain

$$H = \nabla_\Gamma \cdot \frac{\nabla u}{|\nabla u|} = \nabla \cdot \frac{\nabla u}{|\nabla u|} = \frac{1}{|\nabla u|} \sum_{i,j=1}^{n+1} \left(\delta_{ij} - \frac{u_{x_i} u_{x_j}}{|\nabla u|^2} \right) u_{x_i x_j}. \quad (2.11)$$

In the special case that $u(x) = d(x)$, where d is the oriented distance function to Γ , we obtain in view of (2.6)

$$H(x) = \Delta d(x), \quad x \in \Gamma. \quad (2.12)$$

Graph representation. Suppose that

$$U \cap \Gamma = \{(x, v(x)) \mid x \in \Omega\},$$

where $\Omega \subset \mathbb{R}^n$ is open, $x = (x_1, \dots, x_n)$ and $v \in C^2(\Omega)$. Defining $u(x, x_{n+1}) = v(x) - x_{n+1}$ we see that $U \cap \Gamma$ is the zero level set of u and the above considerations imply that

$$H(x, v(x)) = \nabla \cdot \left(\frac{\nabla v(x)}{\sqrt{1 + |\nabla v(x)|^2}} \right), \quad (x, v(x)) \in U \cap \Gamma, \quad (2.13)$$

where ∇ is the gradient in \mathbb{R}^n and the unit normal is chosen as $\nu = \frac{(\nabla v, -1)}{\sqrt{1 + |\nabla v|^2}}$.

Parametric representation. Suppose that there exists an open set $V \subset \mathbb{R}^n$ and a mapping $X \in C^2(V, \mathbb{R}^{n+1})$ such that

$$U \cap \Gamma = X(V), \quad \text{rank } DX(\theta) = n \quad \text{for all } \theta \in V.$$

The vectors $\frac{\partial X}{\partial \theta_1}(\theta), \dots, \frac{\partial X}{\partial \theta_n}(\theta)$ then form a basis of $T_x \Gamma$ at $x = X(\theta)$. We define the metric on Γ by

$$g_{ij}(\theta) = \frac{\partial X}{\partial \theta_i}(\theta) \cdot \frac{\partial X}{\partial \theta_j}(\theta), \quad i, j = 1, \dots, n$$

and let g^{ij} be the components of the inverse matrix of (g_{ij}) . We then have the following formulae for the tangential gradient of a function f (defined in a neighbourhood of Γ) and the mean curvature vector $H\nu$:

$$\nabla_\Gamma f = \sum_{i,j=1}^n g^{ij} \frac{\partial(f \circ X)}{\partial \theta_j} \frac{\partial X}{\partial \theta_i}, \quad (2.14)$$

$$H\nu = -\frac{1}{\sqrt{g}} \sum_{i,j=1}^n \frac{\partial}{\partial \theta_i} \left(g^{ij} \sqrt{g} \frac{\partial X}{\partial \theta_j} \right) \quad (2.15)$$

where $g = \det(g_{ij})$.

2.4. Integration by parts

Let us assume in this section that Γ is in addition compact. The formula for integration by parts on Γ is (*cf.* Gilbarg and Trudinger (1998))

$$\int_{\Gamma} \underline{D}_i f \, dA = \int_{\Gamma} f H \nu_i \, dA \quad i = 1, \dots, n+1, \quad (2.16)$$

where dA denotes the area element on Γ and f is continuously differentiable in a neighbourhood of Γ . Applying (2.16) with $h = f \underline{D}_i g$, summing from $i = 1, \dots, n+1$ and taking into account that $\nabla_{\Gamma} \nu_i \cdot \nu = 0$, we obtain Green's formula,

$$\int_{\Gamma} \nabla_{\Gamma} f \cdot \nabla_{\Gamma} g \, dA = - \int_{\Gamma} f \Delta_{\Gamma} g \, dA. \quad (2.17)$$

In particular, we deduce from (2.10)

$$\int_{\Gamma} H \nu \cdot \phi \, dA = \int_{\Gamma} \nabla_{\Gamma} x \cdot \nabla_{\Gamma} \phi \, dA, \quad (2.18)$$

where ϕ is continuously differentiable in a neighbourhood of Γ with values in \mathbb{R}^{n+1} and $\nabla_{\Gamma} x \cdot \nabla_{\Gamma} \phi = \sum_{i=1}^{n+1} \nabla_{\Gamma} x_i \cdot \nabla_{\Gamma} \phi_i$. This relation will be very important for the numerical treatment of mean curvature flow. The above formulae can be generalized to surfaces with boundaries by including an appropriate integral over $\partial\Gamma$.

2.5. Moving surfaces

In this section we shall be concerned with surfaces that evolve in time. A family $(\Gamma(t))_{t \in (0, T)}$ is called a $C^{2,1}$ -family of hypersurfaces if, for each point $(x_0, t_0) \in \mathbb{R}^{n+1} \times (0, T)$ with $x_0 \in \Gamma(t_0)$, there exists an open set $U \subset \mathbb{R}^{n+1}$, $\delta > 0$ and a function $u \in C^{2,1}(U \times (t_0 - \delta, t_0 + \delta))$ such that

$$U \cap \Gamma(t) = \{x \in U \mid u(x, t) = 0\} \quad \text{and} \quad \nabla u(x, t) \neq 0, \quad x \in U \cap \Gamma(t). \quad (2.19)$$

Suppose in addition that each $\Gamma(t)$ is oriented by a unit normal field $\nu(\cdot, t) \in C^1(\Gamma(t), \mathbb{R}^{n+1})$ and that $\nu \in C^0(\bigcup_{0 < t < T} \Gamma(t) \times \{t\}, \mathbb{R}^{n+1})$. The normal velocity at a point (x_0, t_0) ($x_0 \in \Gamma(t_0)$) is then defined as

$$V(x_0, t_0) = \phi'(t_0) \cdot \nu(x_0, t_0),$$

where $\phi \in C^1((t_0 - \epsilon, t_0 + \epsilon), \mathbb{R}^{n+1})$ satisfies $\phi(t_0) = x_0$ and $\phi(t) \in \Gamma(t)$ for $|t - t_0| < \epsilon$. It can be shown that $V(x_0, t_0)$ is independent of the particular choice of ϕ . Let us calculate $V(x_0, t_0)$ for various representations of $\Gamma(t)$.

Level set representation. Let u be as in (2.19); as above we then have $\nu = \pm \frac{\nabla u}{|\nabla u|}$. If the plus sign applies and $\phi \in C^1((t_0 - \epsilon, t_0 + \epsilon), \mathbb{R}^{n+1})$ satisfies $\phi(t_0) = x_0$ as well as $\phi(t) \in \Gamma(t)$ for $|t - t_0| < \epsilon$, we have

$$0 = \frac{d}{dt} u(\phi(t), t) = \nabla u(\phi(t), t) \cdot \phi'(t) + u_t(\phi(t), t),$$

and hence

$$V(x_0, t_0) = -\frac{u_t(x_0, t_0)}{|\nabla u(x_0, t_0)|}. \quad (2.20)$$

Graph representation. Suppose that

$$U \cap \Gamma(t) = \{(x, v(x, t)) \mid x \in \Omega\},$$

where $\Omega \subset \mathbb{R}^n$ is open and $v \in C^{2,1}(\Omega \times (t_0 - \delta, t_0 + \delta))$. Applying the formula for the level set case to $u(x, x_{n+1}, t) = v(x, t) - x_{n+1}$, we obtain

$$V = -\frac{v_t}{\sqrt{1 + |\nabla v|^2}} \quad (2.21)$$

for the unit normal field $\nu = \frac{(\nabla v, -1)}{\sqrt{1 + |\nabla v|^2}}$.

2.6. Transport theorem for integrals

Consider a family $(\Gamma(t))_{t \in (0, T)}$ of evolving hypersurfaces which satisfies the assumptions made above and suppose in addition that each surface $\Gamma(t)$ is compact. We are interested in the time derivative of certain volume and area integrals.

Lemma 2.1. Let $g \in C^1(Q)$, where Q is an open set containing

$$\bigcup_{0 < t < T} \Gamma(t) \times \{t\}.$$

Suppose in addition that each surface $\Gamma(t)$ is the boundary of an open bounded subset $\Omega(t) \subset \mathbb{R}^{n+1}$. Then

$$\frac{d}{dt} \int_{\Omega(t)} g \, dx = \int_{\Omega(t)} \frac{\partial g}{\partial t} \, dx + \int_{\Gamma(t)} g V \, dA, \quad (2.22)$$

$$\frac{d}{dt} \int_{\Gamma(t)} g \, dA = \int_{\Gamma(t)} \frac{\partial g}{\partial t} \, dA + \int_{\Gamma(t)} g VH \, dA + \int_{\Gamma(t)} \frac{\partial g}{\partial \nu} V \, dA. \quad (2.23)$$

Proof. See the Appendix. □

3. Definition and elementary properties of mean curvature flow

The purpose of this section is to introduce motion by mean curvature and to describe some basic features of this flow. Consider a $C^{2,1}$ -family of hypersurfaces $(\Gamma(t))_{t \in [0, T]} \subset \mathbb{R}^{n+1}$ together with a choice ν of a unit normal.

Definition 1. We say that $(\Gamma(t))_{t \in [0, T]}$ moves by mean curvature if

$$V = -H \quad \text{on } \Gamma(t). \quad (3.1)$$

Here, V denotes the velocity of $\Gamma(t)$ in the direction of ν and H is mean curvature.

As we shall see later, the above equation gives rise to a parabolic equation, or a parabolic system, for the function(s) describing the surfaces $\Gamma(t)$, to which an initial condition

$$\Gamma(0) = \Gamma_0 \quad (3.2)$$

has to be added. If $\Gamma(t)$ has a boundary, then also suitable boundary conditions need to be specified.

In order to give a first idea of this flow we look at the well-known example of the shrinking sphere. Let $\Gamma(t) = \partial B_{r(t)}(x_0) \subset \mathbb{R}^{n+1}$, oriented by the unit outer normal $\nu(x) = \frac{x-x_0}{r(t)}$. Then, $V = r'(t)$, $H = \frac{n}{r(t)}$ on $\Gamma(t)$, so that $\Gamma(t)$ moves by mean curvature provided that $r'(t) = -\frac{n}{r(t)}$. The solution of this ODE is given by $r(t) = \sqrt{r_0^2 - 2nt}$, $0 \leq t < \frac{r_0^2}{2n}$, where $\Gamma_0 = \partial B_{r_0}(x_0)$. Note that $\Gamma(t)$ shrinks to a point as $t \nearrow \frac{r_0^2}{2n}$.

The main feature of mean curvature flow is its area-decreasing property, which is a consequence of the following result.

Lemma 3.1. Let $\Gamma(t)$ be a family of evolving hypersurfaces satisfying $V = -H$ on $\Gamma(t)$ and assume that each $\Gamma(t)$ is compact. Then

$$\int_{\Gamma(t)} V^2 dA + \frac{d}{dt} |\Gamma(t)| = 0,$$

where $|\Gamma|$ is the area of Γ .

Proof. This follows immediately from choosing $g \equiv 1$ in (2.23) and the evolution law (3.1). \square

Since the law (3.1) gives rise to a second order parabolic problem we expect existence of a smooth solution locally in time for a smooth initial hypersurface Γ_0 . Furthermore, maximum and comparison principles are available which can be used to show that two smooth compact solutions which are initially disjoint will stay disjoint (see, *e.g.*, Ecker (2002)). Using the shrinking sphere as a comparison solution, it follows in particular that if $\Gamma(t)$, $0 \leq t < T$ is a smooth solution with $\Gamma_0 \subset B_{r_0}(x_0)$, then $\Gamma(t) \subset B_{\sqrt{r_0^2 - 2nt}}(x_0)$ for $0 \leq t < \min(T, \frac{r_0^2}{2n})$. In general, solutions will develop singularities in finite time before they disappear, but there are certain initial configurations for which they stay smooth until they shrink to a point.

Theorem 3.2. Let $n \geq 2$ and assume that $\Gamma_0 \subset \mathbb{R}^{n+1}$ is a smooth, compact and uniformly convex hypersurface. Then (3.1) and (3.2) have a smooth solution on a finite time interval $[0, T)$ and the $\Gamma(t)$ converge to a

point as $t \nearrow T$. If one rescales the surfaces in such a way that the enclosed volume remains fixed, one has convergence against a sphere as $t \nearrow T$.

Proof. See Huisken (1984). \square

The case $n = 1$ is usually referred to as curve shortening flow.

Theorem 3.3. Assume that $\Gamma_0 \subset \mathbb{R}^2$ is a smooth embedded closed curve. Then (3.1) and (3.2) have a smooth embedded solution on a finite time interval $[0, T)$, which shrinks to a ‘round’ point as $t \nearrow T$.

Proof. Gage and Hamilton (1986) proved this result for convex Γ_0 ; subsequently Grayson (1987) showed that a smooth embedded closed curve remains smooth and embedded and becomes convex in finite time. \square

If the initial curve is not embedded, cusp-like singularities may develop (see Figures 4.2 and 4.3). The papers of Angenent (1991), Altschuler and Grayson (1992) and Deckelnick (1997) propose various methods of how to continue the solution past such a singularity. The analogue of Theorem 3.3 for surfaces does not hold, as can be seen by choosing a suitable dumbbell-shaped initial surface which develops a pinch-off singularity before it shrinks to a point (see Figure 4.5 and Grayson (1989)). This pinch-off leads to a change of the topological type of $\Gamma(t)$, so that the parametric approach – in which the topological type is fixed – will develop a singularity that is difficult to handle. Thus the question arises whether it is possible to introduce a notion of solution that is capable of following the flow through a singularity. Several such notions have been proposed and analysed starting with the pioneering work of Brakke (1978) on varifold solutions, which uses tools from geometric measure theory. In this context we also mention the surface evolver program of Brakke (1992). Level set and phase field methods constitute two completely different approaches which take an Eulerian point of view. We shall discuss these in more detail in Sections 6 and 7.

4. Parametric mean curvature flow

As is mentioned above, in the parametric approach one chooses a suitable reference manifold $M \subset \mathbb{R}^{n+1}$ (of the topological type of the evolving hypersurfaces $\Gamma(t)$) and then looks for maps $X(\cdot, t) : M \rightarrow \mathbb{R}^{n+1}$ ($0 \leq t < T$) such that $\Gamma(t) = X(\cdot, t)(M)$. To fix ideas, let us assume that M is a compact hypersurface without boundary. If we can find X in such a way that

$$\frac{\partial X}{\partial t}(p, t) = -H(X(p, t))\nu(X(p, t)) \quad (p, t) \in M \times (0, T), \quad (4.1)$$

then $V = -H$ on $\Gamma(t)$ follows by taking the dot product with the normal ν . In order to understand (4.1) let $F : \Omega \rightarrow \mathbb{R}^{n+1}$ be a local parametrization

of M defined on an open set $\Omega \subset \mathbb{R}^n$ and set

$$\hat{X}(\theta, t) = X(F(\theta), t), \quad (\theta, t) \in \Omega \times (0, T).$$

Recalling (2.15), the equation (4.1) then turns into

$$\frac{\partial \hat{X}}{\partial t}(\theta, t) - \frac{1}{\sqrt{\hat{g}}} \sum_{i,j=1}^n \frac{\partial}{\partial \theta_i} \left(\hat{g}^{ij} \sqrt{\hat{g}} \frac{\partial \hat{X}}{\partial \theta_j} \right) = 0 \quad (4.2)$$

where $\hat{g}_{ij}(\theta, t) = \frac{\partial \hat{X}}{\partial \theta_i} \cdot \frac{\partial \hat{X}}{\partial \theta_j}$ and \hat{g}^{ij}, \hat{g} are as above. Thus (4.2), and hence (4.1), is a nonlinear parabolic system, which is not defined at points (θ, t) where $\hat{g}(\theta, t) = 0$. In order to close this system, an initial condition $X(p, 0) = X_0(p)$, $p \in M$ needs to be prescribed, where $X_0 : M \rightarrow \mathbb{R}^{n+1}$ is a parametrization of the initial surface Γ_0 .

4.1. Curve shortening flow

Mean curvature evolution in the one-dimensional case is usually referred to as curve shortening flow. In the case of closed curves, a convenient choice of a reference manifold is $M = S^1$, which can be parametrized globally by $F(\theta) = (\cos \theta, \sin \theta)$, $\theta \in [0, 2\pi]$. In the following, for simplicity, let us identify $\hat{X}(\theta, t)$ and $X((\cos \theta, \sin \theta), t)$. Thus, (4.2) becomes

$$X_t - \frac{1}{|X_\theta|} \left(\frac{X_\theta}{|X_\theta|} \right)_\theta = 0 \quad \text{in } I \times (0, T), \quad (4.3)$$

$$X(\cdot, 0) = X_0 \quad \text{in } I, \quad (4.4)$$

where $I = [0, 2\pi]$. In addition, X has to satisfy the periodicity condition

$$X(\theta, t) = X(\theta + 2\pi, t) \quad 0 \leq t < T, \quad \theta \in \mathbb{R}. \quad (4.5)$$

Suppose that $X : \mathbb{R} \times [0, T] \rightarrow \mathbb{R}^2$ is a smooth solution of (4.3)–(4.5), in particular $|X_\theta| > 0$ in $I \times [0, T]$. If we multiply (4.3) by $|X_\theta|$, take the dot product with a test function $\varphi \in H_{\text{per}}^1(I; \mathbb{R}^2) = \{\varphi \in H^1(I; \mathbb{R}^2) \mid \varphi(0) = \varphi(2\pi)\}$ and integrate over I , we obtain

$$\int_I X_t \cdot \varphi |X_\theta| + \int_I \frac{X_\theta \cdot \varphi_\theta}{|X_\theta|} = 0 \quad \text{for all } \varphi \in H_{\text{per}}^1(I; \mathbb{R}^2). \quad (4.6)$$

We use (4.6) in order to discretize in space. For simplicity let $\theta_j = jh$ ($j = 0, \dots, N$) be a uniform grid with grid size $h = 2\pi/N$ and let

$$S_h = \left\{ \varphi_h \in C^0(I; \mathbb{R}^2) \mid \varphi_h|_{[\theta_{j-1}, \theta_j]} \in P_1^2, j = 1, \dots, N; \varphi_h(0) = \varphi_h(2\pi) \right\}$$

be the space of piecewise linear continuous functions with values in \mathbb{R}^2 . The spatial discretization of (4.3) is then given by

$$\int_I X_{ht} \cdot \varphi_h |X_{h\theta}| + \int_I \frac{X_{h\theta} \cdot \varphi_{h\theta}}{|X_{h\theta}|} = 0 \quad \text{for all } \varphi_h \in S_h. \quad (4.7)$$

Denoting the common (scalar) nodal basis by $\{\phi_1, \dots, \phi_N\}$, we can expand $X_h(\theta, t) = \sum_{j=1}^N X_j(t)\phi_j(\theta)$ with vectors $X_j(t) \in \mathbb{R}^2$. This one-dimensional finite element formulation can be rewritten as a difference scheme. To see this, insert $\varphi_h = \phi_j e^k$, ($k = 1, 2$; $j = 1, \dots, N$) into (4.7) and calculate

$$\int_I X_{ht} \cdot \varphi_h |X_{h\theta}| d\theta = \frac{1}{6} |X_j - X_{j-1}| \dot{X}_{j-1} \cdot e^k + \frac{1}{3} (|X_j - X_{j-1}| + |X_{j+1} - X_j|) \dot{X}_j \cdot e^k + \frac{1}{6} |X_{j+1} - X_j| \dot{X}_{j+1} \cdot e^k$$

as well as

$$\int_I \frac{X_{h\theta} \cdot \varphi_{h\theta}}{|X_{h\theta}|} d\theta = \left(-\frac{X_{j+1} - X_j}{q_{j+1}} + \frac{X_j - X_{j-1}}{q_j} \right) \cdot e^k.$$

Here, $q_j = |X_j - X_{j-1}|$ and the dot stands for the time derivative. Thus, (4.7) can be written as

$$\frac{1}{6} q_j \dot{X}_{j-1} + \frac{1}{3} (q_j + q_{j+1}) \dot{X}_j + \frac{1}{6} q_{j+1} \dot{X}_{j+1} = \frac{X_{j+1} - X_j}{q_{j+1}} - \frac{X_j - X_{j-1}}{q_j} \quad (4.8)$$

($j = 1, \dots, N$). If we use mass lumping in (4.8) we get the difference scheme

$$\frac{1}{2} (q_j + q_{j+1}) \dot{X}_j = \frac{X_{j+1} - X_j}{q_{j+1}} - \frac{X_j - X_{j-1}}{q_j}. \quad (4.9)$$

As initial values for X_j we choose

$$X_j(0) = X_0(\theta_j), \quad j = 0, \dots, N, \quad (4.10)$$

so that $X_h(\cdot, 0)$ is the linear interpolant of X_0 . Furthermore we require the periodicity condition

$$X_j = X_{j+N}, \quad j = -1, 0, 1. \quad (4.11)$$

The following proposition shows that the lumped scheme reflects the curve shortening property of the exact solution.

Proposition 4.1. Consider solutions X of (4.3) and $X_h = \sum_{j=1}^N X_j(t)\phi_j(\theta)$ of (4.9) respectively. Then we have for $t \in [0, T]$

$$|X_\theta(\cdot, t)|_t = -|X_t(\cdot, t)|^2 |X_\theta(\cdot, t)| \quad \text{in } I$$

$$\dot{q}_j = -\frac{1}{4} (q_{j-1} + q_j) |\dot{X}_{j-1}|^2 - \frac{1}{4} (q_j + q_{j+1}) |\dot{X}_j|^2, \quad j = 1, \dots, N$$

as long as $q_j > 0$, $j = 1, \dots, N$. Thus, the faces of the polygon with vertices X_1, \dots, X_N decrease in length during time evolution.

Proof. For the proof of the first assertion we differentiate $|\frac{X_\theta}{|X_\theta|}| \equiv 1$ twice with respect to θ and get

$$\frac{X_\theta}{|X_\theta|} \cdot \left(\frac{X_\theta}{|X_\theta|} \right)_\theta = 0, \quad \left| \left(\frac{X_\theta}{|X_\theta|} \right)_\theta \right|^2 = -\frac{X_\theta}{|X_\theta|} \cdot \left(\frac{X_\theta}{|X_\theta|} \right)_{\theta\theta} \quad \text{in } I,$$

which combined with (4.3) gives

$$\begin{aligned} |X_\theta|_t &= \frac{X_\theta}{|X_\theta|} \cdot X_{\theta t} = \frac{X_\theta}{|X_\theta|} \cdot \frac{1}{|X_\theta|} \left(\frac{X_\theta}{|X_\theta|} \right)_{\theta\theta} \\ &= -\frac{1}{|X_\theta|} \left| \left(\frac{X_\theta}{|X_\theta|} \right)_\theta \right|^2 = -|X_t|^2 |X_\theta|. \end{aligned}$$

For the discrete solution we observe that by (4.9) with the unit vectors $T_j = \frac{X_j - X_{j-1}}{q_j}$ we have

$$\begin{aligned} q_j &= T_j \cdot (\dot{X}_j - \dot{X}_{j-1}) \\ &= T_j \cdot \left(\frac{2}{q_j + q_{j+1}} (T_{j+1} - T_j) - \frac{2}{q_{j-1} + q_j} (T_j - T_{j-1}) \right) \\ &= -\frac{2}{q_j + q_{j+1}} (1 - T_j \cdot T_{j+1}) - \frac{2}{q_{j-1} + q_j} (1 - T_{j-1} \cdot T_j) \\ &= -\frac{1}{q_j + q_{j+1}} |T_j - T_{j+1}|^2 - \frac{1}{q_{j-1} + q_j} |T_{j-1} - T_j|^2 \\ &= -\frac{1}{4} (q_{j-1} + q_j) |\dot{X}_{j-1}|^2 - \frac{1}{4} (q_j + q_{j+1}) |\dot{X}_j|^2. \end{aligned}$$

For this we have used the discrete equation (4.9) twice. \square

Under the assumption that a smooth and regular solution of the curve shortening flow (4.3)–(4.5) exists, one obtains the following convergence result together with error estimates for the position vector X and the velocity vector X_t , which by (4.1) is equal to the curvature vector. The proof follows from Dziuk (1994) and is a special case of Theorem 8.4.

Theorem 4.2. Let $X : I \times [0, T] \rightarrow \mathbb{R}^2$ be a periodic smooth solution of the curve shortening flow (4.3)–(4.5) with $|X_\theta| \geq c_0 > 0$ in $I \times [0, T]$. Then there exists an $h_0 > 0$ depending on X and T such that for every $0 < h \leq h_0$ there exists a unique solution $X_h(\theta, t) = \sum_{j=1}^N X_j(t) \phi_j(\theta)$ of the difference scheme (4.9), (4.10) and

$$\max_{[0,T]} \|X - X_h\|_{L^2(I)} + \left(\int_0^T \|X_\theta - X_{h\theta}\|_{L^2(I)}^2 dt \right)^{1/2} \leq ch, \quad (4.12)$$

$$\max_{[0,T]} \|X_t - X_{ht}\|_{L^2(I)} + \left(\int_0^T \|X_{t\theta} - X_{ht\theta}\|_{L^2(I)}^2 dt \right)^{1/2} \leq ch, \quad (4.13)$$

where c depends on X and T .

This algorithm can be generalized without changes to curves evolving in higher codimension, *i.e.*, $X : I \times [0, T] \rightarrow \mathbb{R}^m$ and $m > 2$. The curve solving (4.3) has a velocity only in the normal direction. It is also possible to use

the parametric equation

$$X_t = \frac{X_{\theta\theta}}{|X_\theta|^2}$$

instead, which defines the same curve evolving in the normal direction with a normal velocity being given by the curvature. However, the parametrization is different, with the points on the curve now having a tangential velocity. A finite element error analysis for the motion of a closed curve is given in Deckelnick and Dziuk (1994), while error bounds for the evolution of a curve attached to a fixed boundary with a normal contact condition are proved in Deckelnick and Elliott (1998).

In order to obtain a practical method we still have to discretize in time. Choose a time-step $\tau > 0$ and let $t_m = m\tau$, $m = 0, \dots, M$, $M \leq [\frac{T}{\tau}]$. We let $X_h^m \in S_h$ denote the approximation to $X(\cdot, t_m)$. On the basis of (4.7) we suggest the following scheme:

$$\frac{1}{\tau} \int_I (X_h^{m+1} - X_h^m) \cdot \varphi_h |X_{h\theta}^m| + \int_I \frac{X_{h\theta}^{m+1} \cdot \varphi_{h\theta}}{|X_{h\theta}^m|} = 0 \quad \text{for all } \varphi_h \in S_h. \quad (4.14)$$

Calculations similar to those above yield a time discrete analogue of (4.9), which we formulate as the following algorithm.

Algorithm 1. (Curve shortening flow)

- (1) Let $X_j^0 = X_0(\theta_j)$ ($j = 0, \dots, N$).
- (2) Compute X_j^{m+1} ($j = 0, \dots, N$) from the tridiagonal systems
$$\frac{1}{2\tau} (q_j^m + q_{j+1}^m) (X_j^{m+1} - X_j^m) - \left(\frac{X_{j+1}^{m+1} - X_j^{m+1}}{q_{j+1}^m} - \frac{X_j^{m+1} - X_{j-1}^{m+1}}{q_j^m} \right) = 0.$$
- (3) If $\min_{j=1, \dots, N+1} q_j^{m+1} > 0$ then replace m by $m + 1$ and GOTO 2.

Thus, in each time-step a positive definite and symmetric linear system has to be solved for each component of X_h^{m+1} . Each of these linear systems is of tridiagonal form with two additional entries reflecting the periodicity condition. The system decouples with respect to the dimension of the space in which the curve moves. For practical purposes a redistribution of nodes according to arc length on the curve is sometimes convenient.

Let us go back to the more precise notation $\hat{X}(\theta, t) = X((\cos \theta, \sin \theta), t)$. For later purposes it is convenient to look at (4.14) from a slightly different angle. We introduce the polygon $\Gamma_h^m = \hat{X}_h^m(I)$ along with the space

$$S_h^m = \{\phi_h : \Gamma_h^m \rightarrow \mathbb{R}^2 \mid \phi_h \text{ is affine on each face of } \Gamma_h^m\}. \quad (4.15)$$

Thus, if $\phi_h \in S_h^m$, then ϕ_h is the restriction of an affine function on \mathbb{R}^2 on each face of the polygon and therefore

$$\varphi_h(\theta) = \phi_h(\hat{X}_h^m(\theta)), \quad \theta \in I,$$

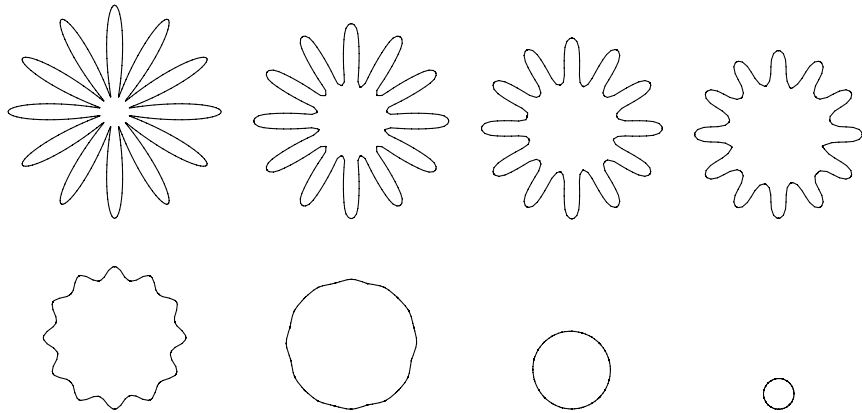


Figure 4.1. Curve shortening flow applied to a star-shaped curve. Time-steps 0, 100, 200, 300, 500, 700, 5000, 7000 (time-step size = 8.5586×10^{-5}), 480 nodes.

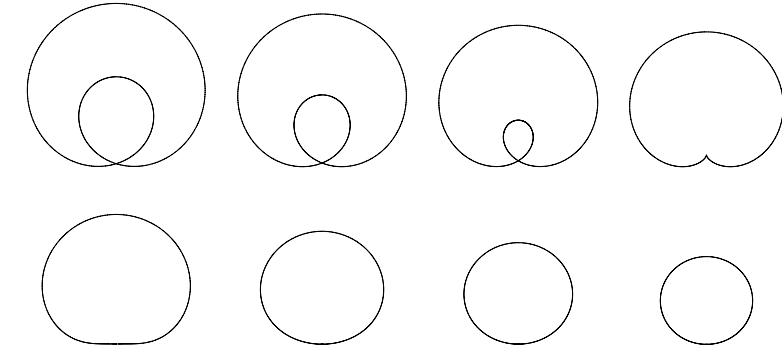


Figure 4.2. Curve shortening flow applied to a curve with a self-intersection. A singularity (cusp) appears. The effect is that the algorithm jumps across the singularity. See Figure 4.3 for a magnified image. Time-steps 0, 1000, 2000, 2500, 3000, 5000, 6000, 7000 (time-step size = 8.5586×10^{-5}), 480 nodes.

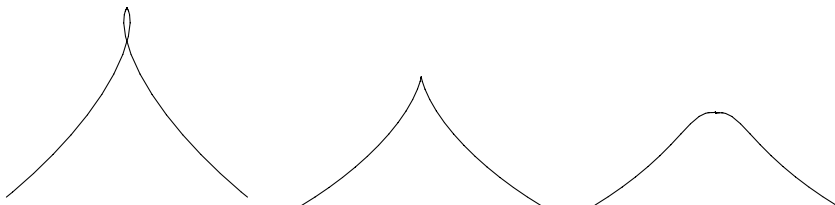


Figure 4.3. Close-up of Figure 4.2. Time-steps 3498 and 3499 and 3505. The parametric theory breaks down.

belongs to \hat{S}_h . Recalling (2.14) we have

$$\nabla_{\Gamma_h^m} \phi_h = \frac{1}{|\hat{X}_{h\theta}^m|} \varphi_{h\theta} \otimes \frac{\hat{X}_{h\theta}^m}{|\hat{X}_{h\theta}^m|}, \quad p = \hat{X}_h^m(\theta),$$

where $(u \otimes v)_{ij} = u_i v_j$ ($u, v \in \mathbb{R}^2$) and $\nabla_{\Gamma_h^m} \phi_h$ is given piecewise on each face of Γ_h^m . Let us define $X_h^{m+1} \in S_h^m$ by $X_h^{m+1}(p) = \hat{X}_h^{m+1}(\theta)$, $p = \hat{X}_h^m(\theta)$. Observing that

$$\nabla_{\Gamma_h^m} X_h^{m+1} \cdot \nabla_{\Gamma_h^m} \phi_h |\hat{X}_{h\theta}^m| = \frac{\hat{X}_{h\theta}^{m+1} \cdot \varphi_{h\theta}}{|\hat{X}_{h\theta}^m|} \quad \text{for all } \varphi_h \in \hat{S}_h$$

we can rewrite (4.14) as

$$\frac{1}{\tau} \int_{\Gamma_h^m} (X_h^{m+1} - \text{id}) \cdot \phi_h \, dA + \int_{\Gamma_h^m} \nabla_{\Gamma_h^m} X_h^{m+1} \cdot \nabla_{\Gamma_h^m} \phi_h \, dA = 0 \quad \text{for all } \phi_h \in S_h^m. \quad (4.16)$$

Note that the dot between the matrices $\nabla_{\Gamma_h^m} X_h^{m+1}$ and $\nabla_{\Gamma_h^m} \phi_h$ is the standard scalar product in \mathbb{R}^4 . The key point about the formulation (4.16) is that Γ_h^{m+1} is now parametrized with the help of the polygon Γ_h^m from the previous time-step, so that the reference manifold M is no longer needed. We can interpret the second integral on the left-hand side of (4.16) as an approximation to

$$\int_{\Gamma(t_{m+1})} \nabla_{\Gamma(t_{m+1})} x \cdot \nabla_{\Gamma(t_{m+1})} \phi \, dA,$$

which equals $-\int_{\Gamma(t_{m+1})} H \nu \cdot \phi \, dA$ by (2.17) and (2.10). Here, H is just the usual curvature of the curve $\Gamma(t_{m+1})$, but of course it is now natural to also use (4.16) for approximating surfaces evolving by mean curvature. We will discuss this issue in the next section.

4.2. Mean curvature flow of surfaces

In this section we shall use a higher-dimensional version of (4.16) in order to approximate parametric surfaces $\Gamma(t) = X(M, t)$, which satisfy (4.1). To begin, we need an analogue of the polygons used in the previous section.

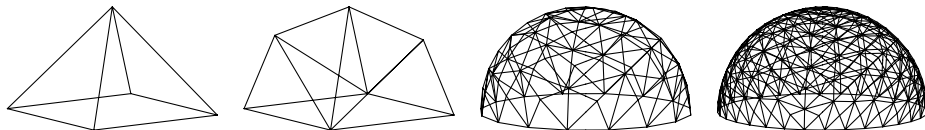


Figure 4.4. Polyhedral surfaces: successively refined grids approximating a half sphere. Macro triangulation (left) and triangulation levels 1, 5 and 7.

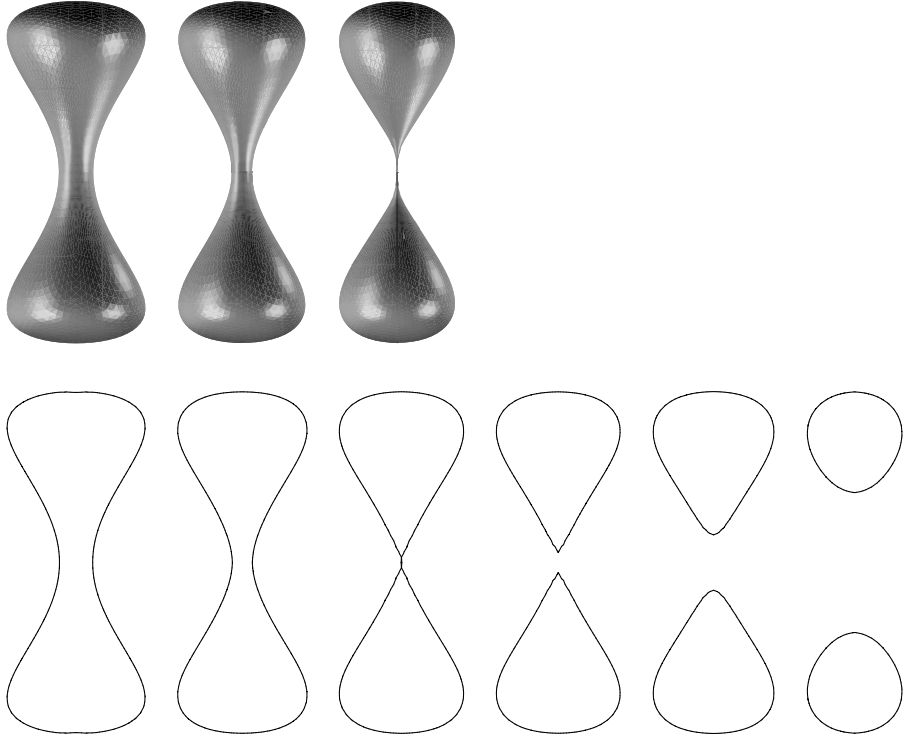


Figure 4.5. First row: Parametric mean curvature flow of a dumbbell-shaped surface. Development of a singularity.
 Second row: Axially symmetric level set computation of the same flow going beyond the topological change of the surface.

Definition 2. We call a set $\Gamma \subset \mathbb{R}^{n+1}$ a *polyhedral surface* if

$$\Gamma = \bigcup_{T \in \mathcal{T}_h} T,$$

where the triangulation \mathcal{T}_h consists of closed, nondegenerate, n -dimensional simplices. The intersection of two adjacent simplices is an $(n - k)$ -dimensional subsimplex of these simplices ($k \in \{1, \dots, n\}$).

Our aim is to construct polyhedral surfaces $\Gamma_h^0, \dots, \Gamma_h^M$ (without boundary) in such a way that Γ_h^m is an approximation to $\Gamma(t_m)$. These surfaces are obtained with the help of the following algorithm. We start the computations with an initial polyhedral Γ_h^0 which approximates the initial surface Γ_0 . In practice there are several ways to construct the initial discrete surface. One way is to map triangulations of charts onto the continuous surface and to glue them together. A much better way is to construct a macro triangulation, that is, a coarse approximation $\tilde{\Gamma}_h^0$ of Γ_0 such that



Figure 4.6. A thin two-dimensional torus shrinks under parametric mean curvature flow to a circle.

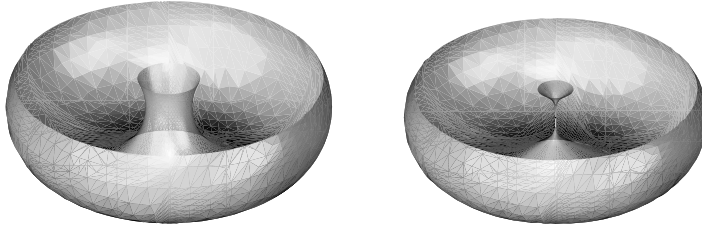


Figure 4.7. A thick two-dimensional torus (cut open) shrinks under parametric mean curvature flow to a sphere developing a singularity.

$\tilde{\Gamma}_h^0 \subset \Gamma_\delta$ (see (2.4), (2.5)) and then to refine this triangulation in \mathbb{R}^{n+1} and project the new nodes x orthogonally onto the smooth surface according to $x' = x - d(x)\nu(x)$ to obtain the new nodes x' of the next-finer triangulation for Γ_h^0 (see Figure 4.4).

Algorithm 2. (Mean curvature flow of surfaces)

Let Γ_h^0 be a polyhedral approximation of Γ_0 .

For $m = 0, 1, \dots, M-1$ define

$$S_h^m = \{\phi_h \in C^0(\Gamma_h^m) \mid \phi_h|_T \text{ is affine for each } T \subset \Gamma_h^m\},$$

and find $X_h^{m+1} \in S_h^m$ with

$$\frac{1}{\tau} \int_{\Gamma_h^m} (X_h^{m+1} - \text{id})\phi_h \, dA + \int_{\Gamma_h^m} \nabla_{\Gamma_h^m} X_h^{m+1} \cdot \nabla_{\Gamma_h^m} \phi_h \, dA = 0 \quad \text{for all } \phi_h \in S_h^m \tag{4.17}$$

Generate the new surface $\Gamma_h^{m+1} = X_h^{m+1}(\Gamma_h^m)$, and if it is a polyhedral surface then GOTO to the next m .

This algorithm is based on a finite element method for partial differential equations on surfaces, developed in Dziuk (1988). Let us have a look at the implementation of the above algorithm. Fix $m \in \{0, \dots, M-1\}$ and denote by $a_1, \dots, a_N \in \mathbb{R}^{n+1}$ the nodes of the polyhedral surface Γ_h^m . The functions $\phi_i : \Gamma_h^m \rightarrow \mathbb{R}$, $i = 1, \dots, N$ are uniquely defined by the requirements

$$\phi_i \in S_h^m, \quad \phi_i(a_j) = \delta_{ij}, \quad i, j = 1, \dots, N.$$

It is not difficult to verify that ϕ_1, \dots, ϕ_N actually form a basis of S_h^m . Now, stiffness and mass matrix are defined by

$$\begin{aligned} S_{ij} &= \int_{\Gamma_h^m} \nabla_{\Gamma_h^m} \phi_i \cdot \nabla_{\Gamma_h^m} \phi_j \, dA, \quad i, j = 1, \dots, N \\ M_{ij} &= \int_{\Gamma_h^m} \phi_i \phi_j \, dA, \quad i, j = 1, \dots, N. \end{aligned}$$

Expanding $(X_h^{m+1})_k(p) = \sum_{j=1}^N \alpha_j^{(k)} \phi_j(p)$ (where $(X_h^{m+1})_k$ is the k th component of X_h^{m+1}), we find that (4.17) is equivalent to the linear systems

$$M\alpha^{(k)} + \tau S\alpha^{(k)} = b^{(k)}, \quad k = 1, \dots, n+1. \quad (4.18)$$

Here, $\alpha^{(k)} = (\alpha_1^{(k)}, \dots, \alpha_N^{(k)})$ and $b^{(k)} \in \mathbb{R}^N$ is given by

$$b_j^{(k)} = \int_{\Gamma_h^m} x_k \phi_j \, dA, \quad j = 1, \dots, N.$$

Since the matrix $M + \tau S$ is symmetric and positive definite, the systems (4.18) can be solved with a conjugate gradient method. The only difference to a ‘Cartesian’ FEM is that the nodes have one more coordinate.

5. Mean curvature flow of graphs

We turn our attention to the mean curvature evolution of surfaces $\Gamma(t)$, which can be written as graphs over some base domain $\Omega \subset \mathbb{R}^n$, that is,

$$\Gamma(t) = \{(x, u(x, t)) \mid x \in \Omega\}.$$

In order to find the differential equation to be satisfied by the height function u , we recall (2.13) and (2.21) to see that the mean curvature H and the velocity V in the direction of $\nu = \frac{(\nabla u, -1)}{\sqrt{1+|\nabla u|^2}}$ are given by

$$H = \nabla \cdot \left(\frac{\nabla u}{\sqrt{1+|\nabla u|^2}} \right), \quad V = -\frac{u_t}{\sqrt{1+|\nabla u|^2}}. \quad (5.1)$$

Thus, the evolution law $V = -H$ on $\Gamma(t)$ translates into the nonlinear parabolic partial differential equation

$$u_t - \sqrt{1 + |\nabla u|^2} \nabla \cdot \left(\frac{\nabla u}{\sqrt{1 + |\nabla u|^2}} \right) = 0 \quad \text{in } \Omega \times (0, T), \quad (5.2)$$

to which we add the following boundary and initial conditions

$$u = g \quad \text{on } \partial\Omega \times (0, T), \quad (5.3)$$

$$u(\cdot, 0) = u_0 \quad \text{in } \Omega, \quad (5.4)$$

where $g : \partial\Omega \rightarrow \mathbb{R}$ and $u_0 : \bar{\Omega} \rightarrow \mathbb{R}$ are given functions. The boundary condition (5.3) implies that the boundaries of the surfaces $\Gamma(t)$ are kept fixed during the evolution. It would also be possible to replace (5.3) by

$$\frac{\partial u}{\partial n} = 0 \quad \text{on } \partial\Omega \times (0, T), \quad (5.5)$$

in which case the surfaces $\Gamma(t)$ would meet the boundary of the cylinder $\Omega \times \mathbb{R}$ at a right angle.

5.1. Analytical results

The main difficulties for the mathematical analysis are due to the fact that the operator

$$A(u) = \sqrt{1 + |\nabla u|^2} \nabla \cdot \left(\frac{\nabla u}{\sqrt{1 + |\nabla u|^2}} \right)$$

is not uniformly parabolic and not in divergence form. Only in one space dimension the equation is in divergence form, since $A(u) = (\arctan u_x)_x$.

Theorem 5.1. Let Ω be a bounded domain in \mathbb{R}^n with $\partial\Omega \in C^{2+\alpha}$ and $u_0 \in C^{2,\alpha}(\bar{\Omega})$.

- (a) Suppose that $g \in C^{2,\alpha}(\bar{\Omega})$ and that the compatibility conditions

$$u_0 = g \quad \text{and} \quad \sqrt{1 + |\nabla u_0|^2} \nabla \cdot \left(\frac{\nabla u_0}{\sqrt{1 + |\nabla u_0|^2}} \right) = 0 \quad \text{on } \partial\Omega$$

are satisfied. If $\partial\Omega$ has nonnegative mean curvature, the initial-boundary value problem (5.2), (5.3), (5.4) has a unique smooth solution which converges to the solution of the minimal surface equation with boundary data g as $t \rightarrow \infty$.

- (b) Suppose that the compatibility condition $\frac{\partial u_0}{\partial n} = 0$ on $\partial\Omega$ holds. Then the initial-boundary value problem (5.2), (5.5), (5.4) has a unique smooth solution which converges to a constant function as $t \rightarrow \infty$.

Proof. See Lieberman (1986) and also Huisken (1989) for (a); (b) is proved in Huisken (1989). \square

The assumption that the boundary of the domain has nonnegative mean curvature is a necessary condition. If it is dropped, the gradient of the solution will become infinite on the boundary: see Oliker and Uraltseva (1993). The main tool in the proof of the previous theorem is the derivation of an evolution equation for the surface element. Our numerical algorithms will be based on a variational formulation of (5.2), (5.3). To derive it, divide (5.2) by

$$Q = \sqrt{1 + |\nabla u|^2}, \quad (5.6)$$

multiply by a test function $\phi \in H_0^1(\Omega)$ and integrate. Integration by parts implies

$$\int_{\Omega} \frac{u_t \phi}{Q} + \int_{\Omega} \frac{\nabla u \cdot \nabla \phi}{Q} = 0, \quad \phi \in H_0^1(\Omega), \quad 0 < t < T. \quad (5.7)$$

It is straightforward to derive from (5.7) the decrease in area.

Lemma 5.2. Suppose that u is a smooth solution of (5.2). Then

$$\int_{\Omega} \frac{u_t^2}{Q} + \frac{d}{dt} \int_{\Omega} Q = 0. \quad (5.8)$$

Proof. Since $u(\cdot, t) = g$ on $\partial\Omega \times (0, T)$ we have $u_t(\cdot, t) = 0$ on $\partial\Omega$ for $0 < t < T$. The relation (5.8) now follows by inserting $\phi = u_t(\cdot, t)$ in (5.7) and observing that $Q_t = \frac{\nabla u \cdot \nabla u_t}{Q}$. \square

Recalling that $V = -\frac{u_t}{Q}$ we may rewrite the relation (5.8) in the more geometric form of Lemma 3.1.

5.2. Spatial discretization

Let \mathcal{T}_h be an admissible nondegenerate triangulation of the domain Ω with mesh size bounded by h , simplices S and $\Omega_h = \bigcup_{S \in \mathcal{T}_h} S$ the corresponding discrete domain. We assume that vertices on $\partial\Omega_h$ are contained in $\partial\Omega$. The space of finite elements of order $s \in \mathbb{N}$ is chosen to be

$$X_h = \{v_h \in C^0(\bar{\Omega}_h) \mid v_h \text{ is a polynomial of order } s \text{ on each } S \in \mathcal{T}_h\}. \quad (5.9)$$

The subspace containing functions with zero boundary values will be denoted by X_{h0} .

We assume that for $s \in \mathbb{N}, p \in [1, \infty]$ there exists an interpolation operator $I_h : H^{s+1,p}(\Omega) \rightarrow X_h$ which satisfies $I_h v \in X_{h0}$ for $v \in H^{s+1,p}(\Omega) \cap H_0^1(\Omega)$, as well as

$$\|v - I_h v\|_{L^p(\Omega \cap \Omega_h)} + h \|\nabla(v - I_h v)\|_{L^p(\Omega \cap \Omega_h)} \leq ch^{s+1} \|v\|_{H^{s+1,p}(\Omega)} \quad (5.10)$$

for all $v \in H^{s+1,p}(\Omega)$. For dimensions $n < p(s+1)$, we can, for instance, choose the usual Lagrange interpolation operator; in higher dimensions a

possible choice is the Clément operator. For what follows we choose piecewise linear finite elements: $s = 1$.

We now use (5.7) in order to define a semidiscrete approximation to the solution of (5.2)–(5.4) as follows: find $u_h(\cdot, t) \in X_h$ with $u_h(\cdot, t) - I_h g \in X_{h0}$ and $u_h(\cdot, 0) = u_{h0} = I_h u_0$ such that

$$\int_{\Omega_h} \frac{u_{ht}\phi_h}{Q_h} + \int_{\Omega_h} \frac{\nabla u_h \cdot \nabla \phi_h}{Q_h} = 0, \quad \text{for all } \phi_h \in X_{h0} \quad (5.11)$$

and all $t \in (0, T)$. Here, we have abbreviated $Q_h = \sqrt{1 + |\nabla u_h|^2}$. The following lemma establishes the global existence of the discrete solution.

Lemma 5.3. The semidiscrete problem has a unique solution u_h which exists globally in time.

Proof. We denote by $a_i, i = 1, \dots, N$ the nodes of the triangulation \mathcal{T}_h and by χ_i the corresponding nodal basis functions. We assume that a_1, \dots, a_{N_1} are the interior nodes, while a_{N_1+1}, \dots, a_N lie on $\partial\Omega_h$. We expand $u_h(\cdot, t) = \sum_{i=1}^{N_1} \alpha_i(t) \chi_i + \sum_{i=N_1+1}^N g(a_i) \chi_i$ and the relation (5.11) then amounts to a nonlinear system of ODEs for $\alpha = (\alpha_1, \dots, \alpha_{N_1})$. Existence of a unique local solution follows from standard ODE theory, while the analogue of (5.8) implies a uniform bound on u_h and therefore on α since X_h is finite-dimensional. This allows us to continue the solution for all times. \square

In order to prove error estimates for the semidiscrete problem we need to make regularity assumptions on the solution of the continuous problem. Let us suppose that u satisfies

$$\int_0^T \|u_t\|_{H^{1,\infty}(\Omega)}^2 dt + \int_0^T \|u_t\|_{H^2(\Omega)}^2 dt \leq N \quad (5.12)$$

for some $N > 0$ (see Deckelnick and Dziuk (1999) for sufficient conditions which imply (5.12)). In the following we shall assume that we have a solution of this kind until the time T . We shall formulate our error estimates in terms of geometric quantities, more specifically in terms of the normals $\nu = \frac{(\nabla u, -1)}{Q}$, $\nu_h = \frac{(\nabla u_h, -1)}{Q_h}$ and the normal velocities $V = -\frac{u_t}{Q}$, $V_h = -\frac{u_{ht}}{Q_h}$ reflecting the form of the *a priori* estimate (5.8).

Theorem 5.4. Let u be a solution of the continuous problem (5.2)–(5.4), which satisfies (5.12). Then

$$\int_0^T \int_{\Omega \cap \Omega_h} (V - V_h)^2 Q_h + \sup_{(0,T)} \int_{\Omega \cap \Omega_h} |\nu - \nu_h|^2 Q_h \leq ch^2.$$

The constant c depends on N .

Proof. Let us give the proof of this theorem for polygonal domains, $\Omega = \Omega_h$. The proof shows how important it is to work with the geometric quantities. The difference of the discrete weak form (5.11) and the corresponding continuous weak form of equation (5.2) reads

$$\int_{\Omega} \left(\frac{u_t}{Q} - \frac{u_{ht}}{Q_h} \right) \phi_h + \int_{\Omega} \left(\frac{\nabla u}{Q} - \frac{\nabla u_{ht}}{Q_h} \right) \cdot \nabla \phi_h = 0 \quad (5.13)$$

for all discrete test functions $\phi_h \in X_{h0}$. As a test function we choose

$$\phi_h = I_h u_t - u_{ht} = (u_t - u_{ht}) - (u_t - I_h u_t).$$

We observe that

$$\begin{aligned} \left(\frac{u_t}{Q} - \frac{u_{ht}}{Q_h} \right) (u_t - u_{ht}) &= (V - V_h)(VQ - V_h Q_h) \\ &= (V - V_h)^2 Q_h + (V - V_h)V(Q - Q_h) \\ &\geq (V - V_h)^2 Q_h - |V - V_h| |V| |Q| \frac{1}{Q} - \frac{1}{Q_h} |Q_h| \\ &\geq \frac{1}{2} (V - V_h)^2 Q_h - \frac{1}{2} |u_t|^2 |\nu - \nu_h|^2 Q_h. \end{aligned} \quad (5.14)$$

Here we have used the fact that

$$\left| \frac{1}{Q} - \frac{1}{Q_h} \right| \leq |\nu - \nu_h|. \quad (5.15)$$

For the gradient term in (5.13) we exploit the fact that the last component of the vector $\nu Q - \nu_h Q_h$ is zero, and get

$$\begin{aligned} \left(\frac{\nabla u}{Q} - \frac{\nabla u_{ht}}{Q_h} \right) \cdot (\nabla u_t - \nabla u_{ht}) &= (\nu - \nu_h) \cdot (\nabla u_t - \nabla u_{ht}, 0) \\ &= (\nu - \nu_h) \cdot (\nu Q - \nu_h Q_h)_t. \end{aligned} \quad (5.16)$$

With the elementary relation

$$(\nu - \nu_h) \cdot \nu = -(\nu - \nu_h) \cdot \nu_h = \frac{1}{2} |\nu - \nu_h|^2,$$

the right-hand side in (5.16) can be estimated as follows:

$$\begin{aligned} &(\nu - \nu_h) \cdot (\nu Q - \nu_h Q_h)_t \\ &= (\nu - \nu_h) \cdot (\nu_t Q - \nu_{ht} Q_h + \nu Q_t - \nu_h Q_{ht}) \\ &= \frac{1}{2} |\nu - \nu_h|^2 (Q_t + Q_{ht}) + (\nu - \nu_h) \cdot (\nu - \nu_h)_t Q_h + (\nu - \nu_h) \cdot \nu_t (Q - Q_h) \\ &= \frac{1}{2} (|\nu - \nu_h|^2 Q_h)_t + \frac{1}{2} |\nu - \nu_h|^2 Q_t + (\nu - \nu_h) \cdot \nu_t (Q - Q_h) \\ &\geq \frac{1}{2} (|\nu - \nu_h|^2 Q_h)_t - \frac{1}{2} |Q_t| |\nu - \nu_h|^2 - |\nu_t| Q |\nu - \nu_h|^2 Q_h, \end{aligned}$$

where again we have used (5.15). With this estimate, (5.14) and (5.16) the error relation (5.13) implies the bound

$$\begin{aligned} & \frac{1}{2} \int_{\Omega} (V - V_h)^2 Q_h + \frac{1}{2} \frac{d}{dt} \int_{\Omega} |\nu - \nu_h|^2 Q_h \\ & \leq \frac{1}{2} (\|u_t\|_{L^\infty(\Omega)}^2 + 3 \|\nabla u_t\|_{L^\infty(\Omega)}^2) \int_{\Omega} |\nu - \nu_h|^2 Q_h \\ & \quad + \int_{\Omega} |V - V_h| |u_t - I_h u_t| + \int_{\Omega} |\nu - \nu_h| |\nabla(u_t - I_h u_t)|. \end{aligned}$$

We estimate the interpolation terms with the help of (5.10), that is,

$$\begin{aligned} & \int_{\Omega} |V - V_h| |u_t - I_h u_t| + \int_{\Omega} |\nu - \nu_h| |\nabla(u_t - I_h u_t)| \\ & \leq c \|u_t\|_{H^2(\Omega)} \left(h^2 \left(\int_{\Omega} (V - V_h)^2 \right)^{\frac{1}{2}} + h \left(\int_{\Omega} |\nu - \nu_h|^2 \right)^{\frac{1}{2}} \right) \\ & \leq \delta \int_{\Omega} (V - V_h)^2 Q_h + \delta \int_{\Omega} |\nu - \nu_h|^2 Q_h + \frac{c}{\delta} \|u_t\|_{H^2(\Omega)}^2 h^2 \end{aligned}$$

for every $\delta > 0$, since $Q_h \geq 1$. After a suitable choice of δ we arrive at

$$\begin{aligned} & \frac{1}{2} \int_{\Omega} (V - V_h)^2 Q_h + \frac{d}{dt} \int_{\Omega} |\nu - \nu_h|^2 Q_h \\ & \leq c (1 + \|u_t\|_{H^{1,\infty}(\Omega)}^2) \int_{\Omega} |\nu - \nu_h|^2 Q_h + c \|u_t\|_{H^2(\Omega)}^2 h^2. \end{aligned}$$

A Gronwall argument and the choice $u_h(\cdot, 0) = I_h u_0$ then finally proves the theorem. \square

Remark 1. It is possible to show that in the two-dimensional case the above error bounds imply that $\sup_{\bar{\Omega} \times [0,T]} Q_h \leq C$ uniformly in h . As a consequence the error estimate can be written down with the help of the usual norms, namely

$$\int_0^T \|u_t - u_{h,t}\|_{L^2(\Omega \cap \Omega_h)}^2 dt + \sup_{(0,T)} \|\nabla(u - u_h)\|_{L^2(\Omega \cap \Omega_h)}^2 \leq ch^2.$$

5.3. Time discretization

Let us choose a time-step $\tau > 0$ and let $t_m = m\tau, m = 0, \dots, M, M \leq [\frac{T}{\tau}]$ as well as $v^m = v(\cdot, m\tau)$ for $m = 0, \dots, M$. Based on (5.11) we suggest the following algorithm.

Algorithm 3. (Mean curvature flow of graphs) Let $u_h^0 = I_h u_0$. For $m = 0, \dots, M - 1$, compute $u_h^{m+1} \in X_h$ such that $u_h^{m+1} - I_h g \in X_{h0}$ and,

for every $\varphi_h \in X_{h0}$,

$$\frac{1}{\tau} \int_{\Omega_h} \frac{u_h^{m+1} \varphi_h}{Q_h^m} + \int_{\Omega_h} \frac{\nabla u_h^{m+1} \cdot \nabla \varphi_h}{Q_h^m} = \frac{1}{\tau} \int_{\Omega_h} \frac{u_h^m \varphi_h}{Q_h^m}. \quad (5.17)$$

with $Q_h^m = \sqrt{1 + |\nabla u_h^m|^2}$.

The above scheme is semi-implicit in time and has the property that in each time-step a linear Laplace-type equation with stiffness matrix weighted by Q_h^m has to be solved. In order to analyse its stability we go back to the basic energy norms introduced in (5.8).

Theorem 5.5. The solution $u_h^m, 0 \leq m \leq M$ of (5.17) satisfies, for every $m \in \{1, \dots, M\}$,

$$\tau \sum_{k=0}^{m-1} \int_{\Omega_h} |V_h^k|^2 Q_h^k + \int_{\Omega_h} Q_h^m \leq \int_{\Omega_h} Q_h^0 \quad (5.18)$$

where $V_h^k = -\frac{(u_h^{k+1} - u_h^k)}{\tau Q_h^k}$ is the discrete normal velocity.

Proof. We choose $\varphi_h = u_h^{k+1} - u_h^k$ as a test function in (5.17) for $m = k$ and get

$$\frac{1}{\tau} \int_{\Omega_h} \frac{(u_h^{k+1} - u_h^k)^2}{Q_h^k} + \int_{\Omega_h} \frac{\nabla u_h^{k+1} \cdot \nabla (u_h^{k+1} - u_h^k)}{Q_h^k} = 0. \quad (5.19)$$

Let us use the notation $\nu_h^k = \frac{(\nabla u_h^k, -1)}{Q_h^k}$. The integrand in the second term can be rewritten as

$$\begin{aligned} \frac{\nabla u_h^{k+1} \cdot \nabla (u_h^{k+1} - u_h^k)}{Q_h^k} &= \frac{(Q_h^{k+1})^2 - 1}{Q_h^k} - \frac{\nabla u_h^{k+1}}{Q_h^{k+1}} \cdot \frac{\nabla u_h^k}{Q_h^k} Q_h^{k+1} \\ &= \frac{(Q_h^{k+1})^2}{Q_h^k} + \frac{1}{2} |\nu_h^{k+1} - \nu_h^k|^2 Q_h^{k+1} - Q_h^{k+1} \\ &= \frac{1}{2} |\nu_h^{k+1} - \nu_h^k|^2 Q_h^{k+1} + Q_h^{k+1} - Q_h^k + \frac{(Q_h^{k+1} - Q_h^k)^2}{Q_h^k}. \end{aligned}$$

We insert this result into (5.19), sum over $k = 0, \dots, m-1$ and obtain the equation

$$\begin{aligned} \tau \sum_{k=0}^{m-1} \int_{\Omega_h} |V_h^k|^2 Q_h^k + \sum_{k=0}^{m-1} \int_{\Omega_h} \frac{(Q_h^{k+1} - Q_h^k)^2}{Q_h^k} + \frac{1}{2} \sum_{k=0}^{m-1} \int_{\Omega_h} |\nu_h^{k+1} - \nu_h^k|^2 Q_h^{k+1} \\ + \int_{\Omega_h} Q_h^m = \int_{\Omega_h} Q_h^0 \end{aligned}$$

which implies the stability estimate (5.18). \square

Let us emphasize that our scheme is unconditionally stable even though the nonlinear expressions are treated explicitly. Other schemes, such as fully explicit and fully implicit variants are discussed in Dziuk (1999a). It is natural to follow the ideas of the semidiscrete case in order to analyse the above algorithm. For the analysis of the fully discrete scheme we need the following regularity assumptions:

$$\begin{aligned} \sup_{t \in (0, T)} (\|u(\cdot, t)\|_{H^{2,\infty}(\Omega)} + \|u_t(\cdot, t)\|_{H^{1,\infty}(\Omega)}) \\ + \int_0^T (\|u_t\|_{H^2(\Omega)}^2 + \|u_{tt}\|^2) \, ds \leq N. \end{aligned} \quad (5.20)$$

This leads to the following result.

Theorem 5.6. Assume that there exists a solution of (5.2)–(5.4) on $[0, T]$, which satisfies (5.20) and let u_h^m , ($m = 1, \dots, M = [\frac{T}{\tau}]$) be the solution of Algorithm 3. Then there exists a $\tau_0 > 0$ such that, for all $0 < \tau \leq \tau_0$,

$$\tau \sum_{m=0}^{M-1} \int_{\Omega \cap \Omega_h} (V^m - V_h^m)^2 Q_h^m \leq c(\tau^2 + h^2), \quad (5.21)$$

$$\sup_{m=0, \dots, M} \int_{\Omega \cap \Omega_h} |\nu^m - \nu_h^m|^2 Q_h^m \leq c(\tau^2 + h^2). \quad (5.22)$$

Proof. This is a special case of the results obtained in Deckelnick and Dziuk (2002a). \square

For computational tests we refer to the anisotropic case; see Table 8.2. Here we give some test results for the usual norms. Error estimates in these norms for the two-dimensional case are contained in Deckelnick and Dziuk (2000). For the tests we have solved the partial differential equation

Table 5.1. Absolute errors in $L^\infty((0, T); L^2(\Omega))$, $L^\infty((0, T); H^1(\Omega))$ and experimental orders of convergence (EOC) for the test problem.

h	E_1	EOC	E_2	EOC
2.0	1.1932	–	0.9428	–
1.0	0.6649	0.84	0.9453	0.00
0.7368	0.2878	2.74	0.5873	1.56
0.4203	0.1067	1.77	0.2919	1.25
0.2219	0.04211	1.46	0.1375	1.18
0.1137	0.01775	1.29	0.06536	1.11
0.05754	0.007986	1.17	0.03168	1.06

(5.2) with a given additional right-hand side. We have chosen $u(x, t) = \sin(|x|^2 - t) - \sin(1 - t)$ and calculated a right-hand side from this function. The computational domain was $\Omega = \{x \in \mathbb{R}^2 \mid |x| < 1\}$ and we used the boundary condition $u = 0$ on $\partial\Omega$. The time interval was $[0, 4]$ and as time-step size we have chosen $\tau = 0.125h$. For two successive grids with grid sizes h_1 and h_2 we computed the absolute errors $E(h_j)$, ($j = 1, 2$) between discrete solution and exact solution for certain norms. The experimental order of convergence was then defined by $\text{EOC} = \log(E(h_1)/E(h_2))/\log(h_1/h_2)$. In Table 5.1 the errors in the norms $E_1 = \sup_{0 \leq m \leq M} \|u^m - u_h^m\|$ with $M\tau = T$ and $E_2 = \sup_{0 \leq m \leq M} \|\nabla(u^m - u_h^m)\|$ are shown. The results confirm the theoretical estimates. Note that the $L^\infty((0, T), L^2(\Omega))$ -error behaves linearly in the grid size h because we have chosen the time-step proportional to the spatial grid size.

6. Mean curvature flow of level sets

If we want to compute topological changes of free boundaries then it is necessary to leave the parametric world, because this fixes the topological type of the interface. One method to do this is to define the interface as the level set of a scalar function:

$$\Gamma(t) = \{x \in \mathbb{R}^{n+1} \mid u(x, t) = 0\}.$$

Let us assume for the moment that $u \in C^{2,1}(\mathbb{R}^{n+1} \times (0, T))$ with $\nabla u \neq 0$ in a neighbourhood of $\bigcup_{t \in (0, T)} \Gamma(t) \times \{t\}$. Recalling (2.11) and (2.20), the relation $V = -H$ on $\Gamma(t)$ would hold if

$$u_t - \sum_{i,j=1}^{n+1} \left(\delta_{ij} - \frac{u_{xi} u_{xj}}{|\nabla u|^2} \right) u_{x_i x_j} = 0 \quad (6.1)$$

in a neighbourhood of $\bigcup_{t \in (0, T)} \Gamma(t) \times \{t\}$. This partial differential equation is highly nonlinear, degenerate parabolic and not defined where the gradient of u vanishes. Therefore, standard methods for parabolic equations fail, but it is possible to develop an existence and uniqueness theory for (6.1) within the framework of viscosity solutions. The corresponding notion involves a pointwise relation and the analysis relies mainly on the maximum principle. It is therefore not straightforward to use finite element methods, which are typically L^2 -methods and normally do not allow a maximum principle. This difficulty will be reflected in the numerical analysis. An example of the evolution of level sets under mean curvature flow is shown in Figure 6.1 (Deckelnick and Dziuk 2001).

Crandall, Ishii and Lions (1992) give a concise introduction to the theory of viscosity solutions, while Giga (2002) describes in detail the application of level set techniques to a large class of geometric evolution equations.

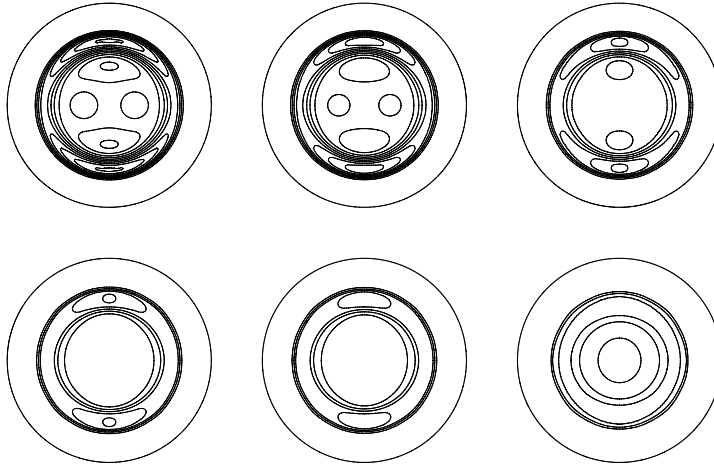


Figure 6.1. Evolution of level lines under mean curvature flow.

Detailed descriptions of computational techniques for level set methods along with a host of applications can be found in the monographs by Sethian (1999) and Osher and Fedkiw (2003).

6.1. Analytical results

Starting from (6.1), we are interested in the following problem:

$$u_t - \sum_{i,j=1}^{n+1} \left(\delta_{ij} - \frac{u_{x_i} u_{x_j}}{|\nabla u|^2} \right) u_{x_i x_j} = 0 \quad \text{in } \mathbb{R}^{n+1} \times (0, \infty) \quad (6.2)$$

$$u(\cdot, 0) = u_0 \quad \text{in } \mathbb{R}^{n+1}. \quad (6.3)$$

An existence and uniqueness theory for (6.2), (6.3) can be carried out within the framework of viscosity solutions.

Definition 3. A function $u \in C^0(\mathbb{R}^{n+1} \times [0, \infty))$ is called a *viscosity subsolution* of (6.2) provided that for each $\phi \in C^\infty(\mathbb{R}^{n+2})$, if $u - \phi$ has a local maximum at $(x_0, t_0) \in \mathbb{R}^{n+1} \times (0, \infty)$, then

$$\begin{aligned} \phi_t - \sum_{i,j=1}^{n+1} \left(\delta_{ij} - \frac{\phi_{x_i} \phi_{x_j}}{|\nabla \phi|^2} \right) \phi_{x_i x_j} &\leq 0 && \text{at } (x_0, t_0), \text{ if } \nabla \phi(x_0, t_0) \neq 0, \\ \phi_t - \sum_{i,j=1}^{n+1} (\delta_{ij} - p_i p_j) \phi_{x_i x_j} &\leq 0 && \text{at } (x_0, t_0) \text{ for some } |p| \leq 1, \\ &&& \text{if } \nabla \phi(x_0, t_0) = 0. \end{aligned} \quad (6.4)$$

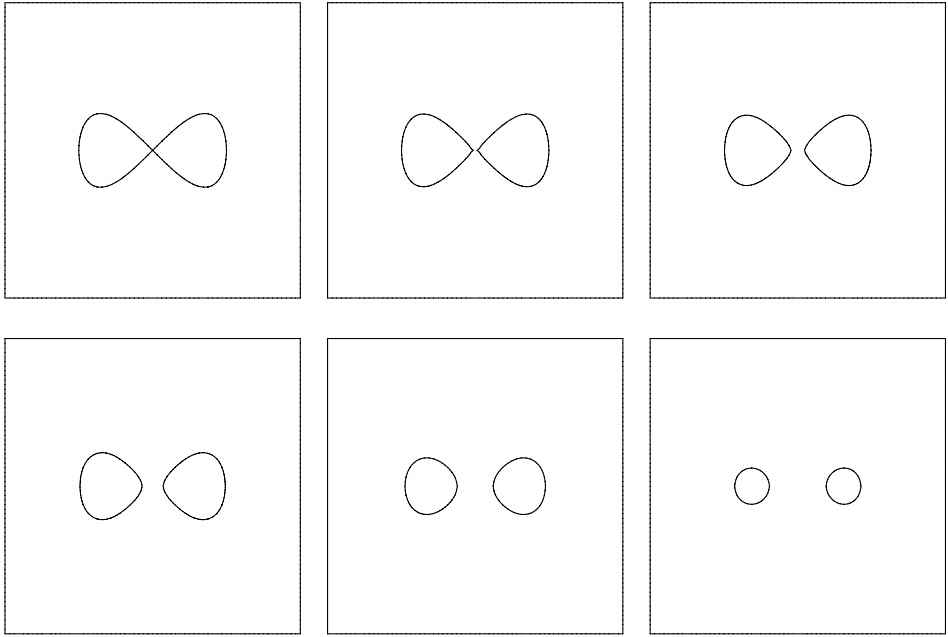


Figure 6.2. Evolution of a lemniscate under level set mean curvature flow: the zero level.

A viscosity supersolution is defined analogously: maximum is replaced by minimum and \leq by \geq . A viscosity solution of (6.2) is a function $u \in C^0(\mathbb{R}^{n+1} \times [0, \infty))$ that is both a subsolution and a supersolution.

We shall assume that the initial function u_0 is smooth and satisfies

$$u_0(x) = 1 \quad \text{for } |x| \geq S \tag{6.5}$$

for some $S > 0$. The following existence and uniqueness theorem is a special case of results proved independently by Evans and Spruck (1991) and Chen, Giga and Goto (1991).

Theorem 6.1. Assume $u_0 : \mathbb{R}^{n+1} \rightarrow \mathbb{R}$ satisfies (6.5). Then there exists a unique viscosity solution of (6.2), (6.3), such that

$$u(x, t) = 1 \quad \text{for } |x| + t \geq R$$

for some $R > 0$ depending only on S .

The level set approach can now be described as follows: given a compact hypersurface Γ_0 , choose a continuous function $u_0 : \mathbb{R}^{n+1} \rightarrow \mathbb{R}$ such that $\Gamma_0 = \{x \in \mathbb{R}^{n+1} \mid u_0(x) = 0\}$. If $u : \mathbb{R}^{n+1} \times [0, \infty) \rightarrow \mathbb{R}$ is the unique viscosity solution of (6.2), (6.3), we then call

$$\Gamma(t) = \{x \in \mathbb{R}^{n+1} \mid u(x, t) = 0\}, \quad t \geq 0$$

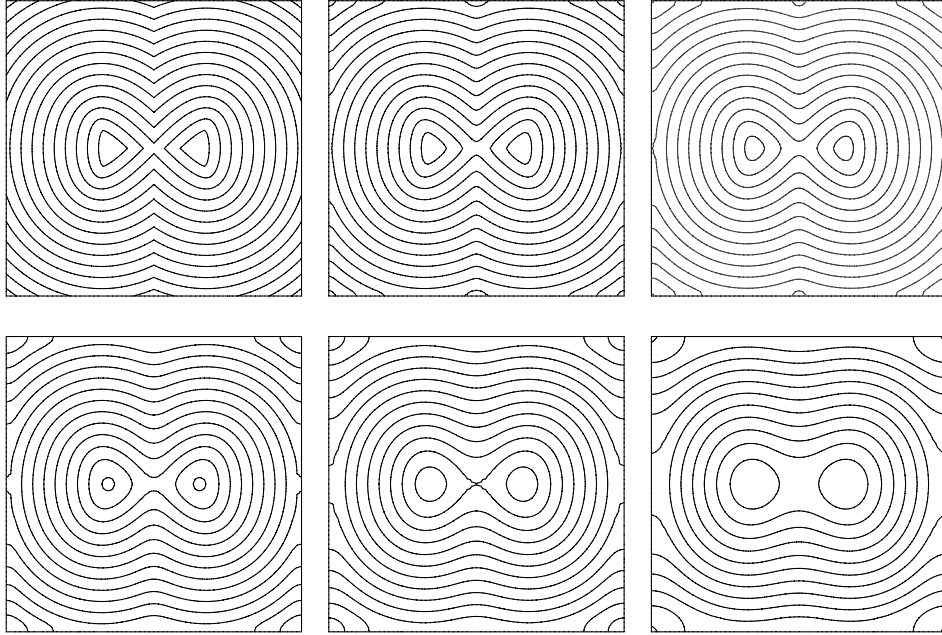


Figure 6.3. Evolution of the oriented distance function of a lemniscate: level lines.

a generalized solution of the mean curvature flow problem. We remark that Evans and Spruck (1991) and Chen, Giga and Goto (1991) also established that the sets $\Gamma(t) = \{x \in \mathbb{R}^{n+1} \mid u(x, t) = 0\}, t > 0$ are independent of the particular choice of u_0 which has Γ_0 as its zero level set, so that the generalized evolution $(\Gamma(t))_{t \geq 0}$ is well defined for a given Γ_0 . As $\Gamma(t)$ exists for all times, it provides a notion of solution beyond singularities in the flow. For this reason, the level set approach has also become very important in the numerical approximation of mean curvature flow and related problems. Note however that it is possible that the set $\Gamma(t)$ may develop an interior for $t > 0$, even if Γ_0 had none, a phenomenon which is referred to as *fattening*. The level set solution has been investigated further in several papers: in particular we mention Evans and Spruck (1992a, 1992b, 1995) and Soner (1993).

6.2. Regularization

Evans and Spruck (1991) proved that the (smooth) solutions u^ϵ of

$$u_t^\epsilon - \sum_{i,j=1}^{n+1} \left(\delta_{ij} - \frac{u_{x_i}^\epsilon u_{x_j}^\epsilon}{\epsilon^2 + |\nabla u^\epsilon|^2} \right) u_{x_i x_j}^\epsilon = 0 \quad \text{in } \mathbb{R}^{n+1} \times (0, \infty), \quad (6.6)$$

$$u^\epsilon(\cdot, 0) = u_0 \quad \text{in } \mathbb{R}^{n+1} \quad (6.7)$$

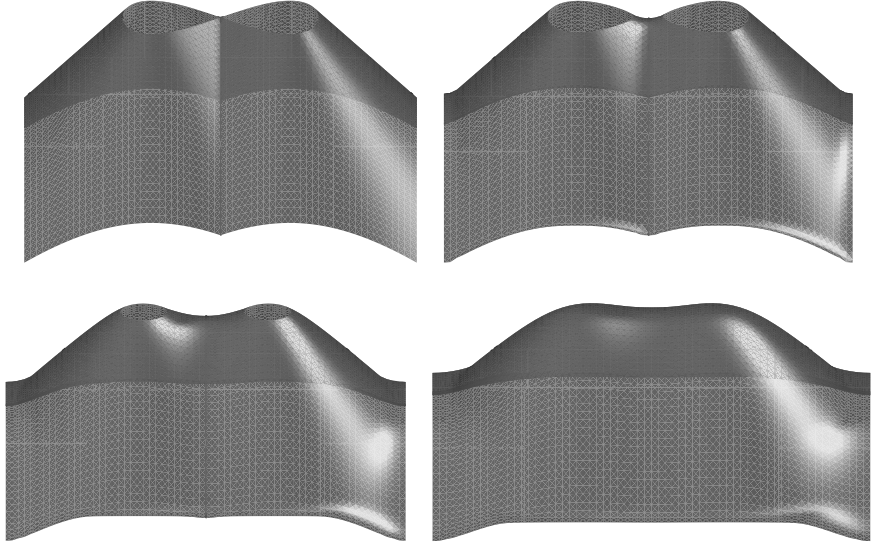


Figure 6.4. Evolution of the oriented distance function of a lemniscate: graph.

converge locally uniformly as $\epsilon \rightarrow 0$ to the unique viscosity solution of (6.2), (6.3). For numerical purposes it is important to know the asymptotic error between the viscosity solution and the solution of the regularized problem quantitatively as $\epsilon \rightarrow 0$. In Deckelnick (2000) there is a proof of the following theorem together with several *a priori* estimates and their dependence on the regularization parameter ϵ .

Theorem 6.2. For every $\alpha \in (0, \frac{1}{2})$, $0 < T < \infty$ there is a constant $C = C(u_0, T, \alpha)$ such that

$$\sup_{0 \leq t \leq T} \|u - u^\epsilon\|_{L^\infty(\mathbb{R}^{n+1})} \leq C\epsilon^\alpha \quad \text{for all } \epsilon > 0.$$

If one wants to calculate approximations to the viscosity solution u of (6.2), (6.3) then, according to Theorem 6.2, it is sufficient to solve the regularized problem (6.6), (6.7), which we have to study for computational purposes, on a bounded domain. For simplicity we choose $\Omega = B_{\tilde{S}}(0)$ with $\tilde{S} > R = R(S)$, where R is the radius from Theorem 6.1, and consider

$$u_{\epsilon t} - \sum_{i,j=1}^{n+1} \left(\delta_{ij} - \frac{u_{\epsilon x_i} u_{\epsilon x_j}}{\epsilon^2 + |\nabla u_\epsilon|^2} \right) u_{\epsilon x_i x_j} = 0 \quad \text{in } \Omega \times (0, \infty), \quad (6.8)$$

$$u_\epsilon = 1 \quad \text{on } \partial\Omega \times (0, \infty), \quad (6.9)$$

$$u_\epsilon(\cdot, 0) = u_0 \quad \text{in } \Omega. \quad (6.10)$$

An application of the parabolic comparison theorem yields the following corollary of Theorem 6.2.

Corollary 6.3. For every $\alpha \in (0, \frac{1}{2})$, $0 < T < \infty$ there is a constant $C = C(u_0, T, \alpha)$ such that

$$\|u - u_\epsilon\|_{L^\infty(\Omega \times (0, T))} \leq C\epsilon^\alpha. \quad (6.11)$$

We are now in position to look at the regularized level set mean curvature flow problem as a problem for graphs. If we scale

$$U = \frac{u_\epsilon}{\epsilon} \quad (6.12)$$

then U is a solution of the mean curvature flow problem for graphs (see (5.2)), that is,

$$U_t - \sqrt{1 + |\nabla U|^2} \nabla \cdot \frac{\nabla U}{\sqrt{1 + |\nabla U|^2}} = 0 \quad \text{in } \Omega \times (0, T). \quad (6.13)$$

This is a theoretical observation and implies that we can apply techniques developed for the mean curvature flow of graphs to the mean curvature flow of level sets. But for computations we shall not use (6.13) but the unscaled version for u_ϵ .

6.3. The approximation of viscosity solutions

Numerical schemes based on the level set approach were first introduced in Osher and Sethian (1988); see also Sethian (1990). Chen, Giga, Hitaka and Honma (1994) proposed a finite difference scheme for which they proved stability with respect to the L^∞ -norm. Walkington (1996) used a finite element approach on the dual mesh to construct a discretization that is stable both with respect to L^∞ and to $W^{1,1}$. Evans (1993) analysed a scheme based on the solution of the usual heat equation, continually re-initialized after short time-steps, and which was proposed in Merriman, Bence and Osher (1994). Crandall and Lions (1996) constructed a finite difference scheme that is both monotone and consistent, and obtained the first convergence result for an approximation of (6.2), (6.3). An error analysis for this scheme can be found in Deckelnick (2000).

Here we want to consider a different finite element scheme which exploits the above-described formal similarity to the graph case. This will also allow us to carry out some basic numerical analysis. In the following we use the abbreviations

$$\nu_\epsilon(v) = \frac{(\nabla v, -\epsilon)}{Q_\epsilon(v)}, \quad Q_\epsilon(v) = \sqrt{\epsilon^2 + |\nabla v|^2}, \quad V_\epsilon(v) = -\frac{v_t}{Q_\epsilon(v)}.$$

Our results for the mean curvature flow of a graph can directly be transformed into a convergence result for the regularized level set problem.

Theorem 6.4. Let u_ϵ be the solution of (6.8), (6.10) and let $u_{\epsilon h}$ be the solution of the semidiscrete problem $u_{\epsilon h}(\cdot, t) \in X_h$ with $u_{\epsilon h}(\cdot, t) - 1 \in X_{h0}$, $u_{\epsilon h}(\cdot, 0) = u_{h0} = I_h u_0$ and

$$\int_{\Omega_h} \frac{u_{\epsilon h t} \phi_h}{Q_\epsilon(u_{\epsilon h})} + \int_{\Omega_h} \frac{\nabla u_{\epsilon h} \cdot \nabla \phi_h}{Q_\epsilon(u_{\epsilon h})} = 0 \quad (6.14)$$

for all $t \in (0, T)$ and all discrete test functions $\phi_h \in X_{h0}$. Then

$$\begin{aligned} \int_0^T \int_{\Omega \cap \Omega_h} (V_\epsilon(u_\epsilon) - V_\epsilon(u_{\epsilon h}))^2 Q_\epsilon(u_{\epsilon h}) &\leq c_\epsilon h^2, \\ \sup_{(0, T)} \int_{\Omega \cap \Omega_h} |\nu_\epsilon(u_\epsilon) - \nu_\epsilon(u_{\epsilon h})|^2 Q_\epsilon(u_{\epsilon h}) &\leq c_\epsilon h^2. \end{aligned}$$

We omit the proof as it is based on the scaling argument (6.12). Unfortunately, the constants c_ϵ contain a term that depends exponentially on $\frac{1}{\epsilon}$, which is due to an application of Gronwall's lemma. Numerical tests, however, suggest that the resulting bound overestimates the error.

In two space dimensions we can prove that the computed solutions $u_{\epsilon h}$ converge in L^∞ to the viscosity solution. The proof is contained in Deckelnick and Dziuk (2001).

Theorem 6.5. Let u be the viscosity solution of (6.2), (6.3) and let $u_{\epsilon h}$ be the solution of the problem (6.14) with $\Omega \subset \mathbb{R}^2$ as in Corollary 6.3. Then there exists a function $h = h(\epsilon) \rightarrow 0$ as $\epsilon \rightarrow 0$ such that

$$\lim_{\epsilon \rightarrow 0} \|u - u_{\epsilon h(\epsilon)}\|_{L^\infty(\Omega \times (0, T))} = 0.$$

Finally, the fully discrete numerical scheme for (regularized) isotropic mean curvature flow of level sets is now a straightforward adaption of Algorithm 3.

Algorithm 4. (Mean curvature flow of level sets) Let $u_{\epsilon h}^0 = I_h u_0$. For $m = 0, \dots, M-1$, compute $u_{\epsilon h}^{m+1} \in X_h$ such that $u_{\epsilon h}^{m+1} - 1 \in X_{h0}$ and, for every $\phi_h \in X_{h0}$,

$$\frac{1}{\tau} \int_{\Omega_h} \frac{u_{\epsilon h}^{m+1} \phi_h}{Q_\epsilon(u_{\epsilon h}^m)} + \int_{\Omega_h} \frac{\nabla u_{\epsilon h}^{m+1} \cdot \nabla \phi_h}{Q_\epsilon(u_{\epsilon h}^m)} = \frac{1}{\tau} \int_{\Omega_h} \frac{u_{\epsilon h}^m \phi_h}{Q_\epsilon(u_{\epsilon h}^m)}. \quad (6.15)$$

For this scheme we have the following convergence result.

Theorem 6.6. Let u_ϵ be the solution of (6.8)–(6.10) and let $u_{\epsilon h}^m$, ($m = 1, \dots, M$) be the solution from Algorithm 4. Then there exists a $\tau_0 > 0$

such that, for all $0 < \tau \leq \tau_0$,

$$\tau \sum_{m=0}^{M-1} \int_{\Omega \cap \Omega_h} (V_\epsilon(u_\epsilon^m) - V_{\epsilon h}^m)^2 Q_\epsilon(u_{\epsilon h}^m) \leq c_\epsilon(\tau^2 + h^2), \quad (6.16)$$

$$\sup_{m=0,\dots,M} \int_{\Omega \cap \Omega_h} |\nu_\epsilon(u_\epsilon^m) - \nu_\epsilon(u_{\epsilon h}^m)|^2 Q_\epsilon(u_{\epsilon h}^m) \leq c_\epsilon(\tau^2 + h^2), \quad (6.17)$$

with $M = [\frac{T}{\tau}]$. Here $V_{\epsilon h}^m = -(u_{\epsilon h}^{m+1} - u_{\epsilon h}^m)/(\tau Q_\epsilon(u_{\epsilon h}^m))$ is the regularized discrete normal velocity.

This result implies the convergence of the fully discrete regularized solution to the viscosity solution.

Theorem 6.7. Let u be the viscosity solution from Theorem 6.1 and let Ω be the domain from Corollary 6.3 in \mathbb{R}^2 . Let $u_{\epsilon h \tau}$ denote the time-interpolated solution of the fully discrete scheme (6.15). Then there exist functions $h = h(\epsilon) \rightarrow 0$ and $\tau = \tau(\epsilon) \rightarrow 0$ as $\epsilon \rightarrow 0$ such that

$$\lim_{\epsilon \rightarrow 0} \|u - u_{\epsilon h(\epsilon)\tau(\epsilon)}\|_{L^\infty(\Omega_h \times (0, T))} = 0.$$

7. Phase field approach to mean curvature flow

7.1. Introduction

The phase field approach to interface evolution is based on physical models for problems involving phase transitions. In this section Ω is a bounded domain in \mathbb{R}^{n+1} and $\Gamma(t)$ is a hypersurface moving through Ω . In the case of two phases one has the notion of an order parameter or phase field function $\varphi : \Omega \times (0, T) \rightarrow \mathbb{R}$ which indicates the phase of a material by associating with the phases the minima of a C^2 double well bulk energy function $W(\cdot) : \mathbb{R} \rightarrow \mathbb{R}$. For simplicity we suppose that $W(r) = W(-r)$ and the minima of $W(\cdot)$ are at ± 1 . The canonical example is

$$W(r) = \frac{1}{4}(r^2 - 1)^2. \quad (7.1)$$

Consider the gradient energy functional

$$E(\varphi) = \int_{\Omega} \left(\frac{\epsilon}{2} |\nabla \varphi|^2 + \frac{W(\varphi)}{\epsilon} \right) dx, \quad (7.2)$$

where ϵ is a small parameter. Steepest descent or gradient flow for this functional leads to the parabolic Allen–Cahn equation (Allen and Cahn 1979)

$$\epsilon \varphi_t - \epsilon \Delta \varphi + \frac{1}{\epsilon} W'(\varphi) = 0 \quad \text{in } \Omega \times (0, T) \quad (7.3)$$

with Neumann boundary conditions. In order to understand the behaviour of this evolution equation for an initial function $\varphi_0 : \Omega \rightarrow \mathbb{R}$, observe that the flow of the ordinary differential equation $\varphi_t = -\frac{W'(\varphi)}{\epsilon^2}$ drives positive values of φ_0 to 1 and negative values to -1 . On the other hand the Laplacian term in the equation (7.3) has a smoothing effect which will diffuse large gradients of the solution. Thus, on the basis of these heuristics, after a short time the solution of (7.3) will develop a structure consisting of bulk regions in which φ is smooth and takes the values ± 1 , and separating these regions there will be interfacial transition layers across which φ changes rapidly from one bulk value to the other. These transition layers are due to the interaction between the regularizing effect of the gradient energy term and the flow associated with the bi-stable potential term W' . It turns out that the motion of these interfacial transition layers approximates mean curvature flow.

We can argue informally to support this in the following way. Let, for $t \in (0, T)$, $\Gamma(t)$ be a smoothly evolving closed and compact hypersurface satisfying $V = -H$. Suppose that $\Gamma(t)$ is the boundary of an open set $\Omega(t) \subset \Omega$ and denote by $d(\cdot, t)$ the signed distance function to $\Gamma(t)$. We consider the semilinear parabolic operator

$$P(v) = \epsilon v_t - \epsilon \Delta v + \frac{1}{\epsilon} W'(v).$$

A calculation yields for $v(x, t) = \psi\left(\frac{d(x,t)}{\epsilon}\right)$, where $\psi : \mathbb{R} \rightarrow \mathbb{R}$, that

$$P(v) = (d_t - \Delta d)\psi'\left(\frac{d}{\epsilon}\right) - \frac{1}{\epsilon}\left(\psi''\left(\frac{d}{\epsilon}\right) - W'\left(\psi\left(\frac{d}{\epsilon}\right)\right)\right).$$

Hence it is natural to define $\psi = \psi(z)$ to be the unique solution of

$$-\psi''(z) + W'(\psi(z)) = 0, \quad z \in \mathbb{R}, \quad (7.4)$$

$$\psi(z) \rightarrow \pm 1, \quad z \rightarrow \pm\infty, \quad \psi(0) = 0, \quad \psi'(z) > 0. \quad (7.5)$$

If W is given by (7.1) we have that $\psi(z) = \tanh(\frac{z}{\sqrt{2}})$ and therefore

$$P(v) = (d_t - \Delta d)\psi'\left(\frac{d}{\epsilon}\right).$$

Recalling (2.12) and (2.20) we obtain $d_t - \Delta d = -V - H = 0$ on $\Gamma(t)$, so that the smoothness of d implies

$$|d_t - \Delta d| \leq C|d|$$

in a neighbourhood U of $\bigcup_{0 < t < T} \Gamma(t) \times \{t\}$. Hence

$$|P(v)| \leq C\epsilon \left| \frac{d}{\epsilon} \psi'\left(\frac{d}{\epsilon}\right) \right| \leq C\epsilon \quad \text{in } U$$

and it follows that $v = \psi\left(\frac{d}{\epsilon}\right)$ is close to being a solution of (7.3) with initial

data $\varphi_0 = \psi\left(\frac{d(\cdot, 0)}{\epsilon}\right)$. That (7.3) is gradient flow for (7.2) is easily shown by testing the equation with φ_t and integrating by parts, leading to

$$\epsilon \int_{\Omega} |\varphi_t|^2 dx + \frac{dE(\varphi)}{dt} = 0,$$

which is the analogue of the energy equation in Lemma 3.1.

A more general isotropic phase field equation is

$$\epsilon \varphi_t = \epsilon \Delta \varphi - \frac{1}{\epsilon} W'(\varphi) + c_W g, \quad (7.6)$$

where g is a forcing term. The constant c_W is a scaling constant dependent on the precise definition of the double well potential W and is given by the formula

$$c_W = \frac{1}{\sqrt{2}} \int_{-1}^1 \sqrt{W(r)} dr. \quad (7.7)$$

The equation of motion that this phase field model approximates is

$$V = -H - g. \quad (7.8)$$

We refer to Rubinstein, Sternberg and Keller (1989) and de Mottoni and Schatzman (1995) for formal and rigorous interface asymptotics relating the Allen–Cahn equation to mean curvature flow. Error bounds for the Hausdorff distance between the zero level set of the phase field function and the interface have been derived (Chen 1992, Bellettini and Paolini 1996). In particular, a convergence rate of $\mathcal{O}(\epsilon^2 |\log \epsilon|^2)$ was established by Bellettini and Paolini (1996). These bounds are proved using comparison theorems for the phase field equation and this can be extended to prove convergence to the viscosity solution of the level set equation in the case of nonsmooth evolution and without the interface thickening (fattening) (Evans, Soner and Souganidis 1992).

7.2. The double obstacle phase field model

We consider the phase field model

$$\epsilon \varphi_t - \epsilon \Delta \varphi + \frac{1}{\epsilon} W'(\varphi) = c_W g. \quad (7.9)$$

The potential W is taken to be of double obstacle form

$$W(r) = \frac{1}{2}(1 - r^2) + I_{[-1,1]}(r), \quad (7.10)$$

where

$$I_{[-1,1]}(r) = \begin{cases} +\infty & \text{for } |r| > 1, \\ 0 & \text{for } |r| \leq 1, \end{cases} \quad (7.11)$$

introduced in the gradient phase field models by Bellettini, Paolini and Verdi

(1990), Blowey and Elliott (1991, 1993b), Chen and Elliott (1994), Paolini and Verdi (1992).

Properly we should interpret $W'(r)$ in the following way:

$$W'(r) = \begin{cases} (-\infty, 1] & \text{if } r = -1, \\ -r & \text{if } |r| < 1, \\ [-1, \infty) & \text{if } r = 1. \end{cases}$$

For this potential, a calculation reveals that the profile of the phase variable in the transition layer given by the solution of (7.4), (7.5) is

$$\psi(r) = \begin{cases} -1 & \text{if } r \leq -\frac{\pi}{2}, \\ \sin(r) & \text{if } |r| < \frac{\pi}{2}, \\ 1 & \text{if } r \geq \frac{\pi}{2}. \end{cases}$$

Furthermore, $c_W = \frac{\pi}{4}$. The double obstacle problem can be written in an equivalent variational inequality formulation. Let \mathcal{K} be the convex set

$$\mathcal{K} = \{\eta \in H^1(\Omega) : |\eta| \leq 1\}.$$

Then the problem is to seek $\varphi \in L^\infty(0, T; \mathcal{K}) \cap H^1(0, T; L^2(\Omega))$ such that $\varphi(\cdot, 0) = \varphi_0$ and

$$\varepsilon \int_{\Omega} \varphi_t(\eta - \varphi) + \varepsilon \int_{\Omega} \nabla \varphi \cdot \nabla(\eta - \varphi) - \frac{1}{\varepsilon} \int_{\Omega} \varphi(\eta - \varphi) \geq \frac{\pi}{4} \int_{\Omega} g(\eta - \varphi) \quad (7.12)$$

for all $\eta \in \mathcal{K}$ and for almost every $t \in (0, T)$. It is well known that this problem has a unique solution.

Theorem 7.1. Suppose that the smooth hypersurfaces $\Gamma(t) \subset \mathbb{R}^{n+1}$ satisfy:

- (i) $\Gamma(t) = \partial\Omega(t)$ for open sets $\Omega(t) \subset \mathbb{R}^{n+1}$;
- (ii) there exists $\delta > 0$ such that $\text{dist}(\Gamma(t), \partial\Omega) \geq \delta$ for $t \in [0, T]$;
- (iii) $|d_t - \Delta d| \leq D_0|d|$ for $|d| \leq \delta, t \in [0, T]$, where $d(\cdot, t)$ is the signed distance function to $\Gamma(t)$;
- (iv) $V = -H$ on $\Gamma(t)$ for $t \in [0, T]$.

Let ε be sufficiently small such that $\frac{1}{2}\pi\varepsilon \leq \delta(1 + 2e^{2D_0T})^{-1}$ and let $\varphi = \varphi_\varepsilon$ be the unique solution of (7.12) with $g = 0$ and initial data $\varphi_0 = \psi\left(\frac{d(\cdot, 0)}{\varepsilon}\right)$. Then, for all $t \in [0, T]$,

$$\begin{aligned} d(x, t) &\geq \frac{1}{2}\pi\varepsilon(1 + 2e^{2D_0t}) \Rightarrow \varphi_\varepsilon(x, t) = 1, \\ d(x, t) &\leq -\frac{1}{2}\pi\varepsilon(1 + 2e^{2D_0t}) \Rightarrow \varphi_\varepsilon(x, t) = -1. \end{aligned}$$

Proof. See Chen and Elliott (1994). □

A consequence of this theorem is that the diffuse interfacial region

$$\{(x, t) : |\varphi_\varepsilon(x, t)| < 1\}$$

is sharply defined with finite width bounded by $c(t)\pi\varepsilon$ and that both the zero level set of $\varphi_\varepsilon(\cdot, t)$ and $\Gamma(t)$ are in a narrow strip of width $c(t)\pi\varepsilon$. Here $c(t) = \frac{1}{2}(1 + e^{2D_0 t})$; but in practice it is observed that this is pessimistic and the growth of the interface width is not usually an issue. A more refined analysis by Nochetto, Paolini and Verdi (1994) revealed in the case of a smooth evolution of the forced mean curvature flow that the Hausdorff distance between the zero level set of φ_ε and the interface of the flow (7.8) is of order $\mathcal{O}(\varepsilon^2)$. Furthermore, there is convergence to the unique viscosity solution of the level set formulation (Nochetto and Verdi 1996a).

7.3. Discretization of the Allen–Cahn equation

We use the same notation for the discrete spaces as in Section 5.2. We will identify any function $\Phi \in X_h$ with the vector $\{\Phi_j\}_{j=1}^N$ of its nodal values, so that $\Phi = \sum_{j=1}^N \Phi_j \chi_j$. By (\cdot, \cdot) we denote the $L^2(\Omega)$ inner product.

For computational convenience we use a discrete inner product $(\cdot, \cdot)_h$ on $C^0(\overline{\Omega})$ defined by

$$(\chi, \eta)_h = \int_{\Omega} I_h(\chi\eta) \, dx \quad \text{for all } \chi, \eta \in C^0(\overline{\Omega}), \quad (7.13)$$

where I_h is the usual Lagrange interpolation operator for X_h . Furthermore, let $\tau = T/M > 0$ be the uniform time-step and $t_m = m\tau$. For any $\{\Phi^m\}_{m=0}^M$, we set $\partial\Phi^m = \tau^{-1}(\Phi^{m+1} - \Phi^m)$. The fully discrete approximation using explicit ($\theta = 0$) and implicit ($\theta = 1$) time-stepping reads as follows.

Algorithm 5. (Allen–Cahn equation) Let $\Phi^0 = I_h\varphi_0$. For $m = 0, \dots, M-1$, find $\Phi^{m+1} \in X_h$, $1 \leq m \leq M-1$, such that, for all $\chi \in X_h$,

$$(\partial\Phi^m, \chi)_h + (\nabla\Phi^{m+\theta}, \nabla\chi) - \frac{1}{\varepsilon^2}(W'(\Phi^{m+\theta}), \chi)_h = \frac{c_W}{\epsilon}(g, \chi)_h. \quad (7.14)$$

For initial data we choose the finite element interpolant of the transition layer profile

$$\Phi^0 = I_h\psi\left(\frac{d_0(x)}{\epsilon}\right),$$

where d_0 is the signed distance function to the initial interface.

The explicit scheme requires the usual time-step constraint for parabolic equations,

$$\tau \leq Ch^2, \quad (7.15)$$

where the constant C depends on the mesh and the L^∞ norm of the initial data through the magnitude of $|W''|$. On the other hand the implicit scheme

requires a time-step constraint in order for the nonlinear equations defining Φ^{m+1} to have a unique solution. This constraint is

$$\tau \leq \alpha\epsilon^2, \quad (7.16)$$

where α is the minimum value of W'' . See Elliott and Stuart (1993) and Chen, Elliott, Gardiner and Zhao (1998).

The analysis of convergence to mean curvature flow requires consideration of the three approximation parameters ϵ, h, τ tending to zero. Standard *a priori* finite element error analysis for fixed ϵ would lead to, for the difference between the finite element solution and the solution of the Allen–Cahn equation, optimal order error bounds in terms of the mesh sizes τ, h but with constants depending on the Gronwall-induced factor $\exp(\frac{T}{\epsilon^2})$. Feng and Prohl (2003) have improved the finite element error analysis of the Allen–Cahn equation using the special structure of the solution. Indeed, they exploit spectral estimates of Chen (1994) which lead to error bounds whose constants show just polynomial growth in $\frac{1}{\epsilon}$. They specifically consider the implicit scheme without numerical integration. As a consequence they derive an error bound of order ϵ^2 between the zero level set of the solution of the Allen–Cahn equation and the limiting surface.

7.4. Discretization of the double obstacle phase field model

We use the finite element setting of Section 7.3. Let $\mathcal{K}^h = \{\chi \in X_h : |\chi| \leq 1\}$. The double obstacle version of Algorithm 5 is as follows.

Algorithm 6. (Double obstacle phase field) Let $\Phi^0 = I_h\varphi_0$. For $m = 0, \dots, M - 1$, find $\Phi^{m+1} \in \mathcal{K}^h$ such that, for all $\chi \in \mathcal{K}^h$,

$$\begin{aligned} & (\partial\Phi^m, \chi - \Phi^{m+1})_h + (\nabla\Phi^{m+\theta}, \nabla\chi - \Phi^{m+1}) \\ & - \frac{1}{\epsilon^2}(\Phi^{m+\theta} + \epsilon c_W g^{m+\theta}, \chi - \Phi^{m+1})_h \geq 0. \end{aligned} \quad (7.17)$$

For initial data we choose the finite element interpolant of the transition layer profile. The explicit scheme is a discrete obstacle variational inequality associated with the mass matrix. Without mass lumping the solution of this nonlinear algebraic problem would require quadratic programming or linear complementarity methods. However, with the mass lumping quadrature rule the explicit scheme is as simple as the explicit scheme for a semilinear parabolic equation. It can be simply written as

$$\Phi^{m+1/2} = \left(\left(1 + \frac{\tau}{\epsilon^2} \right) I - \tau A \right) \Phi^m + c_W \frac{\tau}{\epsilon} g^m, \quad (7.18)$$

$$\Phi^{m+1} = \mathcal{P}\Phi^{m+1/2}. \quad (7.19)$$

Here $A = M^{-1}K$, where M and K are defined by

$$M_{ij} = (\chi_i, \chi_j)_h, \quad K_{ij} = (\nabla\chi_i, \nabla\chi_j),$$

for $1 \leq i, j \leq N$. Furthermore, $\mathcal{P} : \mathbb{R}^N \rightarrow \mathbb{R}^N$ is the component-wise projection onto $[-1, 1]^N$ defined by

$$(\mathcal{P}V)_j = \max(-1, \min(1, V_j)).$$

On the other hand, in linear algebraic form the implicit scheme leads to the discrete variational inequality: find $\Phi^{m+1} \in \mathbb{R}^N$ such that $|\Phi_j| \leq 1$ and

$$\left(\left(1 - \frac{\tau}{\epsilon^2} \right) I + \tau A \right) \Phi^{m+1} \cdot (\chi - \Phi^{m+1}) \geq \left(\Phi^m + c_W \frac{\tau}{\epsilon} g^{m+1} \right) \cdot (\chi - \Phi^{m+1}) \quad (7.20)$$

for all $\chi \in \mathbb{R}^N$ with $|\chi_j| \leq 1$. Because A is symmetric this is equivalent to minimizing a quadratic function subject to bound constraints and can easily be solved by projected SOR (Elliott and Ockendon 1982). Such a system can also be solved by nonlinear multigrid (Kornhuber and Krause 2003).

As for the continuous parabolic variational inequality, a discrete comparison principle holds for these schemes if the triangulation is acute. This provides the basis for a convergence analysis (Nochetto and Verdi 1996b, 1997). For the implicit scheme without numerical integration an $O(\epsilon)$ error bound for the interface is obtained when $\tau = O(h^2) = O(\epsilon^4)$. For the explicit scheme without numerical integration in the potential term an $O(\epsilon^2)$ is proved for $\tau = O(h^2) = O(\epsilon^5)$.

7.5. Implementation

One expects there to be a relationship between ϵ and h in order that the discrete phase field model can approximate the sharp interface motion. Since the convergence analysis in the continuous case relies heavily on understanding the profile of the phase field function across the transition layer, one would expect that for any ϵ the mesh size h should be sufficiently small in order to resolve the interface. Indeed the existing convergence analysis described above indicates that h should tend to zero faster than ϵ . In practice this implies that across the discrete interfacial layer in the normal direction there should be a sufficient number of elements.

In the case of the double obstacle potential, at the m th time-step, the finite elements may be divided into three sets:

$$\begin{aligned} \mathcal{J}_-^h(m) &= \{\Phi_j = -1 \text{ for each element vertex}\}, \\ \mathcal{J}_+^h(m) &= \{\Phi_j = 1 \text{ for each element vertex}\}, \\ \mathcal{I}^h(m) &= \mathcal{T}^h \setminus (\mathcal{J}_-^h(m) \cup \mathcal{J}_+^h(m)). \end{aligned}$$

Clearly the approximation to the interface is the zero level set of Φ^m which lies inside the discrete interfacial region $\mathcal{I}^h(m)$. We view $\mathcal{I}^h(m)$ as a *sharp diffuse interface*, as opposed to the interfacial region associated with the smooth double well, which is not sharply defined. The computational work in evolving the interface is then associated with the small number of

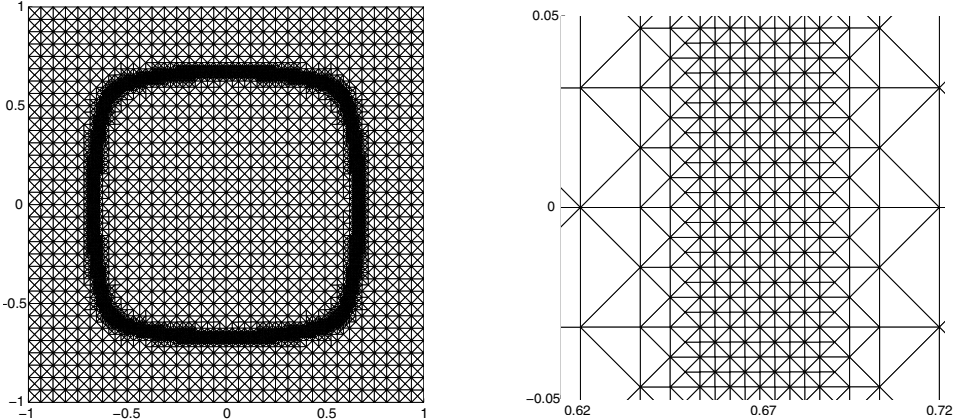


Figure 7.1. Meshes.

elements in this region. As observed above, the time-step, τ , in the phase field calculations is substantially smaller than the mesh size, h . Thus, in a numerical simulation one would expect that, for finite normal velocity of the interface, the sharp diffuse interface should only move by at most the addition or subtraction of a single layer of elements. In the case of the explicit scheme this can be made precise. For nodes in $\mathcal{J}_+^h(m)$ (or $\mathcal{J}_-^h(m)$) whose nearest neighbours are also in $\mathcal{J}_+^h(m)$ (or $\mathcal{J}_-^h(m)$), we find

$$\Phi_j^{m+1/2} = \pm 1 + \frac{\tau}{\epsilon^2}(\pm 1 + c_W \epsilon g^m(a_j))$$

which, provided $|g^m(a_j)| \leq \frac{1}{c_W \epsilon}$, implies that $\Phi_j^{m+1} = \pm 1$. It follows that the *sharp diffuse interface* can not move more than one element per time-step. It also implies that it is only necessary to compute Φ^{m+1} on the closure of the transition layer. This can be exploited in a number of ways.

The two-dimensional *dynamic mesh algorithm* (Nochetto, Paolini and Verdi 1996) is based on the explicit scheme and carries a mesh only in the sharp diffuse interface; it adds and removes triangles where necessary.

The *mask* method (Elliott and Gardiner 1996) keeps an underlying fixed mesh and computes in the sharp diffuse interface only. It is possible to store nodal values only in this region.

An amalgam of the above is an adaptive procedure which uses a fine mesh within the diffuse interface and a coarse mesh outside. In Figure 7.1 a typical mesh is shown for a phase field calculation of anisotropic mean curvature flow. The global mesh is shown together with a zoom. This approach requires a fine mesh slightly larger than the diffuse interface. As the interface region moves the mesh is refined and coarsened appropriately.

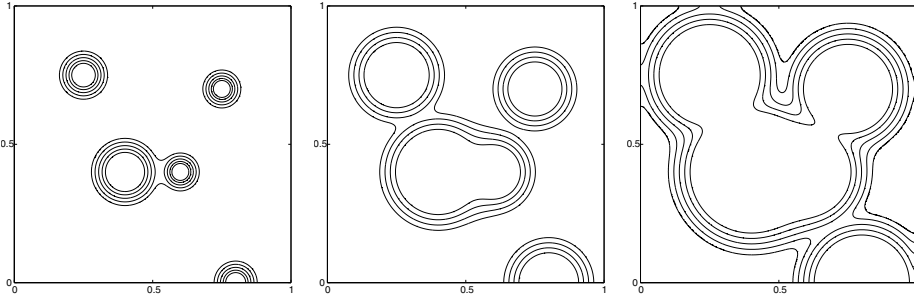


Figure 7.2. Topological change.

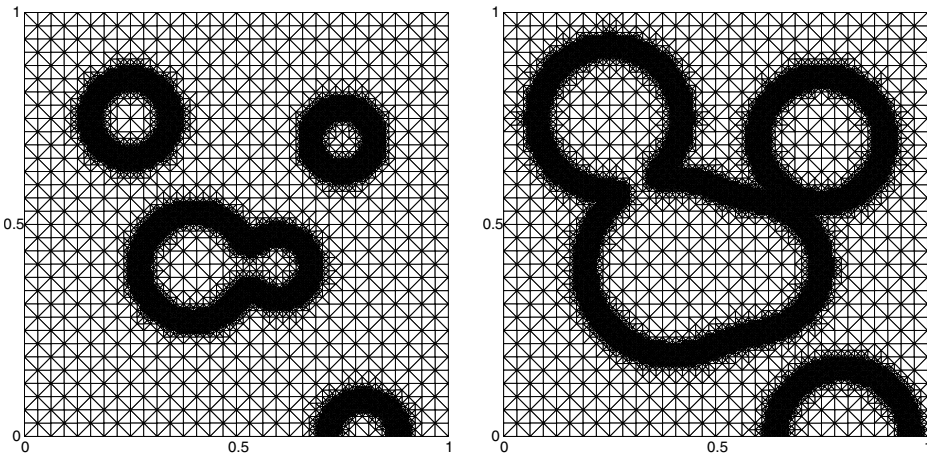


Figure 7.3. Diffuse interfaces with topological change.

Sharp diffuse interface front tracking

Using the double obstacle phase field method and only computing within a sharp diffuse interface as described above can be viewed as a front tracking method, which has the advantage of being able to handle topological change. In Figure 7.2 the interfaces at various times are displayed for a forced mean curvature flow starting from initial circles. Eventually the circles intersect. Meshes associated with these computations are shown in Figure 7.3.

8. Anisotropic mean curvature flow

8.1. The concept of anisotropy

In free boundary problems such as phase transition problems it is often necessary to treat interfaces which are driven by anisotropic curvature. This is induced by modelling an anisotropic surface energy, which generalizes area in the isotropic case to weighted area in the anisotropic case. Anisotropic

surface energy has the form

$$E_\gamma(\Gamma) = \int_{\Gamma} \gamma(\nu) dA, \quad (8.1)$$

where Γ is a surface with normal ν and γ is a given anisotropy function. For $\gamma(p) = |p|$ this energy is the area of Γ . For our purposes it will be necessary to restrict the admissible anisotropies to a certain class.

Definition 4. An anisotropy function $\gamma : \mathbb{R}^{n+1} \rightarrow \mathbb{R}$ is called *admissible* if

$$(1) \quad \gamma \in C^3(\mathbb{R}^{n+1} \setminus \{0\}), \quad \gamma(p) > 0 \text{ for } p \in \mathbb{R}^{n+1} \setminus \{0\};$$

(2) γ is positively homogeneous of degree one, *i.e.*,

$$\gamma(\lambda p) = |\lambda| \gamma(p) \quad \text{for all } \lambda \neq 0, p \neq 0; \quad (8.2)$$

(3) there exists $\gamma_0 > 0$ such that

$$D^2\gamma(p)q \cdot q \geq \gamma_0 |q|^2 \quad \text{for all } p, q \in \mathbb{R}^{n+1}, \quad |p| = 1, \quad p \cdot q = 0. \quad (8.3)$$

It is not difficult to verify that (8.2) implies

$$D\gamma(p) \cdot p = \gamma(p), \quad D^2\gamma(p)p \cdot q = 0, \quad (8.4)$$

$$D\gamma(\lambda p) = \frac{\lambda}{|\lambda|} D\gamma(p), \quad D^2\gamma(\lambda p) = \frac{1}{|\lambda|} D^2\gamma(p) \quad (8.5)$$

for all $p \in \mathbb{R}^{n+1} \setminus \{0\}$, $q \in \mathbb{R}^{n+1}$ and $\lambda \neq 0$. The convexity assumption (8.3) will be crucial for analysis and numerical methods.

Anisotropy is normally visualized by using the Frank diagram \mathcal{F} and the Wulff shape \mathcal{W} :

$$\begin{aligned} \mathcal{F} &= \{p \in \mathbb{R}^{n+1} \mid \gamma(p) \leq 1\}, \\ \mathcal{W} &= \{q \in \mathbb{R}^{n+1} \mid \gamma^*(q) \leq 1\}. \end{aligned}$$

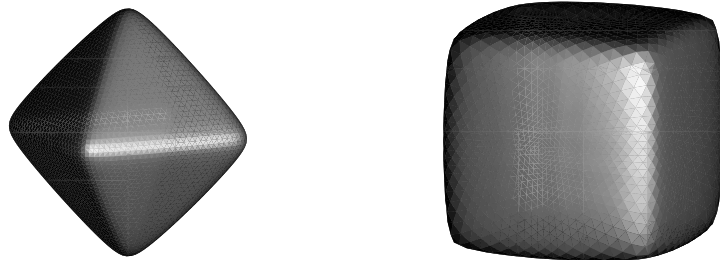


Figure 8.1. Frank diagram (left) and Wulff shape (right) for the regularized l^1 -anisotropy $\gamma(p) = \sum_{j=1}^3 \sqrt{\varepsilon^2 |p_j|^2 + p_j^2}$.

Here γ^* is the dual of γ , which is given by

$$\gamma^*(q) = \sup_{p \in \mathbb{R}^{n+1} \setminus \{0\}} \frac{p \cdot q}{\gamma(p)}. \quad (8.6)$$

Let us consider some examples. Note that not all of them are admissible.

The choice $\gamma(p) = |p|$ is called the isotropic case; in particular we have that $\mathcal{F} = \mathcal{W} = \{p \in \mathbb{R}^{n+1} \mid |p| \leq 1\}$ is the closed unit ball.

A typical choice for anisotropy is the discrete l^r -norm for $1 \leq r \leq \infty$,

$$\gamma(p) = \|p\|_{l^r} = \left(\sum_{k=1}^{n+1} |p_k|^r \right)^{\frac{1}{r}}, \quad 1 \leq r < \infty, \quad (8.7)$$

with the obvious modification for $r = \infty$.

For a given positive definite $(n+1) \times (n+1)$ matrix G , the anisotropy function

$$\gamma(p) = \sqrt{Gp \cdot p} \quad (8.8)$$

models an anisotropy which is defined by a (constant) Riemannian metric. In Figure 8.2 we show the Frank diagram and Wulff shape for the anisotropy

$$\gamma(p) = \sqrt{(5.5 + 4.5 \operatorname{sign}(p_1))p_1^2 + p_2^2 + p_3^2}. \quad (8.9)$$

One anisotropy function often used in a physical context is

$$\gamma(p) = \left(1 - A \left(1 - \frac{\|p\|_{l^4}^4}{\|p\|_{l^2}^4} \right) \right) \|p\|_{l^2} \quad (8.10)$$

where A is a parameter. For $A < 0.25$ the Frank diagram is convex.

For more information on this subject, including anisotropies that may depend on space, see Bellettini and Paolini (1996).

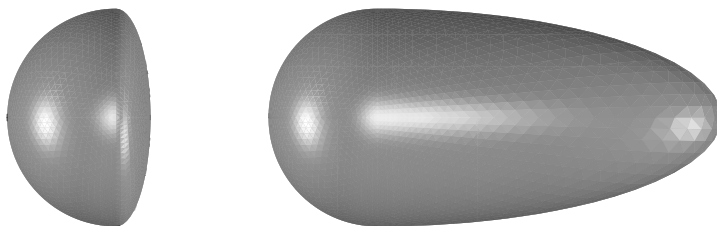


Figure 8.2. Frank diagram \mathcal{F} (left) and Wulff shape \mathcal{W} (right) for the anisotropy (8.9).

8.2. Anisotropic distance function

Let γ be an admissible anisotropy function. We can associate with γ a nonsymmetric metric Υ on \mathbb{R}^{n+1} by setting

$$\Upsilon(x, y) = \gamma^*(x - y), \quad x, y \in \mathbb{R}^{n+1}. \quad (8.11)$$

It is possible to prove that Υ is equivalent to the standard Euclidean metric. Suppose next that $\Omega \subset \mathbb{R}^{n+1}$ is a bounded open set with smooth boundary Γ . Using Υ we now define an anisotropic signed distance function $d_\gamma : \mathbb{R}^{n+1} \rightarrow \mathbb{R}$ by

$$d_\gamma(x) = \begin{cases} \inf_{y \in \Gamma} \Upsilon(x, y), & x \in \mathbb{R}^{n+1} \setminus \bar{\Omega}, \\ 0, & x \in \Gamma, \\ -\inf_{y \in \Gamma} \Upsilon(x, y), & x \in \Omega. \end{cases}$$

Lemma 8.1. There exists an open neighbourhood U of Γ such that $d_\gamma \in C^2(U)$ and

$$\gamma(\nabla d_\gamma) = 1, \quad (8.12)$$

$$D^2 d_\gamma D\gamma(\nabla d_\gamma) = 0. \quad (8.13)$$

8.3. Anisotropic mean curvature

Our goal is to generalize the notion of mean curvature to the anisotropic setting. Suppose that γ is an admissible anisotropy function and that $\Gamma \subset \mathbb{R}^{n+1}$ is an oriented hypersurface with normal ν . We define the Cahn–Hoffmann vector ν_γ on Γ by

$$\nu_\gamma(x) = D\gamma(\nu(x)), \quad x \in \Gamma, \quad (8.14)$$

and the anisotropic mean curvature by

$$H_\gamma(x) = \nabla_\Gamma \cdot \nu_\gamma(x), \quad x \in \Gamma. \quad (8.15)$$

Note that $H_\gamma = H$ in the isotropic case $\gamma(p) = |p|$. The following lemma shows that H_γ is a natural generalization of mean curvature as the first variation of the area functional with respect to normal variations.

Lemma 8.2. Suppose that Γ is compact. For $\phi \in C_0^\infty(U)$ (U a neighbourhood of Γ) define $F_\epsilon(x) = x + \epsilon\phi(x)\nu(x)$, $x \in U$ as well as $\Gamma_\epsilon = F_\epsilon(\Gamma)$. Then,

$$\frac{d}{d\epsilon} E_\gamma(\Gamma_\epsilon)|_{\epsilon=0} = \int_\Gamma H_\gamma \phi \, dA.$$

Proof. Let $d(\cdot, \epsilon) : \mathbb{R}^{n+1} \rightarrow \mathbb{R}$ denote the signed distance function to Γ_ϵ . Consider $g : U \times (-\epsilon_0, \epsilon_0) \rightarrow \mathbb{R}$, defined by

$$g(x, \epsilon) = \gamma(\nu_\epsilon(x)) = \gamma(\nabla d(x, \epsilon)),$$

where ∇ acts on the x variables only. Now (2.23), (2.20) and (2.6) imply

$$\begin{aligned} \frac{d}{d\epsilon} E_\gamma(\Gamma_\epsilon)|_{\epsilon=0} &= \frac{d}{d\epsilon} \int_{\Gamma_\epsilon} g(\cdot, \epsilon) dA|_{\epsilon=0} \\ &= \int_{\Gamma} \frac{\partial g}{\partial \epsilon}(\cdot, 0) dA - \int_{\Gamma} g(\cdot, 0) \frac{\partial d}{\partial \epsilon}(\cdot, 0) H dA - \int_{\Gamma} \frac{\partial g}{\partial \nu}(\cdot, 0) \frac{\partial d}{\partial \epsilon}(\cdot, 0) dA. \end{aligned}$$

It is not difficult to see that $\frac{\partial d}{\partial \epsilon}(\cdot, 0) = -\phi(x)$, $x \in \Gamma$, which also implies that

$$\frac{\partial g}{\partial \epsilon}(\cdot, 0) = D\gamma(\nu) \cdot \nabla \frac{\partial d}{\partial \epsilon}(\cdot, 0) = D\gamma(\nu) \cdot \nabla_\Gamma \frac{\partial d}{\partial \epsilon}(\cdot, 0) = -\nu_\gamma \cdot \nabla_\Gamma \phi.$$

Here we have used the definition of ν_γ and the fact that $\nabla \frac{\partial d}{\partial \epsilon}(\cdot, 0) \cdot \nu = 0$ on Γ . Thus,

$$\begin{aligned} \frac{d}{d\epsilon} E_\gamma(\Gamma_\epsilon)|_{\epsilon=0} &= - \int_{\Gamma} \nu_\gamma \cdot \nabla_\Gamma \phi dA + \int_{\Gamma} \gamma(\nu) \phi H dA + \int_{\Gamma} \frac{\partial g}{\partial \nu}(\cdot, 0) \phi dA \\ &= \int_{\Gamma} \nabla_\Gamma \cdot \nu_\gamma \phi dA + \int_{\Gamma} \frac{\partial g}{\partial \nu}(\cdot, 0) \phi dA, \end{aligned}$$

where the last identity follows from (2.16). Finally, observing that $\frac{\partial g}{\partial \nu}(\cdot, 0) = \gamma_{p_i}(\nu) d_{x_i x_j}(\cdot, 0) d_{x_j}(\cdot, 0) = 0$, and recalling the definition of H_γ , the claim follows. \square

Let us next calculate H_γ for various descriptions of Γ .

Level set representation. Suppose that Γ is given as in (2.1) and oriented by $\nu = \frac{\nabla u}{|\nabla u|}$. Since γ_{p_i} is homogeneous of degree 0, we have (see also (2.2))

$$\begin{aligned} H_\gamma &= \nabla_\Gamma \cdot \nu_\gamma = \sum_{i=1}^{n+1} D_i \left(\gamma_{p_i} \left(\frac{\nabla u}{|\nabla u|} \right) \right) = \sum_{i=1}^{n+1} D_i (\gamma_{p_i}(\nabla u)) \\ &= \sum_{i,j=1}^{n+1} \gamma_{p_i p_j}(\nabla u) u_{x_i x_j} - \sum_{i,k,l=1}^{n+1} \gamma_{p_i p_l}(\nabla u) u_{x_l x_k} \frac{u_{x_k}}{|\nabla u|} \frac{u_{x_i}}{|\nabla u|}. \end{aligned}$$

Recalling (8.4) we therefore deduce

$$H_\gamma = \sum_{i,j=1}^{n+1} \gamma_{p_i p_j}(\nabla u) u_{x_i x_j}. \quad (8.16)$$

Graph representation. If Γ is locally given as the graph of the function $x' \mapsto v(x')$, $x' = (x_1, \dots, x_n)$ with normal $\nu = \frac{(\nabla_{x'} v, -1)}{\sqrt{1 + |\nabla_{x'} v|^2}}$, formula (8.16) applied to $u(x', x_{n+1}) = v(x') - x_{n+1}$ gives

$$H_\gamma = \sum_{i,j=1}^n \gamma_{p_i p_j}(\nabla_{x'} v, -1) v_{x_i x_j}. \quad (8.17)$$

Let us next derive an analogue of (2.16) with H replaced by H_γ . Observing that $\underline{D}_k \nu_l = \underline{D}_l \nu_k$ and recalling that $\underline{D}_k x_l = \delta_{kl} - \nu_k \nu_l$, we obtain

$$\begin{aligned} H_\gamma \nu_l &= \underline{D}_k (\gamma_{p_k}(\nu)) \nu_l = \underline{D}_k (\gamma_{p_k}(\nu) \nu_l) - \gamma_{p_k}(\nu) \underline{D}_k \nu_l \\ &= \underline{D}_k (\gamma_{p_k}(\nu) \nu_l) - \gamma_{p_k}(\nu) \underline{D}_l \nu_k \\ &= \underline{D}_k (\gamma_{p_k}(\nu) \nu_l) - \underline{D}_l (\gamma(\nu)) \\ &= \underline{D}_k (\gamma_{p_k}(\nu) \nu_l) - \underline{D}_k (\gamma(\nu) (\delta_{kl} - \nu_k \nu_l)) - \gamma(\nu) \nu_l \underline{D}_k \nu_k \\ &= \underline{D}_k (\gamma_{p_k}(\nu) \nu_l) - \underline{D}_k (\gamma(\nu) \underline{D}_k x_l) - \gamma(\nu) H \nu_l, \end{aligned}$$

where summation over k is from 1 to $n + 1$. For a smooth test function $\phi = (\phi_1, \dots, \phi_{n+1})$ we multiply the above relation by ϕ_l , sum over l and integrate over Γ . Using (2.16) we infer

$$\begin{aligned} \int_{\Gamma} H_\gamma \nu \cdot \phi &= - \sum_{k,l=1}^{n+1} \int_{\Gamma} \gamma_{p_k}(\nu) \nu_l \underline{D}_k \phi_l + \sum_{k,l=1}^{n+1} \int_{\Gamma} \gamma_{p_k}(\nu) \nu_l H \nu_k \phi_l \\ &\quad + \sum_{k,l=1}^{n+1} \int_{\Gamma} \gamma(\nu) \underline{D}_k x_l \underline{D}_k \phi_l - \sum_{l=1}^{n+1} \int_{\Gamma} \gamma(\nu) H \nu_l \phi_l \end{aligned}$$

and (8.4) yields

$$\int_{\Gamma} H_\gamma \nu \cdot \phi = - \sum_{k,l=1}^{n+1} \int_{\Gamma} \gamma_{p_k}(\nu) \nu_l \underline{D}_k \phi_l + \sum_{k,l=1}^{n+1} \int_{\Gamma} \gamma(\nu) \underline{D}_k x_l \underline{D}_k \phi_l. \quad (8.18)$$

This relation will be at the heart of the numerical methods in the parametric case. For additional information on the subject of weighted mean curvature including the crystalline case, see Taylor (1992).

8.4. Motion by anisotropic mean curvature with mobility

Having introduced the notion of anisotropic mean curvature we can now formulate the following generalization of (3.1):

$$\beta(\nu) V = -H_\gamma + g \quad \text{on } \Gamma(t). \quad (8.19)$$

Here, $\beta : S^n \rightarrow \mathbb{R}$ is a given positive and smooth function of degree zero. In applications where $\Gamma(t)$ models a sharp phase-interface, the coefficient β measures the drag opposing interfacial motion and the function $\frac{1}{\beta}$ is called mobility. The function g represents the energy difference in the bulk phases. A detailed derivation of (8.19) from the force balances and the second law of thermodynamics can be found in Angenent and Gurtin (1989) and Gurtin (1993). Taylor, Cahn and Handwerker (1992) give an overview of various mathematical approaches to (8.19).

In what follows we shall consider the simpler problem

$$\beta(\nu)V = -H_\gamma \quad \text{on } \Gamma(t), \quad (8.20)$$

even though all our techniques can be generalized to (8.19). It can be shown (see Bellettini and Paolini (1996)) that for the choice $\beta(\nu) = \frac{1}{\gamma(\nu)}$ there is an explicit solution of (8.20) consisting of shrinking boundaries of Wulff shapes; the sets

$$\Gamma(t) = \{p \in \mathbb{R}^{n+1} \mid \gamma^*(p) = \sqrt{r(0)^2 - 2nt}\}$$

satisfy $\frac{1}{\gamma(\nu)}V = -H_\gamma$ and are therefore a generalization of the shrinking circles from the isotropic case. We also have the following analogue of Lemma 3.1.

Lemma 8.3. Let $\Gamma(t)$ be a family of evolving hypersurfaces satisfying (8.20) on $\Gamma(t)$, and assume that each $\Gamma(t)$ is compact. Then

$$\int_{\Gamma(t)} \beta(\nu)V^2 dA + \frac{d}{dt} \int_{\Gamma(t)} \gamma(\nu) = 0.$$

Proof. In the same way as in the proof of Lemma 8.2, we derive

$$\frac{d}{dt} \int_{\Gamma(t)} \gamma(\nu) = \int_{\Gamma(t)} H_\gamma V,$$

and the claim follows from the evolution law (8.20). \square

8.5. Anisotropic curve shortening flow

Let us consider a family $\Gamma(t)$ of closed curves in \mathbb{R}^2 which move according to (8.20). As in Section 4.1 we describe the evolution by means of a mapping $X: \mathbb{R} \times [0, T] \rightarrow \mathbb{R}^2$ which satisfies $X(\theta, t) = X(\theta + 2\pi, t)$ for $t \in [0, T]$, $\theta \in \mathbb{R}$. The curves $\Gamma(t) = X(\cdot, t)$ will move by (8.20) provided that

$$\beta(\nu)X_t = -H_\gamma\nu. \quad (8.21)$$

Using the notation $(a_1, a_2)^\perp = (-a_2, a_1)$ we may write $\nu = \tau^\perp$, where $\tau = \frac{X_\theta}{|X_\theta|}$ is the unit tangent to the curve $\Gamma(t)$. Equation (8.21) amounts to a system of partial differential equations for the vector function X . In order to write down this system, let $\varphi \in H_{\text{per}}^1(I; \mathbb{R}^2)$, $I = [0, 2\pi]$, be a test function, which we can think of as being defined on $\Gamma(t)$ via $\phi(X(\theta, t)) = \varphi(\theta)$. It follows from (8.18) that

$$\begin{aligned} \int_{\Gamma(t)} H_\gamma \nu \cdot \phi &= - \sum_{k,l=1}^2 \int_{\Gamma(t)} \gamma_{p_k}(\nu) \nu_l \underline{D}_k \phi_l + \sum_{k,l=1}^2 \int_{\Gamma(t)} \gamma(\nu) \underline{D}_k x_l \underline{D}_k \phi_l \\ &= - \sum_{k,l=1}^2 \int_{\Gamma(t)} (\gamma_{p_k}(\nu) \nu_l - \gamma(\nu) \delta_{kl}) \underline{D}_k \phi_l, \end{aligned}$$

since $\underline{D}_k x_l = \delta_{kl} - \nu_k \nu_l$. Using $\nabla_\Gamma \phi_l = \frac{\varphi_{l,\theta}}{|X_\theta|} \tau$ and recalling that $\gamma(p) = D\gamma(p) \cdot p$, we obtain after some calculations

$$\sum_{k,l=1}^2 (\gamma_{p_k}(\nu) \nu_l - \gamma(\nu) \delta_{kl}) \underline{D}_k \phi_l = -D\gamma(\nu) \cdot \frac{\varphi_\theta^\perp}{|X_\theta|}.$$

In conclusion we have

$$\int_{\Gamma(t)} H_\gamma \nu \cdot \varphi \, dA = \int_0^{2\pi} D\gamma(X_\theta^\perp) \cdot \varphi_\theta^\perp \, d\theta,$$

so that we obtain the following weak form of (8.21):

$$\int_0^{2\pi} \beta \left(\frac{X_\theta^\perp}{|X_\theta|} \right) X_t \cdot \varphi |X_\theta| \, d\theta + \int_0^{2\pi} D\gamma(X_\theta^\perp) \cdot \varphi_\theta^\perp \, d\theta = 0 \quad \text{for all } \varphi \in H_{\text{per}}^1(I; \mathbb{R}^2). \quad (8.22)$$

We shall base our numerical scheme on this formulation. The classical form of (8.22) is

$$\beta \left(\frac{X_\theta^\perp}{|X_\theta|} \right) X_t + \frac{1}{|X_\theta|} \frac{\partial}{\partial \theta} (D\gamma(X_\theta^\perp)^\perp) = 0 \quad \text{in } I \times (0, T). \quad (8.23)$$

For the convenience of the reader we explicitly write down the two equations of this system:

$$\begin{aligned} \beta \left(\frac{X_\theta^\perp}{|X_\theta|} \right) X_{1t} |X_\theta| - \gamma_{p_2 p_2}(-X_{2\theta}, X_{1\theta}) X_{1\theta\theta} + \gamma_{p_2 p_1}(-X_{2\theta}, X_{1\theta}) X_{2\theta\theta} &= 0, \\ \beta \left(\frac{X_\theta^\perp}{|X_\theta|} \right) X_{2t} |X_\theta| - \gamma_{p_1 p_1}(-X_{2\theta}, X_{1\theta}) X_{2\theta\theta} + \gamma_{p_1 p_2}(-X_{2\theta}, X_{1\theta}) X_{1\theta\theta} &= 0. \end{aligned}$$

It is easy to see that this system can be written as

$$\beta \left(\frac{X_\theta^\perp}{|X_\theta|} \right) X_t - a \left(\frac{X_\theta^\perp}{|X_\theta|} \right) \frac{1}{|X_\theta|} \frac{\partial}{\partial \theta} \left(\frac{X_\theta}{|X_\theta|} \right) = 0,$$

where

$$a(p) = \gamma_{pp}(p) p^\perp \cdot p^\perp, \quad p \in \mathbb{R}^2 \setminus \{0\}.$$

Note that (8.3) implies $a(p) \geq \gamma_0 > 0$ for all $p \in \mathbb{R}^2, |p| = 1$. Analytical results for this problem which generalize the theory for the isotropic case ($a = 1$) have been obtained by Gage (1993). We shall continue to use the form (8.22) because this equation only contains first derivatives of the anisotropy function γ . Recall the definition of S_h from Section 4.1. A discrete solution of (8.22) will be a function $X_h : [0, T] \rightarrow S_h$, such that

$$X_h(\cdot, 0) = X_{h0} = I_h X_0 = \sum_{j=1}^N X_0(\theta_j) \phi_j,$$

and for all discrete test functions $\varphi_h \in S_h$

$$\int_0^{2\pi} \beta \left(\frac{X_{h\theta}}{|X_{h\theta}|} \right) X_{ht} \cdot \varphi_h |X_{h\theta}| d\theta + \int_0^{2\pi} D\gamma(X_{h\theta}^\perp) \cdot \varphi_{h\theta}^\perp d\theta = 0. \quad (8.24)$$

In the same way as in the isotropic case we can write

$$X_h(\theta, t) = \sum_{j=1}^N X_j(t) \phi_j(\theta)$$

with $X_j(t) \in \mathbb{R}^2$, and find that the discrete weak equation (8.24) is equivalent to the following system of $2N$ ordinary differential equations:

$$\begin{aligned} \frac{1}{6} \beta_j q_j \dot{X}_{j-1} + \frac{1}{3} (\beta_j q_j + \beta_{j+1} q_{j+1}) \dot{X}_j + \frac{1}{6} \beta_{j+1} q_{j+1} \dot{X}_{j+1} \\ + D\gamma(X_{j+1}^\perp - X_j^\perp)^\perp - D\gamma(X_j^\perp - X_{j-1}^\perp)^\perp = 0, \end{aligned}$$

for $j = 1, \dots, N$, where $X_0(t) = X_N(t)$, $X_{N+1} = X_1(t)$, and

$$q_j = |X_j - X_{j-1}|, \quad \beta_j = \beta \left(\frac{X_j - X_{j-1}}{q_j} \right).$$

Furthermore, the initial values are given by

$$X_j(0) = X_0(\theta_j), \quad j = 1, \dots, N.$$

We again use mass lumping, which is equivalent to a quadrature formula. Thus we replace this system by the lumped scheme

$$\frac{1}{2} (\beta_j q_j + \beta_{j+1} q_{j+1}) \dot{X}_j + D\gamma(X_{j+1}^\perp - X_j^\perp)^\perp - D\gamma(X_j^\perp - X_{j-1}^\perp)^\perp = 0 \quad (8.25)$$

together with the initial conditions $X_j(0) = X_0(\theta_j)$ for $j = 1, \dots, N$. We are now ready to say what we mean by a discrete solution of anisotropic curve shortening flow. The above system is equivalent to the one we use in the following definition of discrete anisotropic curve shortening flow.

Definition 5. A solution of the discrete anisotropic curve shortening flow for the initial curve $\Gamma_{h0} = X_{h0}([0, 2\pi])$ is a polygon $\Gamma_h(t) = X_h([0, 2\pi], t)$, which is parametrized by a piecewise linear mapping $X_h(\cdot, t) \in S_h$, $t \in [0, T]$, such that $X_h(\cdot, 0) = X_{h0}$ and for all $\varphi_h \in S_h$

$$\begin{aligned} & \int_0^{2\pi} \beta \left(\frac{X_{h\theta}}{|X_{h\theta}|} \right) X_{ht} \cdot \varphi_h |X_{h\theta}| d\theta + \int_0^{2\pi} D\gamma(X_{h\theta}^\perp) \cdot \varphi_{h\theta}^\perp d\theta \\ & + \frac{1}{6} h^2 \int_0^{2\pi} \beta \left(\frac{X_{h\theta}}{|X_{h\theta}|} \right) X_{h\theta t} \cdot \varphi_{h\theta} |X_{h\theta}| d\theta = 0. \end{aligned} \quad (8.26)$$

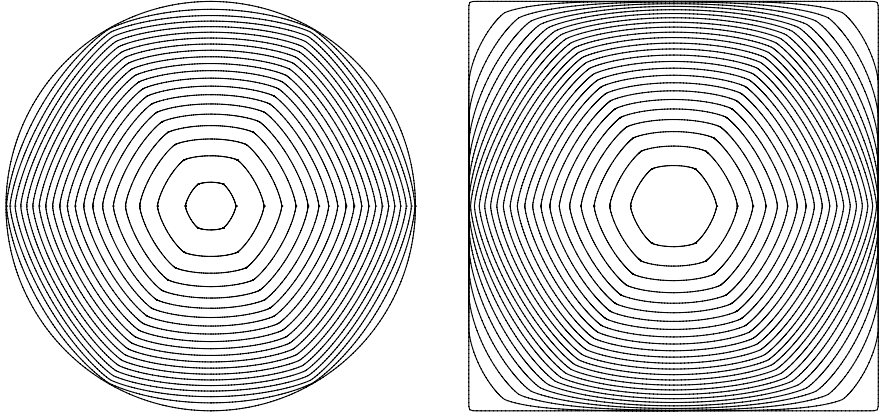


Figure 8.3. Anisotropic curve shortening flow with a sixfold anisotropy function applied to a circle (left) and to a square (right).

Here h is the constant grid size of the uniform grid in $[0, 2\pi]$. The last term of (8.26) is introduced by mass lumping. One could also define the discrete curve shortening flow without this quantity, but then the geometric property of length shortening would not be true for the discrete problem.

Dziuk (1999b) proved the following convergence result for $\beta = 1$. It is easily extended to the case of general β . We formulate the result for the geometric quantities normal, length and normal velocity. The error estimates in standard norms then follow easily.

Theorem 8.4. Suppose that $\beta : S^2 \rightarrow \mathbb{R}$ is a smooth positive function. Let X be a solution of the anisotropic curve shortening flow (8.23) on the interval $[0, T]$ with $X(\cdot, 0) = X_0$, $\min_{[0, 2\pi] \times [0, T]} |X_\theta| \geq c_0 > 0$ and $X_t \in L^2((0, T), H^2(0, 2\pi))$. Then there is an $h_0 > 0$ such that, for all $0 < h \leq h_0$, there exists a unique solution X_h of the discrete anisotropic curve shortening flow (8.26) on $[0, T]$ with $X_h(\cdot, 0) = X_{h0} = I_h X_0$, and the error between smooth and discrete solution can be estimated as follows:

$$\begin{aligned} \sup_{(0, T)} \int_0^{2\pi} |\nu - \nu_h|^2 |X_{h\theta}| d\theta + \sup_{(0, T)} \int_0^{2\pi} (|X_\theta| - |X_{h\theta}|)^2 d\theta &\leq ch^2, \\ \int_0^T \int_0^{2\pi} |X_t - X_{ht}|^2 |X_{h\theta}| d\theta dt &\leq ch^2. \end{aligned}$$

The constants depend on c_0 , T and $\|X_t\|_{L^2((0, T), H^2(0, 2\pi))}$.

Table 8.1. Convergence test for anisotropic curve shortening flow.

h	E_1	EOC ₁	E_2	EOC ₂	E_3	EOC ₃	E_4	EOC ₄
0.3927	0.4929		1.049		0.1236		1.042	
0.1964	0.2544	0.954	0.5467	0.940	0.04703	1.39	0.5500	0.922
0.09818	0.1327	0.939	0.2762	0.985	0.02060	1.19	0.2787	0.981
0.04909	0.06698	0.986	0.1345	0.996	0.009875	1.06	0.1398	0.995
0.02454	0.03354	0.998	0.06928	0.999	0.004882	1.02	0.06996	0.999
0.01227	0.01680	0.998	0.03465	1.0	0.002434	1.0	0.03499	1.0

We tested the algorithm with an exact solution,

$$X(\theta, t) = \sqrt{1 - 2t} (\cos g(\theta), \sin g(\theta)),$$

where we have chosen $g(\theta) = \theta + 0.1 \sin \theta$. The anisotropy function is $\gamma(p) = |p| - 0.25p_1$. We compute the errors

$$E_1 = \|X_t - X_{ht}\|_{L^2((0,T), L^2(\Gamma_h))}, \quad E_2 = \|\nu - \nu_h\|_{L^\infty((0,T), L^2(\Gamma_h))},$$

$$E_3 = \||X_\theta| - |X_{h\theta}|\|_{L^2((0,T), L^2(S^1))}, \quad E_4 = \|X_\theta - X_{h\theta}\|_{L^\infty((0,T), L^2(S^1))}$$

with $\Gamma_h = X_h([0, 2\pi], \cdot)$. For two successive grid sizes h_1 and h_2 with corresponding errors $E(h_1)$ and $E(h_2)$, the experimental order of convergence $\text{EOC} = \ln(E(h_1)/E(h_2))/\ln(h_1/h_2)$ is calculated and shown in Table 8.1 from Dziuk (1999b). The time-step τ was chosen $\tau = 0.5 h^2$ for these computations. We emphasize that the algorithm for anisotropic curve shortening flow does not use the second derivatives of the anisotropy function γ .

The system (8.25) can be formally written in complex tridiagonal form. For details and a suitable time discretization we refer to Dziuk (1999b). Let us finally mention that in Girao (1995) simple closed convex curves evolving by (8.20) are computed by approximating the smooth anisotropy by a crystalline one. Also, an error analysis for the resulting method is given.

8.6. Anisotropic curvature flow of graphs

Let us next turn to the evolution of hypersurfaces which are given as graphs, *i.e.*, $\Gamma(t) = \{(x, u(x, t)) \mid x \in \Omega\}$. In order to translate (8.20) into an evolution equation for u we recall that

$$H_\gamma = \sum_{i,j=1}^n \gamma_{p_i p_j} (\nabla u, -1) u_{x_i x_j} = \sum_{i=1}^n \frac{\partial}{\partial x_i} (\gamma_{p_i} (\nabla u, -1)).$$

Furthermore, since $V = -\frac{u_t}{Q}$ with $Q = \sqrt{1 + |\nabla u|^2}$ we see that (8.20) leads to the following nonlinear partial differential equation,

$$\beta\left(\frac{(\nabla u, -1)}{Q}\right)u_t - Q \sum_{i=1}^n \frac{\partial}{\partial x_i}(\gamma_{p_i}(\nabla u, -1)) = 0 \quad \text{in } \Omega \times (0, T), \quad (8.27)$$

to which we add the following initial and boundary conditions:

$$\begin{aligned} u &= g && \text{on } \partial\Omega \times (0, T), \\ u(\cdot, 0) &= u_0 && \text{in } \Omega. \end{aligned}$$

In the sequel we shall again assume that this problem has a solution u which satisfies (5.12) and refer to Deckelnick and Dziuk (1999) for a corresponding existence and uniqueness result.

Discretization in space and estimate of the error

As in the isotropic case we may use a variational approach even though the differential equation is not in divergence form. Starting from (8.27) we obtain, with the abbreviation $\nu = \frac{(\nabla u, -1)}{Q}$,

$$\int_{\Omega} \frac{\beta(\nu) u_t \varphi}{Q} + \sum_{i=1}^n \int_{\Omega} \gamma_{p_i}(\nabla u, -1) \varphi_{x_i} = 0 \quad (8.28)$$

for all $\varphi \in H_0^1(\Omega)$, $t \in (0, T)$ together with the above initial and boundary conditions. We now consider a semidiscrete approximation of (8.28): find $u_h(\cdot, t) \in X_h$ with $u_h(\cdot, t) - I_h g \in X_{h0}$ such that

$$\int_{\Omega_h} \frac{\beta(\nu_h) u_{h,t} \varphi_h}{Q_h} + \sum_{i=1}^n \int_{\Omega_h} \gamma_{p_i}(\nabla u_h, -1) \varphi_{h,x_i} = 0 \quad \text{for all } \varphi_h \in X_{h0}, \quad (8.29)$$

for all $t \in (0, T]$, where we have set

$$Q_h = \sqrt{1 + |\nabla u_h|^2}, \quad \nu_h = \frac{(\nabla u_h, -1)}{Q_h}.$$

As an initial condition we use $u_h(\cdot, 0) = u_h^0 = I_h u_0$. Our main result gives an error bound for the important geometric quantities V and ν . The proof is contained in Deckelnick and Dziuk (1999).

Theorem 8.5. Suppose that (8.27) has a solution u that satisfies (5.12). Then (8.29) has a unique solution u_h and

$$\int_0^T \|V - V_h\|_{L^2(\Gamma_h(t))}^2 dt + \sup_{t \in (0, T)} \|(\nu - \nu_h)(\cdot, t)\|_{L^2(\Gamma_h(t))}^2 \leq Ch^2.$$

Here, $\Gamma_h(t) = \{(x, u_h(x, t)) \mid x \in \Omega_h \cap \Omega\}$ and V, V_h are as in Theorem 5.4.

Fully discrete scheme, stability and error estimate

Let us next consider discretization in time in order to get a practical method. Compared to the isotropic case, our problem has become more complicated because of the presence of two additional nonlinearities, namely the functions β and γ . In order to keep the computational effort as small as possible it would be desirable to have a method that only requires the solution of a linear problem at each time-step. This can be achieved by treating the nonlinearities in an explicit way and guaranteeing stability via the introduction of an additional stabilizing term. We start again from the variational formulation (8.28) and choose a time-step $\tau > 0$. Using the notation from Section 5.3 our scheme reads as follows.

Algorithm 7. (Anisotropic mean curvature flow of graphs) Given u_h^m , find $u_h^{m+1} \in X_h$ such that $u_h^{m+1} - I_h g \in X_{h0}$ and

$$\begin{aligned} \frac{1}{\tau} \int_{\Omega_h} \frac{\beta(\nu_h^m)(u_h^{m+1} - u_h^m)}{Q_h^m} \varphi_h + \sum_{i=1}^n \int_{\Omega_h} \gamma_{p_i}(\nu_h^m) \varphi_{hx_i} \\ + \lambda \int_{\Omega_h} \frac{\gamma(\nu_h^m)}{Q_h^m} \nabla(u_h^{m+1} - u_h^m) \cdot \nabla \varphi_h = 0 \end{aligned} \quad (8.30)$$

for all $\varphi_h \in X_{h0}$. Here we have set $u_h^0 = I_h u_0$ as well as

$$Q_h^m = \sqrt{1 + |\nabla u_h^m|^2}, \quad \nu_h^m = \frac{(\nabla u_h^m, -1)}{Q_h^m}.$$

The above scheme is semi-implicit and requires the solution of a linear system in each time-step. We shall see that it is unconditionally stable provided the parameter λ is chosen appropriately.

Theorem 8.6. Let $\bar{\gamma} = \frac{1}{\sqrt{5}-1} \max \{ \sup_{|p|=1} |\nabla \gamma(p)|, \sup_{|p|=1} |D^2 \gamma(p)| \}$. Then we have for $0 \leq M \leq [\frac{T}{\tau}]$

$$\begin{aligned} \tau \sum_{m=1}^{M-1} \int_{\Omega_h} \frac{\beta(\nu_h^m)}{Q_h^m} \left| \frac{u_h^{m+1} - u_h^m}{\tau} \right|^2 + \lambda \tau \sum_{m=1}^{M-1} \int_{\Omega_h} \frac{\gamma(\nu_h^m)}{Q_h^m} \left(\frac{Q_h^{m+1} - Q_h^m}{\sqrt{\tau}} \right)^2 \\ + \left(\lambda \inf_{|p|=1} \gamma(p) - \bar{\gamma} \right) \tau \sum_{m=1}^{M-1} \int_{\Omega_h} \left| \frac{\nu_h^{m+1} - \nu_h^m}{\sqrt{\tau}} \right|^2 Q_h^{m+1} + \int_{\Omega_h} \gamma(\nu_h^M) Q_h^M \\ \leq \int_{\Omega_h} \gamma(\nu_h^0) Q_h^0. \end{aligned}$$

In particular, if λ is chosen in such a way that $\lambda \inf_{|p|=1} \gamma(p) > \bar{\gamma}$, then we have for $\Gamma_h^m = \{(x, u_h^m(x)) \mid x \in \Omega_h\}$

$$E_\gamma(\Gamma_h^m) \leq E_\gamma(\Gamma_h^0) \quad \text{for all } 0 \leq m \leq \left[\frac{T}{\tau} \right]. \quad (8.31)$$

Thus we have proved stability for the semi-implicit scheme without any restriction on the time-step size. An error analysis for the above scheme has been carried out in Deckelnick and Dziuk (2002a). The precise result is as follows.

Theorem 8.7. Suppose that $\lambda \inf_{|p|=1} \gamma(p) > \bar{\gamma}$ ($\bar{\gamma}$ as in Theorem 8.6). Then there exists $\tau_0 > 0$ such that, for all $0 < \tau \leq \tau_0$,

$$\sum_{m=0}^{[\frac{T}{\tau}]-1} \tau \int_{\Omega \cap \Omega_h} (V^m - V_h^m)^2 Q_h^m + \max_{0 \leq m \leq [\frac{T}{\tau}]} \int_{\Omega \cap \Omega_h} |\nu^m - \nu_h^m|^2 Q_h^m \leq c(\tau^2 + h^2).$$

We have run numerical tests for anisotropic mean curvature flow of graphs. The Wulff shape shrinks homothetically during the evolution. We have chosen the very strong anisotropy $\gamma(p) = \sqrt{0.01p_1^2 + p_2^2 + p_3^2}$. The equation $\gamma^*(x, u(x, t)) = \sqrt{1 - 4t}$ defines a solution of the differential equation when the mobility is chosen as $\beta = 1/\gamma$. The exact solution is given by $u(x, t) = \sqrt{1 - 4t - 100x_1^2 - x_2^2}$. The condition on the stabilizing parameter λ (see Theorem 8.6) is satisfied for $\lambda = 81.0$. We use $\tau = 0.01h$ as a uniform time-step size. The coupling between time-step size and spatial grid size is done in order not to spoil the asymptotic orders of convergence. For a discussion with respect to the choice of λ and τ we refer to Deckelnick and Dziuk (2002a). Table 8.2 shows the grid size h , the errors

$$E(V) = \left(\sum_{m=0}^M \tau \int_{\Omega_h} |V^m - V_h^m|^2 Q_h^m \right)^{\frac{1}{2}},$$

$$E(\nu) = \left(\max_{0 \leq m \leq M} \int_{\Omega_h} |\nu^m - \nu_h^m|^2 Q_h^m \right)^{\frac{1}{2}},$$

Table 8.2. Convergence test for anisotropic mean curvature flow of graphs.

h	$E(\nu)$	EOC	$E(V)$	EOC	$L^\infty(H^1)$	EOC
7.0711e-2	9.7027e-2	—	2.3278e-2	—	1.3366e-1	—
3.5355e-2	2.3213e-2	2.06	6.0827e-3	1.94	4.4935e-2	1.57
2.6050e-2	2.4818e-2	-0.22	7.5203e-3	-0.70	4.5372e-2	-0.03
1.4861e-2	1.3868e-2	1.04	4.1117e-3	1.08	2.4163e-2	1.12
7.8462e-3	7.0232e-3	1.07	1.9806e-3	1.14	1.2256e-2	1.06
4.0210e-3	3.5368e-3	1.03	1.0176e-3	1.00	6.1725e-3	1.03
2.0342e-3	1.8103e-3	0.98	5.2675e-4	0.97	3.1225e-3	1.00
1.0229e-3	9.2938e-4	0.97	2.6988e-4	0.97	1.5799e-3	0.99

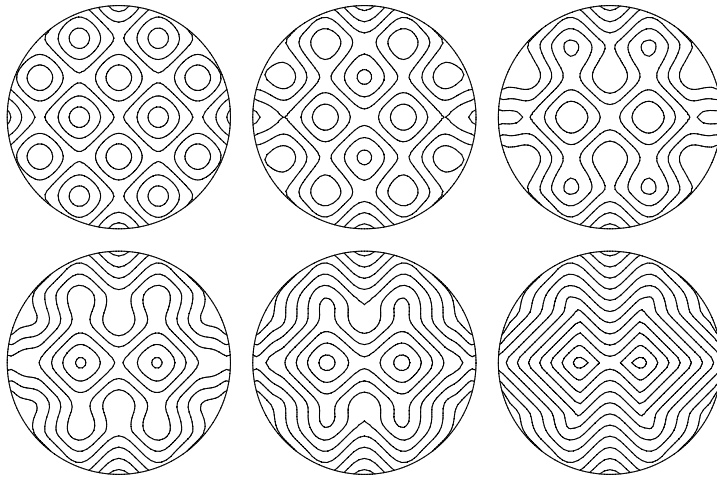


Figure 8.4. Level lines for the time-steps 0, 250, 500, 750, 3000 for a regularized crystalline anisotropy.

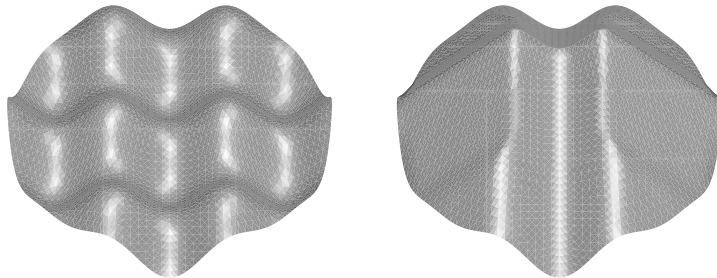


Figure 8.5. Initial value and stationary solution for a regularized crystalline anisotropy.

and the corresponding experimental orders of convergence (EOC) between two successive grid sizes. We add a column with the $L^\infty((0, T), H^1(\Omega))$ error. Obviously the results of the asymptotic error estimates of Theorem 8.7 are reproduced in our test computations. We add a long time computation from Deckelnick and Dziuk (2002a). As an anisotropy function we used an anisotropy which is a regularized form of $\gamma(p) = |p|_{l^\infty}$ (see also Figure 8.1 for the dual situation). We have chosen a nonzero constant right-hand side for the equation. In Figure 8.4 we show the level lines of the initial function, of four time-steps and of the stationary solution. The boundary values were kept fixed during the evolution. We can see that the octahedral shape develops during the evolution. In Figure 8.5 we show the initial graph and the stationary graph. The domain was the unit disk.

8.7. Anisotropic mean curvature flow of level sets

Here we briefly sketch how the level set approach can be adapted to the anisotropic case. Let us look for solutions of (8.20) in the form

$$\Gamma(t) = \{x \in \mathbb{R}^{n+1} \mid u(x, t) = 0\}$$

where the scalar function u has to be determined. The relations (2.20) and (8.16) lead to the following nonlinear partial differential equation

$$\beta \left(\frac{\nabla u}{|\nabla u|} \right) u_t - |\nabla u| \sum_{j,k=1}^{n+1} \gamma_{p_j p_k} (\nabla u) u_{x_j x_k} = 0 \quad \text{in } \mathbb{R}^{n+1} \times (0, \infty), \quad (8.32)$$

which is degenerate parabolic since $D^2\gamma(p)p = 0$. We regularize the equation by using an extension of the anisotropy to $n+2$ space dimensions. Let us assume that there is an admissible weight function $\bar{\gamma} = \bar{\gamma}(p_1, \dots, p_{n+1}, p_{n+2})$ such that

$$\bar{\gamma}(p_1, \dots, p_{n+1}, 0) = \gamma(p_1, \dots, p_{n+1}).$$

In the following we denote this extension again by γ . Rather than treating (8.32) we introduce for a (small) positive parameter ϵ the regularized problem

$$\beta \left(\frac{\nabla u_\epsilon}{\sqrt{\epsilon^2 + |\nabla u_\epsilon|^2}} \right) u_{\epsilon t} - \sqrt{\epsilon^2 + |\nabla u_\epsilon|^2} \sum_{j,k=1}^{n+1} \gamma_{p_j p_k} (\nabla u_\epsilon, -\epsilon) u_{\epsilon x_j x_k} = 0.$$

We consider this differential equation on $\Omega \times (0, T)$, where $\Omega \subset \mathbb{R}^{n+1}$ is a bounded smooth domain and $T > 0$ is some final time. Furthermore, appropriate initial and boundary conditions need to be added, which can be done similarly to the isotropic case. The numerical approximation of the resulting problem follows the ideas of the graph case. The same applies to the analysis of the schemes, where of course one has to bear in mind the dependency on the regularization parameter ϵ .

8.8. Anisotropic phase field

We turn now to the setting of Section 7. Anisotropic phase field models are based on the following anisotropic interfacial energy functional

$$E_\gamma(\varphi) = \int_{\Omega} \left(\epsilon A(\nabla \varphi) + \frac{1}{\epsilon} W(\varphi) \right) dx, \quad (8.33)$$

where $A : \mathbb{R}^{n+1} \rightarrow \mathbb{R}$ is smooth, convex and positively homogeneous of degree two which replaces the quadratic gradient energy used in the isotropic case. In order to relate it to the anisotropic energy density used in this section we set

$$A(p) = \frac{1}{2} \gamma(p)^2, \quad p \in \mathbb{R}^{n+1}. \quad (8.34)$$

The double well bulk energy function W may be chosen as in the isotropic situation. The L^2 -gradient flow of E_γ leads to the following quasilinear parabolic equation:

$$\epsilon\varphi_t - \epsilon\nabla \cdot DA(\nabla\varphi) + \frac{1}{\epsilon}W'(\varphi) = 0 \quad \text{in } \Omega \times (0, T). \quad (8.35)$$

For small ϵ and suitable initial data, (8.35) approximates the following anisotropic mean curvature flow:

$$\frac{1}{\gamma(\nu)}V = -H_\gamma \quad \text{on } \Gamma(t). \quad (8.36)$$

This can be motivated in a similar manner to the isotropic case. For convenience we suppose that W is a smooth double well. Set

$$P(v) = \epsilon v_t - \epsilon\nabla \cdot DA(\nabla v) + \frac{1}{\epsilon}W'(v) \quad (8.37)$$

and

$$v(x, t) = \psi\left(\frac{d_\gamma(x, t)}{\epsilon}\right),$$

where ψ is the transition profile defined by (7.4) and (7.5) and $d_\gamma(\cdot, t)$ denotes the anisotropic signed distance function to the smoothly evolving interface $\Gamma(t)$ which satisfies (8.36) on $\Gamma(t)$. A calculation shows

$$\begin{aligned} v_t &= \psi'\left(\frac{d_\gamma}{\epsilon}\right)\frac{d_{\gamma,t}}{\epsilon}, \quad \nabla v = \psi'\left(\frac{d_\gamma}{\epsilon}\right)\frac{\nabla d_\gamma}{\epsilon}, \\ D^2v &= \psi\left(\frac{d_\gamma}{\epsilon}\right)\frac{\nabla d_\gamma \otimes \nabla d_\gamma}{\epsilon^2} + \psi'\left(\frac{d_\gamma}{\epsilon}\right)\frac{D^2d_\gamma}{\epsilon}, \end{aligned}$$

and using (8.4), (8.5) as well as Lemma 8.1, we obtain

$$\begin{aligned} P(v) &= \psi'\left(\frac{d_\gamma}{\epsilon}\right)|\nabla d_\gamma|\left(\frac{d_{\gamma,t}}{|\nabla d_\gamma|} - \gamma\left(\frac{\nabla d_\gamma}{|\nabla d_\gamma|}\right)\sum_{i,j=1}^{n+1}\gamma_{p_ip_j}(\nabla d_\gamma)d_{\gamma,x_ix_j}\right) \\ &\quad + \frac{1}{\epsilon}\left(-\psi''\left(\frac{d_\gamma}{\epsilon}\right) + W'\left(\psi\left(\frac{d_\gamma}{\epsilon}\right)\right)\right). \end{aligned}$$

Observing that

$$\frac{d_{\gamma,t}}{|\nabla d_\gamma|} - \gamma\left(\frac{\nabla d_\gamma}{|\nabla d_\gamma|}\right)\sum_{i,j=1}^{n+1}\gamma_{p_ip_j}(\nabla d_\gamma)d_{\gamma,x_ix_j} = -V - \gamma(\nu)H_\gamma = 0 \quad \text{on } \Gamma(t)$$

and choosing ψ as in (7.4), (7.5) we see that v is close to being a solution of $P(v) = 0$ in a neighbourhood of $\bigcup_{0 < t < T} \Gamma(t) \times \{t\}$.

Kinetic anisotropy and a generalized double obstacle phase field model
As a generalization of (8.35) we consider the phase field model

$$\varepsilon\beta(\nabla\varphi)\varphi_t - \varepsilon\nabla \cdot DA(\nabla\varphi) + \frac{1}{\epsilon}W'(\varphi) = c_W\rho(\varphi)g. \quad (8.38)$$

Here, the potential W is taken to be of double obstacle form,

$$W(r) = W_0(r) + I_{[-1,1]}(r), \quad (8.39)$$

where $W_0 \in C^2[-1, 1]$ and

$$I_{[-1,1]}(r) = \begin{cases} +\infty & \text{for } |r| > 1, \\ 0 & \text{for } |r| \leq 1. \end{cases}$$

A possible example of W_0 is

$$W_0(r) = \frac{1}{4(1+\xi^2)}[(r^2 - 1 - \xi^2)^2 - \xi^4] \quad (8.40)$$

with $\xi \in (0, \infty)$. For $\xi = 0$, W_0 takes the classical smooth double well Ginzburg–Landau quadratic form $\frac{1}{4}(r^2 - 1)^2$, whereas for $\xi \rightarrow \infty$ we recover the classical double obstacle potential

$$W(r) = \frac{1}{2}(1 - r^2) + I_{[-1,1]}(r). \quad (8.41)$$

The function ρ is nonnegative and even with a positive integral across the transition region $[-1, 1]$. As above one can show that the zero level set of φ approximates an interface which evolves according to the anisotropic forced mean curvature flow:

$$\frac{\beta(\nu)}{\gamma(\nu)}V = -H_\gamma - g. \quad (8.42)$$

Properly (8.38) should be written as the parabolic variational inequality

$$\begin{aligned} & \epsilon \int_{\Omega} \beta(\nabla\varphi)\varphi_t(\eta - \varphi) + \epsilon \int_{\Omega} DA(\nabla\varphi) \cdot (\nabla\eta - \nabla\varphi) + \frac{1}{\epsilon} \int_{\Omega} W'_0(\varphi)(\eta - \varphi) \\ & \geq c_W \int_{\Omega} \rho(\varphi)g(\eta - \varphi) \quad \text{for all } \eta \in \mathcal{K} = \{\eta \in H^1(\Omega) : |\eta| \leq 1\}, \end{aligned} \quad (8.43)$$

which is treated in the viscosity sense in Elliott and Schätzle (1997) because of the singularity in β at the origin.

Convergence

The phase field approximation of anisotropic interface motion can be established as in the isotropic case for smooth potential W (McFadden, Wheeler, Braun, Coriell and Sekerka 1993, Wheeler and McFadden 1996). Convergence of the double obstacle model to the unique viscosity solution of the anisotropic level set equation was proved in Elliott and Schätzle (1997) even in the case of kinetic anisotropy. The error bounds for smoothly

evolving flows are again $O(\epsilon^2)$ (Elliott and Schätzle 1996, Elliott, Paolini and Schätzle 1996).

Discretization of anisotropic phase field equation

The numerical approximation of (8.43) follows the approach used for the isotropic Allen–Cahn equation (Section 7.3). We use the same notation for the finite element spaces and time discretizations. In order to implement the method it is necessary to use a regularization β_ϵ of β .

Fully explicit time-stepping

The fully discrete approximation of (8.43) using explicit time-stepping reads as follows.

Algorithm 8. (Anisotropic double obstacle phase field) Let $\Phi^0 = I_h \varphi_0$. For $m = 0, \dots, M - 1$, find $\Phi^{m+1} \in \mathcal{K}_h$ such that, for all $\chi \in \mathcal{K}_h$,

$$\begin{aligned} & \epsilon(\beta_\epsilon(\nabla\Phi^m)\partial\Phi^m, \chi - \Phi^{m+1})_h + \epsilon(DA(\nabla\Phi^m), \nabla\chi - \nabla\Phi^{m+1}) \\ & + \frac{1}{\epsilon}(W'_0(\Phi^m), \chi - \Phi^{m+1})_h - c_W(\rho(\Phi^m)g^m, \chi - \Phi^{m+1})_h \geq 0. \end{aligned} \quad (8.44)$$

This scheme is as simple to implement as in the isotropic situation. Let M_β^m , K^m , M_ρ^m , and M_W^m be defined by

$$\begin{aligned} (M_\beta^m)_{ij} &= (\beta_\epsilon(\nabla\Phi^m)\chi_i, \chi_j)_h, \quad (K^m)_{ij} = (D^2 A(\nabla\Phi^m)\nabla\chi_i, \nabla\chi_j)_h, \\ (M_\rho^m)_j &= c_W(\rho(\Phi^m)g^m, \chi_j)_h, \quad (M_W^m)_j = (W'_0(\Phi^m), \chi_j)_h \end{aligned}$$

for $1 \leq i, j \leq N$, $0 \leq m \leq M$. Here we made use of the fact that $DA(\nabla\Phi^m) = D^2 A(\nabla\Phi^m)\nabla\Phi^m$, which follows from (8.4) and the fact that DA is homogeneous of degree 1. The variational formulation (8.44) is then equivalent to the following matrix formulation

$$M_\beta^m \Phi^{m+1/2} = (M_\beta^m - \tau K^m) \Phi^m + \frac{\tau}{\epsilon} M_\rho^m - \frac{\tau}{\epsilon^2} M_W^m \quad (8.45)$$

and it remains to project $\Phi^{m+1/2}$ component-wise yielding $\Phi^{m+1} = \mathcal{P}\Phi^{m+1/2}$. The use of the mass lumping in (8.45), which diagonalizes M_β^m , is crucial to eliminate any iteration in solving (8.45).

Semi-implicit time-stepping scheme

A semi-implicit scheme is obtained by treating the gradient energy term implicitly, yielding the following method.

Algorithm 9. Let $\Phi^0 = I_h \varphi_0$. For $m = 0, \dots, M - 1$, find $\Phi^{m+1} \in \mathcal{K}_h$ such that, for all $\chi \in \mathcal{K}_h$,

$$\begin{aligned} & \epsilon(\beta_\epsilon(\nabla\Phi^m)\partial\Phi^m, \chi - \Phi^{m+1})_h + \epsilon(DA(\nabla\Phi^{m+1}), \nabla\chi - \nabla\Phi^{m+1}) \\ & + \frac{1}{\epsilon}(W'_0(\Phi^m), \chi - \Phi^{m+1})_h - c_W(\rho(\Phi^m)g^m, \chi - \Phi^{m+1})_h \geq 0. \end{aligned} \quad (8.46)$$

The algebraic problem is now a convex optimization problem with obstacle constraints.

These schemes are stable in the sense of satisfying energy norm bounds analogous to those enjoyed by the solution of the PDE. The stability constraints are analogous to those holding in the isotropic case. However, owing to the anisotropy in the discrete elliptic operator there is a lack of a comparison principle which has proved a barrier to proving convergence.

9. Fourth order flows

9.1. Surface diffusion

In this paragraph we study various ways to approximate surfaces which evolve according to surface diffusion, that is,

$$V = \Delta_\Gamma H_\gamma \quad \text{on } \Gamma(t). \quad (9.1)$$

Here, H_γ denotes the anisotropic mean curvature of the surface $\Gamma(t)$ as it was introduced in (8.15). This evolution has interesting geometrical properties: if $\Gamma(t)$ is a closed surface bounding a domain $\Omega(t)$, then the volume of $\Omega(t)$ is preserved and the weighted surface area of $\Gamma(t)$ decreases. At present, the existence and uniqueness theory for surface diffusion is limited to the isotropic case $\gamma(q) = |q|, q \in \mathbb{R}^{n+1}$. For example, it is known that for closed curves in the plane or closed surfaces in \mathbb{R}^3 , balls are asymptotically stable subject to small perturbations: see Elliott and Garcke (1997) and Escher, Mayer and Simonett (1998). However, topological changes such as pinch-off are possible (Giga and Ito 1998, Mayer and Simonett 2000) and a one-dimensional graph may lose its graph property. An example of pinch-off is shown in Figure 9.1. We start with the axially symmetric initial surface given by

$$r_0(x) = 1 + 0.05(\sin(5.5x) + \sin(5x)), \quad x \in (0, 8\pi). \quad (9.2)$$

Pinch-off happens after a very long computation time. Note the different scaling of the x - and the r -axis. This example was first computed in Coleman, Falk and Moakher (1995).

9.2. Surface diffusion for axially symmetric surfaces

In applications one is interested in the stability of so-called whiskers, which are axially symmetric cylindrical bodies of small diameter with respect to their length: see Nichols and Mullins (1965) and Coleman, Falk and Moakher (1995). Let us consider an axially symmetric cylindrical body, whose boundary

$$\Gamma(t) = \{\mathbf{x} \in \mathbb{R}^3 \mid \mathbf{x} = (x, r(x, t) \cos \phi, r(x, t) \sin \phi), x \in [0, L], \phi \in [0, 2\pi]\}$$

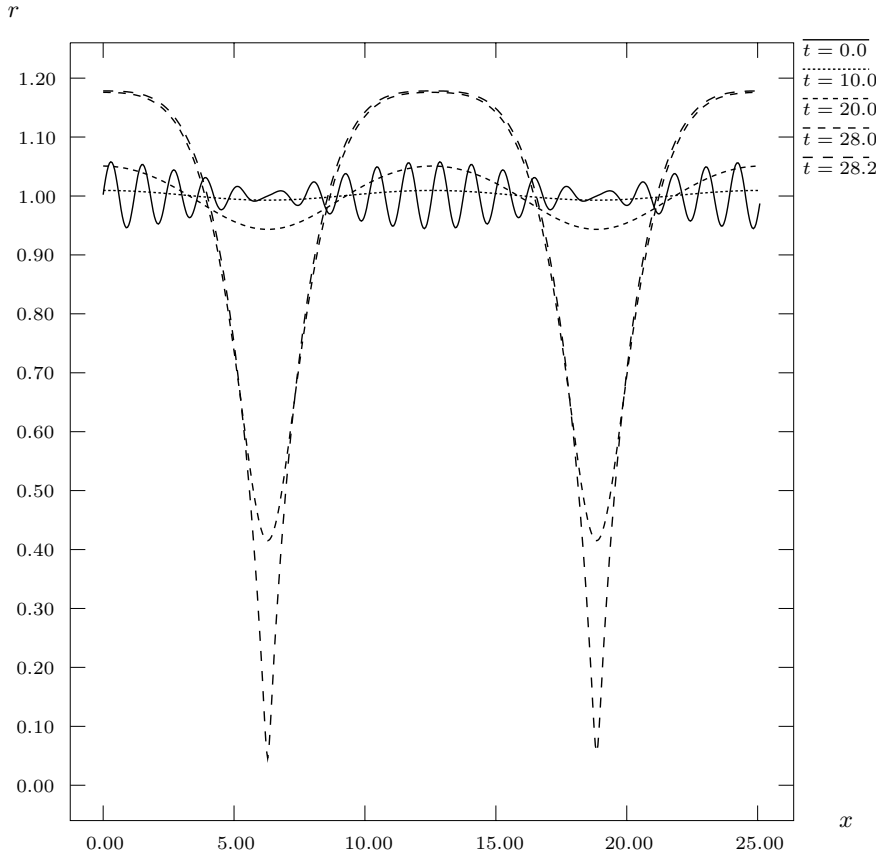


Figure 9.1. Evolution of the initial surface given by (9.2) for $t = 0.0, 10.0, 20.0, 28.0$ and 28.2 .

evolves by $V = \Delta_\Gamma H$. We assume that the radius r is a smooth positive function, which is periodic in x , so that $r(0, t) = r(L, t)$. In these coordinates the mean curvature of $\Gamma(t)$ is

$$H = \frac{1}{r\sqrt{1+r_x^2}} - \frac{r_{xx}}{\sqrt{1+r_x^2}^3} = \frac{1}{r\sqrt{1+r_x^2}} - \left(\frac{r_x}{\sqrt{1+r_x^2}} \right)_x, \quad (9.3)$$

while normal velocity and the surface Laplacian, respectively, are given by

$$V = \frac{r_t}{\sqrt{1+r_x^2}}, \quad \Delta_\Gamma H = \frac{1}{r\sqrt{1+r_x^2}} \left(\frac{rH_x}{\sqrt{1+r_x^2}} \right)_x.$$

It follows from these two equations that r satisfies the quasilinear fourth order parabolic problem

$$r_t = \frac{1}{r} \left(\frac{rH_x}{\sqrt{1+r_x^2}} \right)_x \quad \text{in } I \times (0, T], \quad (9.4)$$

$$r(0, t) = r(L, t) \quad \text{in } (0, T], \quad (9.5)$$

$$H(0, t) = H(L, t) \quad \text{in } (0, T], \quad (9.6)$$

$$r(\cdot, 0) = r_0 \quad \text{in } I, \quad (9.7)$$

where $I = (0, L)$ and H is given by (9.3). The initial function r_0 is assumed to be periodic and positive.

For discretization purposes it is convenient to split the fourth order problem into two coupled second order equations for the radial variable r and the mean curvature H resulting in the following variational form:

$$\int_I rr_t \eta \, dx + \int_I \frac{rH_x \eta_x}{\sqrt{1+r_x^2}} \, dx = 0 \quad (9.8)$$

$$\int_I rH \zeta \, dx - \int_I \sqrt{1+r_x^2} \zeta \, dx - \int_I \frac{rr_x \zeta_x}{\sqrt{1+r_x^2}} \, dx = 0 \quad (9.9)$$

for all $\eta, \zeta \in H_{\text{per}}^1(I) = \{\eta \in H^1(I) \mid \eta(0) = \eta(L)\}$. We note that Coleman, Falk and Moakher (1995) proposed a similar second order splitting and used $R = r^2$ and H as the variables.

We employ (9.8), (9.9) in order to define a semidiscrete scheme using linear finite elements to approximate r and H . Let $0 = x_0 < x_1 < \dots < x_N = L$, $h_j = x_j - x_{j-1}$ and $h = \max_{1 \leq j \leq N} h_j$. We shall make an inverse assumption of the form $h \leq \rho h_j$ for all $j = 1, \dots, N$, where $\rho > 0$ is independent of h . The spatial discretization is based on piecewise linear finite elements,

$$X_h = \{\phi_h \in C^0(\bar{I}) \mid \phi_h|_{[x_{j-1}, x_j]} \in P^1, 1 \leq j \leq N, \phi_h(0) = \phi_h(L)\}.$$

Our discrete problem now reads: find $r_h, H_h : [0, T] \rightarrow X_h$ such that

$$\int_I r_h r_{h,t} \eta_h \, dx + \int_I \frac{r_h H_{h,x} \eta_{h,x}}{\sqrt{1+r_{h,x}^2}} \, dx = 0, \quad (9.10)$$

$$\int_I r_h H_h \zeta_h \, dx - \int_I \sqrt{1+r_{h,x}^2} \zeta_h \, dx - \int_I \frac{r_h r_{h,x} \zeta_{h,x}}{\sqrt{1+r_{h,x}^2}} \, dx = 0 \quad (9.11)$$

for all $\eta_h, \zeta_h \in X_h$, $t \in [0, T]$ and with $r_h(0) = I_h r_0$, where I_h denotes the Lagrange interpolation operator. In Deckelnick, Dziuk and Elliott (2003a) a convergence analysis for the above scheme is carried out. The principal results are error bounds for position and mean curvature as described in the following theorem.

Theorem 9.1. Let us assume that (9.4)–(9.7) has a sufficiently smooth positive solution on a maximal time interval $[0, T_{\max})$. Then the discrete solution (r_h, H_h) exists on $[0, T]$ for all $T < T_{\max}$ and there is an $h_0 > 0$ such that, for all $0 < h \leq h_0$,

$$\sup_{(0,T)} \|r - r_h\|_{H^1(I)}^2 + \int_0^T \|H - H_h\|_{H^1(I)}^2 dt \leq Ch^2. \quad (9.12)$$

9.3. Surface diffusion for graphs

The anisotropic surface diffusion (1.8) of a graph $\Gamma(t) = \{(x, u(x, t)) | x \in \Omega\}$ sitting above a domain $\Omega \subset \mathbb{R}^n$ leads to a highly nonlinear fourth order geometric partial differential equation. For graphs the Laplace–Beltrami operator applied to anisotropic mean curvature H_γ reads

$$\Delta_\Gamma H_\gamma = \frac{1}{Q} \nabla \cdot \left(Q \left(I - \frac{\nabla u \otimes \nabla u}{Q^2} \right) \nabla H_\gamma \right), \quad (9.13)$$

where we have again written $Q = \sqrt{1 + |\nabla u|^2}$. Recalling (8.17) as well as $V = -\frac{u_t}{Q}$, we see that (1.8) for graphs is equivalent to the partial differential equation

$$u_t + \nabla \cdot \left(Q \left(I - \frac{\nabla u}{Q} \otimes \frac{\nabla u}{Q} \right) \nabla \left(\sum_{i,j=1}^n \gamma_{p_i p_j} (\nabla u, -1) u_{x_i x_j} \right) \right) = 0. \quad (9.14)$$

As in the previous section, it is convenient to split the fourth order problem into two second order problems as follows:

$$u_t = \nabla \cdot \left(Q \left(I - \frac{\nabla u}{Q} \otimes \frac{\nabla u}{Q} \right) \nabla w \right), \quad (9.15)$$

$$w = - \sum_{i,j=1}^n \gamma_{p_i p_j} (\nabla u, -1) u_{x_i x_j}. \quad (9.16)$$

The system is closed using Neumann boundary conditions and an initial condition for u :

$$Q \left(I - \frac{\nabla u}{Q} \otimes \frac{\nabla u}{Q} \right) \nabla w \cdot \nu_{\partial\Omega} = 0, \quad (9.17)$$

$$D\gamma(\nabla u, -1) \cdot (\nu_{\partial\Omega}, 0) = 0, \quad (9.18)$$

$$u(\cdot, 0) = u_0. \quad (9.19)$$

The first equation, (9.17), is the zero mass flux condition, whereas the second equation, (9.18), is the natural variational boundary condition which defines w as the variational derivative or chemical potential for the surface energy functional. Note that an initial condition on w is not required. The

problem (9.15)–(9.18) can easily be rewritten in variational form, namely

$$\int_{\Omega} u_t \eta + \int_{\Omega} Q \left(I - \frac{\nabla u}{Q} \otimes \frac{\nabla u}{Q} \right) \nabla w \cdot \nabla \eta = 0, \quad (9.20)$$

$$\int_{\Omega} w \psi - \sum_{j=1}^n \int_{\Omega} \gamma_{p_j}(\nabla u, -1) \psi_{x_j} = 0 \quad (9.21)$$

for all $\eta, \psi \in H^1(\Omega)$, $t \in (0, T]$.

Replacing $H^1(\Omega)$ by the space X_h of piecewise linear finite elements we immediately arrive at a natural way to discretize in space. A finite element error analysis for the resulting semidiscrete scheme in the isotropic case was carried out by Bänsch, Morin and Nochetto (2004) for graphs in arbitrary space dimension. The time discretization follows the ideas of the discretization techniques introduced in Algorithm 7 and Theorem 8.7, leading to the following.

Algorithm 10. (Anisotropic surface diffusion of graphs) Let $\tau > 0$ be the time-step size with $M\tau = T$ and assume that $\lambda > 0$ is as in Theorem 8.7. Let the initial value $u_{h0} \in X_h$. For $m = 1, \dots, M$, compute $u_h^{m+1}, w_h^{m+1} \in X_h$ such that

$$\begin{aligned} \frac{1}{\tau} \int_{\Omega} (u_h^{m+1} - u_h^m) \eta_h + \int_{\Omega} Q_h^m \left(I - \frac{\nabla u_h^m}{Q_h^m} \otimes \frac{\nabla u_h^m}{Q_h^m} \right) \nabla w_h^{m+1} \cdot \nabla \eta_h &= 0, \\ \int_{\Omega} w_h^{m+1} \psi_h - \lambda \int_{\Omega} \frac{\gamma(\nabla u_h^m, -1)}{(Q_h^m)^2} \nabla(u_h^{m+1} - u_h^m) \cdot \nabla \psi_h \\ &\quad - \sum_{i=1}^n \int_{\Omega} \gamma_{p_i}(\nabla u_h^m, -1) \psi_{hx_i} \\ -\tau \int_{\Omega} Q_h^m \left(I - \frac{\nabla u_h^m}{Q_h^m} \otimes \frac{\nabla u_h^m}{Q_h^m} \right) \nabla(u_h^{m+1} - u_h^m) \cdot \nabla \psi_h &= 0 \end{aligned}$$

for all discrete test functions $\eta_h, \psi_h \in X_h$. Here $Q_h^m = \sqrt{1 + |\nabla u_h^m|^2}$.

Note that in each time-step a linear system of equations has to be solved. An error analysis for this scheme is carried out in Deckelnick, Dziuk and Elliott (2003b).

Theorem 9.2. Let u be a sufficiently smooth solution of anisotropic surface diffusion (9.14), (9.17)–(9.19) on the domain $\Omega \times (0, T)$ and set $w = -H_\gamma$. Let X_h be the space of continuous piecewise linear finite elements.

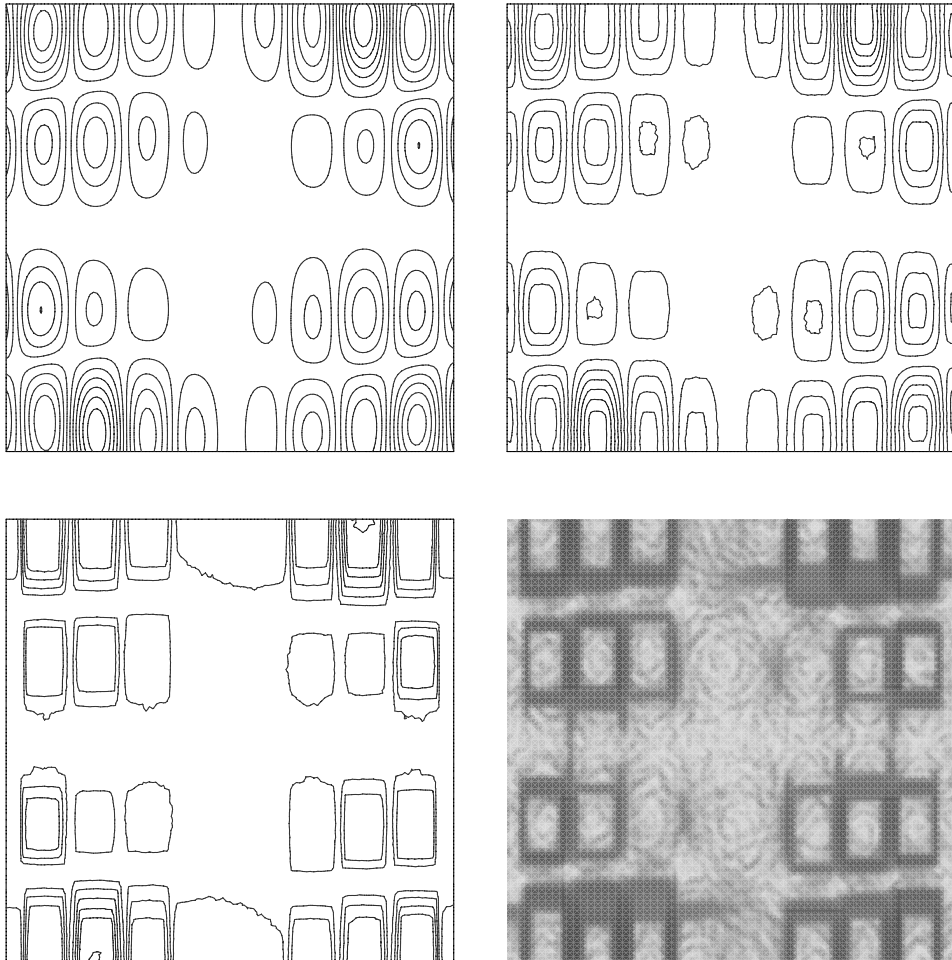


Figure 9.2. Anisotropic surface diffusion with a very strong anisotropy. Level lines are shown for the time-steps 0, 10, 200 and a view from a position vertically above the graph for time-step 300.

Then for the discrete solution u_h^m, w_h^m ($m = 1, \dots, M$) we have the error estimates

$$\begin{aligned} \max_{m=1,\dots,M} \|u^m - u_h^m\|_{L^2(\Omega)}^2 + \tau \sum_{m=1}^M \|w^m - w_h^m\|_{L^2(\Omega)}^2 &\leq c(\tau^2 + h^2), \\ \max_{m=1,\dots,M} \int_{\Omega} \frac{|\nabla(u^m - u_h^m)|^2}{Q_h^m} + \tau \sum_{m=1}^M \int_{\Omega} \frac{|\nabla(w^m - w_h^m)|^2}{Q_h^{m-1}} &\leq c(\tau^2 + h^2). \end{aligned}$$

Here $u^m = u(\cdot, m\tau)$, $w^m = w(\cdot, m\tau)$.

The proof uses ideas that were developed for the motion of graphs by anisotropic mean curvature. There is neither a restriction on the space dimension nor a coupling of time-step size and grid size. In two dimensions inverse estimates yield $L^\infty((0, T), H^1(\Omega))$ -convergence for u and convergence in $L^2((0, T), H^1(\Omega))$ for w .

In Figure 9.2 we show computational results for anisotropic surface diffusion of a graph. The anisotropy is chosen to be a regularized l^1 norm (see Figure 8.1),

$$\gamma(p) = \sum_{j=1}^3 \sqrt{p_j^2 + \varepsilon^2 |p|^2} \quad (9.22)$$

with $\varepsilon = 10^{-3}$. Thus the Frank diagram is a smoothed octahedron and the Wulff shape is a smoothed cube. The initial data were taken to depend on three random numbers $r_1, r_2, r_3 \in (0, 1)$,

$$\begin{aligned} u_0(x) = & 0.25 (\sin(2\pi r_1 x_1) + 0.25 \sin(3\pi r_2 x_2)) \times \\ & (0.1 \sin(2\pi r_3 x_1) + \sin(5\pi r_1 x_2)) \sin(2\pi r_2 x_1 x_2). \end{aligned} \quad (9.23)$$

We used Neumann boundary conditions and the right-hand side (for the curvature equation) $f = 1 - x_1^2 - x_2^2$. The level lines for some time-steps are shown in Figure 9.2. The Wulff shape (a smooth cube) appears in the solution as a consequence of the right-hand side f . For more computational results we refer to Deckelnick, Dziuk and Elliott (2003b).

9.4. Phase field model for surface diffusion

Just as the phase field model for mean curvature flow is gradient flow for the gradient energy functional and leads to a second order parabolic equation, a phase field model for surface diffusion may also be based on the same energy functional and a suitable approximation of the Laplace–Beltrami operator leading to a nonlinear degenerate fourth order parabolic equation. The appropriate setting is in the context of the Cahn–Hilliard equation for phase separation in binary alloys. The phase function φ may be viewed as the difference in mass fractions of the two species so that the values $\varphi = \pm 1$ are associated with the pure materials. Stable phases of the alloy are then associated with the minima of a double well bulk energy W , which in the regular solution form is

$$W(\varphi) = \frac{\theta}{2} [(1 + \varphi) \ln[1 + \varphi] + (1 - \varphi) \ln[1 - \varphi]] + \frac{1}{2}(1 - \varphi^2).$$

This homogeneous free energy function is non-convex with a double well, for $|\theta| < 1$, and $W'(\varphi)$ is said to be the homogeneous chemical potential.

The Cahn–Hilliard gradient energy functional is then

$$E(\varphi) = \int_{\Omega} \left[\frac{\epsilon}{2} |\nabla \varphi|^2 + \frac{1}{\epsilon} W(\varphi) \right]. \quad (9.24)$$

The functional derivative of this energy is used to define the chemical potential

$$w = -\epsilon \Delta \varphi + \frac{W'(\varphi)}{\epsilon}. \quad (9.25)$$

Mass conservation is

$$\partial_t \varphi + \nabla \cdot \mathcal{J} = 0, \quad (9.26)$$

where \mathcal{J} is the mass flux and typically for diffusion

$$\mathcal{J} = -\mathcal{M}(\varphi) \nabla w \quad (9.27)$$

with the degenerate mobility $\mathcal{M}(\varphi) = 1 - \varphi^2$. The upshot is a fourth order Cahn–Hilliard equation with degenerate mobility. Interface asymptotics (Cahn, Elliott and Novick-Cohen 1996) show that, as $\theta(\epsilon)$ and ϵ tend to zero, the zero level set of φ approximates a surface evolving by surface diffusion. Computational results in a setting which includes a forcing due to an electric field may be found in Barrett, Nürnberg and Styles (2004).

9.5. Willmore flow

Our starting point is the Willmore functional

$$E(X) = \frac{1}{2} \int_{\Gamma} H^2 dA, \quad \Gamma = X(M), \quad (9.28)$$

where M is an n -dimensional reference manifold and $X : M \rightarrow \mathbb{R}^{n+1}$ is a smooth immersion. Considering variations $X_\epsilon(p) = X(p) + \epsilon \phi(p)$, $p \in M$, where $\phi : M \rightarrow \mathbb{R}^{n+1}$ is smooth and vanishes near ∂M , one obtains the formula

$$\begin{aligned} \langle E'(X), \phi \rangle &= \frac{d}{d\epsilon} E(X_\epsilon)|_{\epsilon=0} \\ &= \int_{\Gamma} \Delta_{\Gamma} X \cdot (\Delta_{\Gamma} \phi + 2\nu \nabla_{\Gamma} \nu \cdot \nabla_{\Gamma} \phi) + \frac{1}{2} \int_{\Gamma} H^2 \nabla_{\Gamma} X \cdot \nabla_{\Gamma} \phi \\ &= \int_{\Gamma} \nabla_{\Gamma}(H\nu) \cdot \nabla_{\Gamma} \phi - 2 \int_{\Gamma} H \nabla_{\Gamma} \nu \cdot \nabla_{\Gamma} \phi + \frac{1}{2} \int_{\Gamma} H^2 \nabla_{\Gamma} X \cdot \nabla_{\Gamma} \phi, \end{aligned} \quad (9.29)$$

where we have used (2.10). Note that $\nabla_{\Gamma} X \cdot \nabla_{\Gamma} \phi = \sum_{j,k=1}^{n+1} D_j X_k D_j \phi_k$. Willmore flow then arises as the L^2 -gradient flow of the Willmore functional, that is,

$$\int_{\Gamma} X_t \cdot \phi dA = -\langle E'(X), \phi \rangle. \quad (9.30)$$

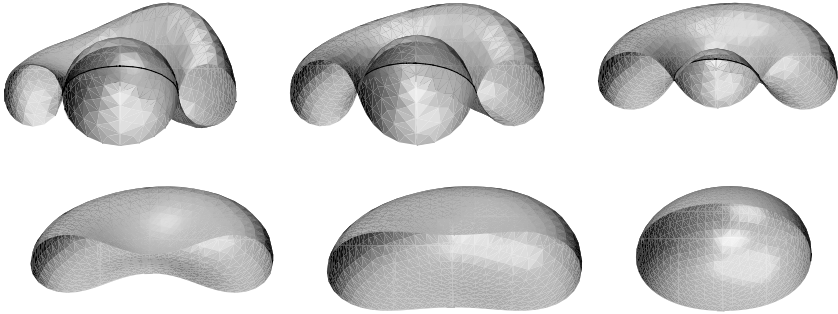


Figure 9.3. Surface relaxing under Willmore flow, cut open at $x_2 = 0$.

Using integration by parts one obtains the nonlinear evolution equation of fourth order, that is,

$$X_t = \Delta_\Gamma(H\nu) - 2\nabla_\Gamma \cdot (H\nabla_\Gamma\nu) + H\nabla_\Gamma H - \frac{1}{2}H^3\nu. \quad (9.31)$$

If we take the scalar product of the above expression with ν and observe that $\Delta_\Gamma\nu \cdot \nu = -|\nabla_\Gamma\nu|^2$, we obtain the evolution law

$$V = \Delta_\Gamma H + H|\nabla_\Gamma\nu|^2 - \frac{1}{2}H^3 \quad \text{on } \Gamma(t). \quad (9.32)$$

Note that from Section 2.3 we have

$$|\nabla_\Gamma\nu|^2 = \sum_{j,k=1}^{n+1} (\underline{D}_j\nu_k)^2 = \kappa_1^2 + \cdots + \kappa_n^2.$$

For two-dimensional surfaces Γ we then have

$$|\nabla_\Gamma\nu|^2 = \kappa_1^2 + \kappa_2^2 = (\kappa_1 + \kappa_2)^2 - 2\kappa_1\kappa_2 = H^2 - 2K$$

with Gauss curvature K . This leads to the evolution law

$$V = \Delta_\Gamma H + \frac{1}{2}H^3 - 2KH. \quad (9.33)$$

Compared with the surface diffusion problem (1.7) additional dimension-dependent nonlinearities appear. Up to now analytical results for the above evolution law have been primarily obtained for the case of closed surfaces. In Simonett (2001) it is shown that a unique local solution of (9.32) satisfying $\Gamma(0) = \Gamma_0$ exists provided that Γ_0 is a compact closed immersed and orientable $C^{2,\alpha}$ -surface in \mathbb{R}^3 . The solution exists globally in time if Γ_0 is sufficiently close to a sphere in $C^{2,\alpha}$. Using different methods, Kuwert and Schätzle (2004a) obtain global existence of solutions provided that $\int_{\Gamma_0} |A^\circ|^2$ is sufficiently small, where A° denotes the trace-free part of the second fundamental form. They were subsequently able to remove the smallness

assumption and to prove the existence of a global smooth solution provided that $E(X_0) \leq 16\pi$, where $\Gamma_0 = X_0(S^2)$ (see Kuwert and Schätzle (2004b) and note that our definition differs from theirs by a factor of 2). There is numerical evidence (Mayer and Simonett 2002) that the above condition is optimal in the sense that the flow develops a singularity if the initial surface has energy greater than 16π . A major problem in the numerical solution of this problem is the treatment of Gauss curvature, which is a nonlinear expression of the principal curvatures and – contrary to mean curvature – is not easily accessible to variational methods.

The elastic flow of curves

Let us start with the one-dimensional parametric problem. The Bernoulli model of an elastic rod (Truesdell 1983) described by a closed curve $X : S^1 \rightarrow \mathbb{R}^2$ uses the curvature integral (9.28) as elastic energy. Since this energy can be minimized by scaling, one usually adds length multiplied by a parameter $\lambda > 0$ resulting in the functional

$$E_\lambda(X) = \frac{1}{2} \int_{\Gamma} H^2 ds + \lambda \int_{\Gamma} 1 ds.$$

Let us introduce $Y = H\nu$, where H is just the usual curvature of a curve. We then obtain from (9.29) and the Frenet formula $\nabla_{\Gamma}\nu = H\tau \otimes \tau$ (with the unit tangent τ)

$$\begin{aligned} \langle E'_\lambda(X), \phi \rangle &= \int_{\Gamma} \nabla_{\Gamma} Y \cdot \nabla_{\Gamma} \phi ds - 2 \int_{\Gamma} H \nabla_{\Gamma} \nu \cdot \nabla_{\Gamma} \phi \\ &\quad + \frac{1}{2} \int_{\Gamma} H^2 \nabla_{\Gamma} X \cdot \nabla_{\Gamma} \phi + \lambda \int_{\Gamma} Y \cdot \phi \\ &= \int_{\Gamma} \nabla_{\Gamma} Y \cdot \nabla_{\Gamma} \phi - \frac{3}{2} \int_{\Gamma} H^2 \nabla_{\Gamma} X \cdot \nabla_{\Gamma} \phi + \lambda \int_{\Gamma} Y \cdot \phi. \end{aligned}$$

Thus one may expect the gradient flow for E_λ to be given by the equation

$$X_t = \Delta_{\Gamma} Y - \frac{3}{2} \nabla_{\Gamma} \cdot (H^2 \nabla_{\Gamma} X) - \lambda Y. \quad (9.34)$$

Long time existence for this problem has been proved by Polden (1996). Just as in Section 4.1 we think of X as a mapping from $\mathbb{R} \times [0, T]$ into \mathbb{R}^2 . We then have the following system to be satisfied by X and Y :

$$X_t - \frac{1}{|X_\theta|} \left(\frac{Y_\theta}{|X_\theta|} \right)_\theta + \frac{3}{2} \frac{1}{|X_\theta|} \left(|Y|^2 \frac{X_\theta}{|X_\theta|} \right)_\theta + \lambda Y = 0, \quad (9.35)$$

$$Y + \frac{1}{|X_\theta|} \left(\frac{X_\theta}{|X_\theta|} \right)_\theta = 0 \quad (9.36)$$

in $[0, 2\pi] \times (0, T)$. In addition, X has to satisfy the initial condition $X(\cdot, 0) = X_0$ in $I = [0, 2\pi]$ and the periodicity condition $X(\theta, t) = X(\theta + 2\pi, t)$ for

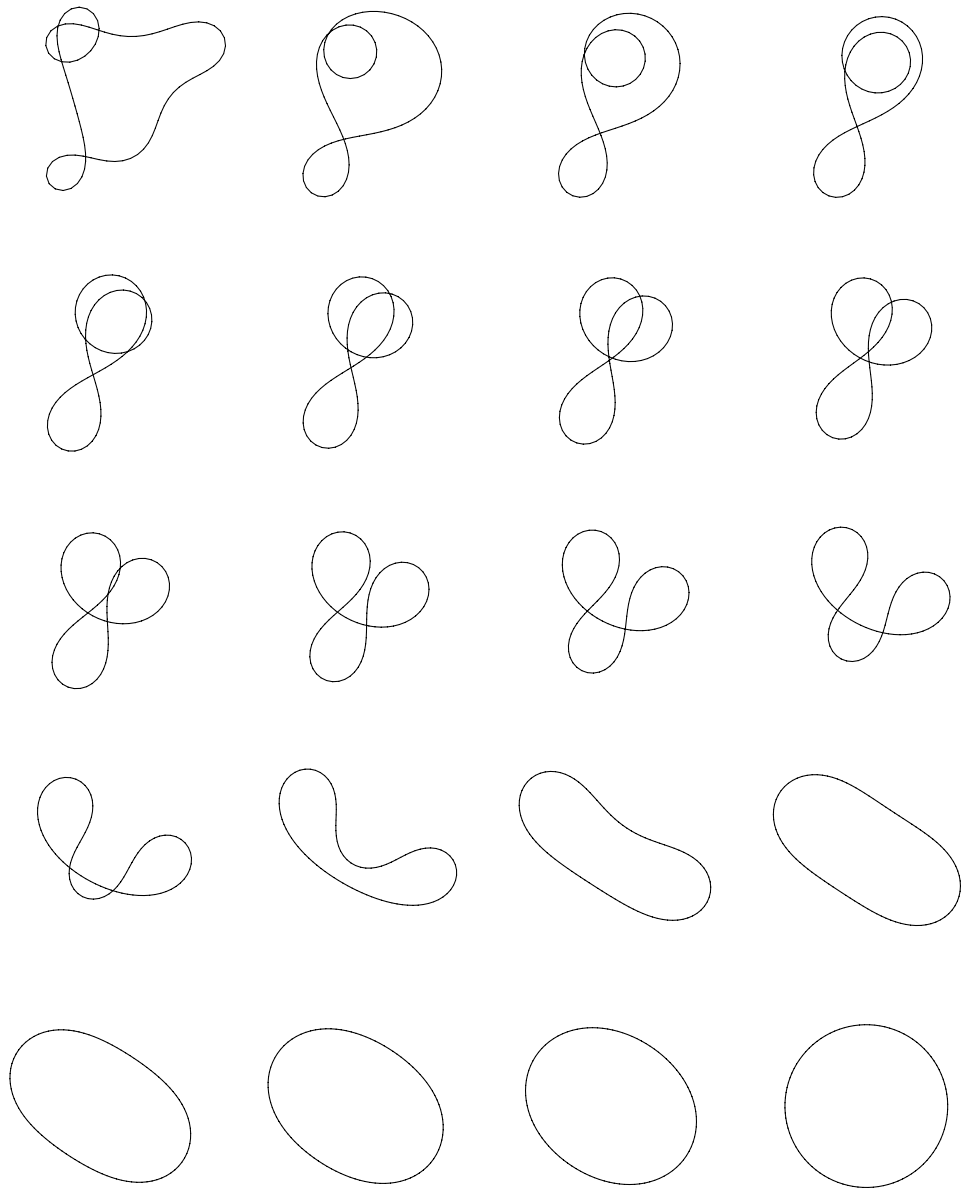


Figure 9.4. Time series of the two-dimensional length-preserving elastic flow (graphically scaled).

$0 \leq t < T$, $\theta \in \mathbb{R}$. As in the derivation of (4.6) we obtain a variational formulation of (9.35), (9.36),

$$\begin{aligned} \int_I X_t \cdot \varphi |X_\theta| + \int_I \frac{Y_\theta \cdot \varphi_\theta}{|X_\theta|} - \frac{3}{2} \int_I |Y|^2 \frac{X_\theta \cdot \varphi_\theta}{|X_\theta|} + \lambda \int_I Y \cdot \varphi |X_\theta| = 0, \\ \int_I Y \cdot \psi |X_\theta| - \int_I \frac{X_\theta \cdot \psi_\theta}{|X_\theta|} = 0 \end{aligned}$$

for all test functions $\varphi, \psi \in H_{\text{per}}^1([0, 2\pi]; \mathbb{R}^2)$. We use this weak form of our problem for a finite element discretization in space, which in one space dimension leads to a suitable difference scheme. The derivation of this scheme follows the derivation of (4.9), additionally using mass lumping in both equations. Let us denote by ϕ_1, \dots, ϕ_N the basis of the finite element space S_h introduced in Section 4.1. Then, expanding $X_h(\theta, t) = \sum_{j=1}^N X_j(t) \phi_j(\theta)$, $Y_h(\theta, t) = \sum_{j=1}^N Y_j(t) \phi_j(\theta)$ with vectors $X_j(t), Y_j(t) \in \mathbb{R}^2$, yields the following system of $2N$ ordinary differential equations:

$$\begin{aligned} \frac{1}{2}(q_j + q_{j+1})(\dot{X}_j + \lambda Y_j) + \frac{Y_j - Y_{j-1}}{q_j} - \frac{Y_{j+1} - Y_j}{q_{j+1}} \\ - p_j \frac{X_j - X_{j-1}}{q_j} + p_{j+1} \frac{X_{j+1} - X_j}{q_{j+1}} = 0 \end{aligned} \quad (9.37)$$

$$\frac{1}{2}(q_j + q_{j+1})Y_j - \frac{X_j - X_{j-1}}{q_j} + \frac{X_{j+1} - X_j}{q_{j+1}} = 0 \quad (9.38)$$

($j = 1, \dots, N$), where $X_0 = X_N, X_{N+1} = X_1, Y_0 = Y_N, Y_{N+1} = Y_1$, and the initial values are given by $X_j(0) = X_0(\theta_j)$ ($j = 1, \dots, N$). Furthermore,

$$q_j = |X_j - X_{j-1}|, \quad p_j = \frac{1}{2}(|Y_{j-1}|^2 + Y_{j-1} \cdot Y_j + |Y_j|^2). \quad (9.39)$$

A more detailed description can be found in Dziuk, Kuwert and Schätzle (2002). The paper actually treats curves in arbitrary codimension both showing long time existence of solutions as well as numerical examples. We include here a computation which shows the unravelling of a planar knotted curve under the length-preserving elastic flow in Figure 9.4.

Parametric Willmore flow of surfaces

The equation for Willmore flow of two-dimensional surfaces in \mathbb{R}^3 is much more difficult to treat. This is because Gauss curvature appears in the equation (9.33) for Willmore flow. Mean curvature H is given as a divergence expression (see (2.9)), so that in the discretization of parametric mean curvature flow, for example, we were able to formulate the mean curvature vector in a weak form, which then lead to a finite element scheme for parametric mean curvature flow. We were able to define the mean curvature vector of a polyhedron as a continuous and piecewise linear vector-valued

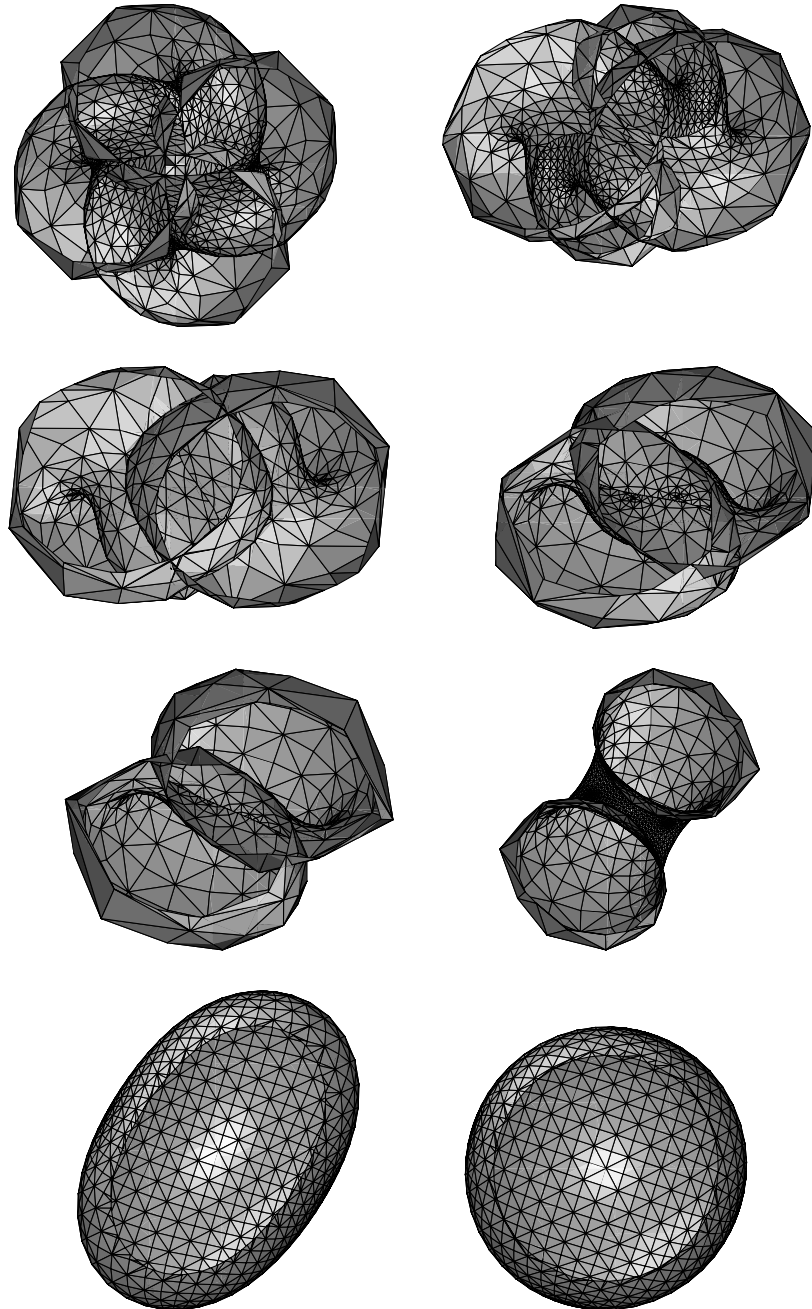


Figure 9.5. Half of a sphere eversion: the unravelling of a perturbed Willmore sphere under parametric Willmore flow (scaled graphically). Time-steps 0, 5600, 6000, 6400, 6800, 7000, 7200, 7400, 7600 and 8000.

function. Rusu (2001) employed a trick to remove Gauss curvature from the equations. Let us briefly describe the underlying idea, which we think is very important for applications of Willmore flow. For simplicity we look at closed surfaces. Going back to (9.29) and introducing the mean curvature vector $Y = H\nu$ as a new variable, we have

$$\langle E'(X), \phi \rangle = \int_{\Gamma} \nabla_{\Gamma} Y \cdot \nabla_{\Gamma} \phi - 2 \int_{\Gamma} Y \cdot \nu \nabla_{\Gamma} \nu \cdot \nabla_{\Gamma} \phi + \frac{1}{2} \int_{\Gamma} |Y|^2 \nabla_{\Gamma} X \cdot \nabla_{\Gamma} \phi.$$

Integration by parts gives

$$\int_{\Gamma} Y \cdot \nu \nabla_{\Gamma} \nu \cdot \nabla_{\Gamma} \phi = \int_{\Gamma} (\nabla_{\Gamma} Y \cdot \nabla_{\Gamma} \phi - (\nu \nabla_{\Gamma} Y) \cdot (\nu \nabla_{\Gamma} \phi)).$$

If we insert this identity into the above expression for $E'(X)$ we obtain

$$\langle E'(X), \phi \rangle = - \int_{\Gamma} R(\nu) \nabla_{\Gamma} Y \cdot \nabla_{\Gamma} \phi + \frac{1}{2} \int_{\Gamma} |Y|^2 \nabla_{\Gamma} X \cdot \nabla_{\Gamma} \phi$$

with the reflection matrix $R_{kl}(\nu) = \delta_{kl} - 2\nu_k \nu_l$. Starting from (9.30) we can now write down a variational formulation for parametric Willmore flow which uses position X and mean curvature vector Y as variables: find $X : M \times [0, T) \rightarrow \mathbb{R}^3$ such that

$$\begin{aligned} \int_{\Gamma} X_t \cdot \phi \, dA - \int_{\Gamma} R(\nu) \nabla_{\Gamma} Y \cdot \nabla_{\Gamma} \phi \, dA + \frac{1}{2} \int_{\Gamma} |Y|^2 \nabla_{\Gamma} X \cdot \nabla_{\Gamma} \phi \, dA &= 0, \\ \int_{\Gamma} Y \cdot \psi \, dA - \int_{\Gamma} \nabla_{\Gamma} X \cdot \nabla_{\Gamma} \psi \, dA &= 0 \end{aligned}$$

for all test functions $\phi, \psi \in H^1(\Gamma)^3$. Here, $\Gamma = \Gamma(t) = X(M, t)$. Furthermore we require the initial condition $X(\cdot, 0) = X_0$. We observe that all quantities are well defined for a polyhedral surface Γ so that it is possible to use this formulation in order to approximate solutions by linear finite elements (see Rusu (2001) for more details and Clarenz, Diewald, Dziuk, Rumpf and Rusu (2004) for applications to problems in image restoration).

9.6. Willmore flow of graphs

If the two-dimensional surface $\Gamma = \{(x, u(x, t)) \mid x \in \Omega\}$ is a graph above some domain $\Omega \subset \mathbb{R}^2$, then we can directly derive a fourth order parabolic partial differential equation for u . We write the equation (9.33) for a graph. In order to write down this equation we note that the quantities V, H, K and $\Delta_{\Gamma} H$ appearing in (9.33) are expressed in terms of u as in (5.1) and

$$K = \frac{\det D^2 u}{Q^4}, \quad (9.40)$$

$$\Delta_{\Gamma} H = \frac{1}{Q} \nabla \cdot \left(Q \left(I - \frac{\nabla u}{Q} \otimes \frac{\nabla u}{Q} \right) \nabla H \right). \quad (9.41)$$

We can rewrite the last equation as

$$\Delta_\Gamma H = \nabla \cdot \left(\frac{1}{Q} \left(I - \frac{\nabla u \otimes \nabla u}{Q^2} \right) \nabla (QH) \right) - H \nabla \cdot \left(\frac{1}{Q} \left(I - \frac{\nabla u \otimes \nabla u}{Q^2} \right) \nabla Q \right). \quad (9.42)$$

With the expression (5.1) for H we conclude

$$\frac{1}{Q} \left(I - \frac{\nabla u \otimes \nabla u}{Q^2} \right) \nabla Q = \frac{1}{Q} \left(\nabla Q - \frac{\Delta u}{Q} \nabla u \right) + H \frac{\nabla u}{Q}, \quad (9.43)$$

and a calculation shows that

$$\nabla \cdot \left(\frac{1}{Q} \left(\nabla Q - \frac{\Delta u}{Q} \nabla u \right) \right) = -2K. \quad (9.44)$$

Inserting (9.43) and (9.44) into (9.42), we obtain

$$\begin{aligned} \Delta_\Gamma H &= \nabla \cdot \left(\frac{1}{Q} \left(I - \frac{\nabla u \otimes \nabla u}{Q^2} \right) \nabla (QH) \right) + 2HK - H \nabla \cdot \left(H \frac{\nabla u}{Q} \right) \\ &= \nabla \cdot \left(\frac{1}{Q} \left(I - \frac{\nabla u \otimes \nabla u}{Q^2} \right) \nabla (QH) \right) + 2HK - \frac{1}{2} \nabla \cdot \left(\frac{H^2}{Q} \nabla u \right) - \frac{1}{2} H^3. \end{aligned}$$

Comparing this expression with (9.33), we obtain a fourth order parabolic partial differential equation for u ,

$$u_t + Q \nabla \cdot \left(\frac{1}{Q} \left(I - \frac{\nabla u \otimes \nabla u}{Q^2} \right) \nabla (QH) \right) - \frac{1}{2} Q \nabla \cdot \left(\frac{H^2}{Q} \nabla u \right) = 0 \quad \text{in } \Omega \times (0, T). \quad (9.45)$$

As before we can split the fourth order problem into two second order equations. The above equation suggests using the height u and

$$w = -QH$$

as variables which is different from the case of surface diffusion. Note that Gauss curvature no longer appears. The above ideas were introduced by Droske and Rumpf (2004) for a level set approach to Willmore flow.

The finite element approach is now based on dividing (9.45) by Q , multiplying by a test function $\varphi \in H_0^1(\Omega)$ and integrating by parts. This leads to

$$\int_{\Omega} \frac{u_t \varphi}{Q} + \int_{\Omega} \frac{1}{Q} \left(I - \frac{\nabla u \otimes \nabla u}{Q^2} \right) \nabla w \cdot \nabla \varphi + \frac{1}{2} \int_{\Omega} \frac{w^2}{Q^3} \nabla u \cdot \nabla \varphi = 0, \quad (9.46)$$

$$\int_{\Omega} \frac{w \zeta}{Q} - \int_{\Omega} \frac{\nabla u \cdot \nabla \zeta}{Q} = 0, \quad (9.47)$$

for all $\varphi, \zeta \in H_0^1(\Omega)$. As boundary conditions we choose

$$u = u_0 \quad \text{on } \partial\Omega \times [0, T] \cup \Omega \times \{0\}, \quad (9.48)$$

$$w = 0 \quad \text{on } \partial\Omega \times [0, T] \quad (9.49)$$

with a given function u_0 , which is independent of time. For the error estimates we need the following regularity of the continuous solution:

$$\frac{\partial^k u}{\partial t^k} \in L^\infty((0, T); H^{4-2k, \infty}(\Omega)) \cap L^2((0, T); H^{5-2k}(\Omega)), \quad k = 0, 1, 2. \quad (9.50)$$

Thus we need high compatibility of initial and boundary data. The spatially discrete problem now reads as follows. Find $(u_h(t), w_h(t))$, $0 \leq t \leq T$, such that $u_h(t) - I_h u_0 \in X_{h0}$, $w_h(t) \in X_{h0}$, $u_h(0) = u_{0h} \in X_{h0}$ and

$$\begin{aligned} \int_\Omega \frac{u_{ht}\varphi h}{Q_h} + \int_\Omega \frac{1}{Q_h} \left(I - \frac{\nabla u_h \otimes \nabla u_h}{Q_h^2} \right) \nabla w_h \cdot \nabla \varphi_h \\ + \frac{1}{2} \int_\Omega \frac{w_h^2}{Q_h^3} \nabla u_h \cdot \nabla \varphi_h = 0 \quad \text{for all } \varphi_h \in X_{h0}, \\ \int_\Omega \frac{w_h \zeta_h}{Q_h} - \int_\Omega \frac{\nabla u_h \cdot \nabla \zeta_h}{Q_h} = 0 \quad \text{for all } \zeta_h \in X_{h0}. \end{aligned}$$

The discrete initial value $u_h(\cdot, 0) = u_{0h} \in X_h$ is chosen as the ‘minimal surface projection’

$$\int_\Omega \frac{\nabla u_{0h} \cdot \nabla \zeta_h}{\sqrt{1 + |\nabla u_{0h}|^2}} = \int_\Omega \frac{\nabla u_0 \cdot \nabla \zeta_h}{\sqrt{1 + |\nabla u_0|^2}} \quad \text{for all } \zeta_h \in X_{h0}, \quad (9.51)$$

of the continuous initial value u_0 .

Theorem 9.3. Let us assume that (9.45), (9.48), (9.49) has a unique solution u on the interval $[0, T]$, which satisfies (9.50). Also suppose that u_{0h} is defined as the projection (9.51) of u_0 . Then

$$\sup_{0 \leq t \leq T} \|(u - u_h)(t)\| + \sup_{0 \leq t \leq T} \|(w - w_h)(t)\| \leq ch^2 |\log h|^2, \quad (9.52)$$

$$\sup_{0 \leq t \leq T} \|\nabla(u - u_h)(t)\| \leq ch, \quad (9.53)$$

$$\int_0^T \|u_t - u_{ht}\|^2 dt \leq ch^4 |\log h|^4, \quad (9.54)$$

$$\int_0^T \|\nabla(w - w_h)\|^2 dt \leq ch^2. \quad (9.55)$$

Appendix

Proof of Lemma 2.1. We prove (2.23), leaving (2.22) to the reader. Fix $t_0 \in (0, T)$. For $x \in \Gamma(t_0)$ let $U_x, \delta_x > 0$ and u be as in (2.19). By the implicit function theorem there exists an open set $\tilde{U}_x \subset U_x$, $0 < \tilde{\delta}_x \leq \delta_x$ such that $\tilde{U}_x \times (t_0 - \tilde{\delta}_x, t_0 + \tilde{\delta}_x) \subset Q$ and $\tilde{U}_x \cap \Gamma(t)$ can be written as a graph over some open set $\Omega_x \subset \mathbb{R}^n$ for $|t - t_0| < \tilde{\delta}_x$. Since $\Gamma(t_0) \subset \cup_{x \in \Gamma(t_0)} \tilde{U}_x$ and

$\Gamma(t_0)$ is compact, there exist a_1, \dots, a_N with $\Gamma(t_0) \subset \cup_{j=1}^N \tilde{U}_j$, $\tilde{U}_j = \tilde{U}_{a_j}$. Let $Q_j = \tilde{U}_j \times (t_0 - \tilde{\delta}_j, t_0 + \tilde{\delta}_j)$ and let $\eta_j \in C_0^\infty(Q_j)$, $1 \leq j \leq N$, be a partition of unity which satisfies $\sum_{j=1}^N \eta_j(x, t) = 1$ for (x, t) in a neighbourhood of $\Gamma(t_0) \times \{t_0\}$. For t close to t_0 we then have

$$\frac{d}{dt} \int_{\Gamma(t)} g(x, t) dA = \sum_{j=1}^N \frac{d}{dt} \int_{\tilde{U}_j \cap \Gamma(t)} \eta_j(x, t) g(x, t) dA. \quad (9.56)$$

Let us fix $j \in \{1, \dots, N\}$; by construction there exists $\Omega \subset \mathbb{R}^n$ and $v \in C^{2,1}(\Omega \times (t_0 - \tilde{\delta}_j, t_0 + \tilde{\delta}_j))$ such that w.l.o.g.

$$\tilde{U}_j \cap \Gamma(t) = \{(x', v(x', t)) \mid x' = (x_1, \dots, x_n) \in \Omega\}.$$

Abbreviating $h = \eta_j g$, we have

$$\int_{\tilde{U}_j \cap \Gamma(t)} h(x, t) dA = \int_{\Omega} h(x', v(x', t), t) \sqrt{1 + |\nabla_{x'} v|^2} dx'$$

so that we obtain, for t close to t_0 ,

$$\begin{aligned} \frac{d}{dt} \int_{\tilde{U}_j \cap \Gamma(t)} h dA &= \int_{\Omega} (h_{x_{n+1}} v_t + h_t) \sqrt{1 + |\nabla_{x'} v|^2} + \int_{\Omega} h \frac{\nabla_{x'} v \cdot \nabla_{x'} v_t}{\sqrt{1 + |\nabla_{x'} v|^2}} \\ &= \int_{\Omega} (h_{x_{n+1}} v_t + h_t) \sqrt{1 + |\nabla_{x'} v|^2} - \int_{\Omega} h \nabla_{x'} \cdot \left(\frac{\nabla_{x'} v}{\sqrt{1 + |\nabla_{x'} v|^2}} \right) v_t \\ &\quad - \int_{\Omega} (\nabla_{x'} h + h_{x_{n+1}} \nabla_{x'} v) \cdot \frac{\nabla_{x'} v}{\sqrt{1 + |\nabla_{x'} v|^2}} v_t \end{aligned}$$

where we have used integration by parts observing that $\text{supp } h(\cdot, t) \subset \Omega$. Recalling that $\nu = \frac{(\nabla_{x'} v, -1)}{\sqrt{1 + |\nabla_{x'} v|^2}}$ and $H = \nabla_{x'} \cdot \left(\frac{\nabla_{x'} v}{\sqrt{1 + |\nabla_{x'} v|^2}} \right)$ we finally get

$$\frac{d}{dt} \int_{\tilde{U}_j \cap \Gamma(t)} h dA = \int_{\tilde{U}_j \cap \Gamma(t)} \left(\frac{\partial h}{\partial \nu} V + h_t + h V H \right) dA.$$

Note that the above identity has been derived under the implicit assumption that $\nabla_{x'} v_t$ exists; the general case can be justified with the help of an approximating argument. If we return to (9.56) and recall that $\sum_{j=1}^N \eta_j \equiv 1$ in a neighbourhood of $\Gamma(t_0) \times \{t_0\}$, we obtain (2.23) at $t = t_0$. \square

Acknowledgements

We would like to thank Michael Fried and Alfred Schmidt for providing figures of calculations for the Stefan problem with undercooling and Vanessa Styles for providing figures of phase field calculations. The work was supported by the Deutsche Forschungsgemeinschaft via DFG-Forschergruppe ‘Non-linear partial differential equations: Theoretical and numerical analysis’ and

via DFG-Graduiertenkolleg: ‘Nichtlineare Differentialgleichungen: Modellierung, Theorie, Numerik, Visualisierung’. Partial support was provided by EPSRC/network research ‘Computation and numerical analysis for multi-scale and multiphysics modelling’. The graphical presentations were performed with the packages GRAPE and Xgraph.

REFERENCES

- S. Allen and J. Cahn (1979), ‘A microscopic theory for antiphase boundary motion and its application to antiphase domain coarsening’, *Acta Metall.* **27**, 1084–1095.
- R. Almgren (1993), ‘Variational algorithms and pattern formation in dendritic solidification’, *J. Comput. Phys.* **106**, 337–354.
- S. J. Altschuler and M. A. Grayson (1992), ‘Shortening space curves and flow through singularities’, *J. Differential Geom.* **35**, 283–298.
- S. Angenent (1991), ‘Parabolic equations for curves on surfaces, Part II: Intersections, blow-up and generalized solutions’, *Ann. of Math.* **133**, 171–215.
- S. Angenent and M. Gurtin (1989), ‘Multiphase thermomechanics with interfacial structure, 2: Evolution of an isothermal interface’, *Arch. Rat. Mech. Anal.* **108**, 323–391.
- G. Aubert and P. Kornprobst (2002), *Mathematical Problems in Image Processing*, Vol. 147 of *Applied Mathematical Sciences*, Springer.
- E. Bänsch and A. Schmidt (2000), ‘Simulation of dendritic crystal growth with thermal convection’, *Interfaces Free Bound.* **2**, 95–115.
- E. Bänsch, P. Morin and R. H. Nochetto (2004), ‘Surface diffusion of graphs: Variational formulation, error analysis and simulation’, *SIAM J. Numer. Anal.* **42**, 773–799.
- J. W. Barrett, R. Nürnberg and V. Styles (2004), ‘Finite element approximation of a phase field model for void electromigration’, *SIAM J. Numer. Anal.* **42**, 738–772.
- G. Bellettini and M. Paolini (1995), ‘Quasi-optimal error estimates for the mean curvature flow with a forcing term’, *Differential Integral Equations* **8**, 735–752.
- G. Bellettini and M. Paolini (1996), ‘Anisotropic motion by mean curvature in the context of Finsler geometry’, *Hokkaido Math. J.* **25**, 537–566.
- G. Bellettini, M. Novaga and M. Paolini (1999), ‘Facet-breaking for three dimensional crystals evolving by mean curvature’, *Interfaces Free Bound.* **1**, 39–55.
- G. Bellettini, M. Novaga and M. Paolini (2001), ‘Characterization of facet-breaking for non-smooth mean curvature flow in the convex case’, *Interfaces Free Bound.* **3**, 415–446.
- G. Bellettini, M. Paolini and C. Verdi (1990), ‘ Γ -convergence of discrete approximations to interfaces with prescribed mean curvature’, *Rendiconti Mat. Acc. Lincei* **9**, 317–328.
- J. F. Blowey and C. M. Elliott (1991), ‘The Cahn–Hilliard gradient theory for phase separation with non-smooth free energy, Part I: Mathematical Analysis’, *European J. Appl. Math.* **2**, 233–280.

- J. F. Blowey and C. M. Elliott (1993a), ‘The Cahn–Hilliard gradient theory for phase separation with non-smooth free energy, Part II: Numerical Analysis’, *European J. Appl. Math.* **3**, 147–179.
- J. F. Blowey and C. M. Elliott (1993b), Curvature dependent phase boundary motion and parabolic obstacle problems, in *Proc. IMA Workshop on Degenerate Diffusion, 1991* (W. Ni, L. Peletier and J. L. Vasquez, eds) Springer, IMA **47**, pp. 19–60.
- J. F. Blowey and C. M. Elliott (1994), A phase field model with a double obstacle potential, in *Motion by Mean Curvature and Related Topics* (G. Buttazzo and A. Visintin, ed.), de Gruyter, New York, pp. 1–22.
- K. A. Brakke (1978), *The Motion of a Surface by its Mean Curvature*, Princeton University Press, NJ.
- K. A. Brakke (1992), ‘The surface evolver’, *Exp. Math.* **1**, 141–165.
- R. J. Braun, S. R. Coriell, G. B. McFadden and A. A. Wheeler (1993), ‘Phase field models for anisotropic interfaces’, *Phys. Rev. E* **48**, 2016–2024.
- E. Burman and M. Picasso (2003), ‘Anisotropic, adaptive finite elements for the computation of a solutal dendrite’, *Interfaces Free Bound.* **5**, 103–127.
- G. Caginalp (1986), ‘An analysis of a phase field model of a free boundary’, *Arch. Rat. Mech. Anal.* **92**, 206–245.
- J. W. Cahn and J. E. Hilliard (1958), ‘Free energy of a nonuniform system I: Interfacial free energy’, *J. Chem. Phys.* **28**, 258–267.
- J. W. Cahn and J. E. Taylor (1994), ‘Surface motion by surface diffusion’, *Acta Metall. Mater.* **42**, 1045–1063.
- J. W. Cahn, C. M. Elliott and A. Novick-Cohen (1996), ‘The Cahn–Hilliard equation with a concentration dependent mobility: motion by minus the Laplacian of the mean curvature’, *European J. Appl. Math.* **7**, 287–301.
- V. Caselles, R. Kimmel, G. Sapiro and C. Sbert (1997), ‘Minimal surfaces: a geometric three dimensional segmentation approach’, *Numer. Math.* **77**, 423–451.
- A. Chambolle (2004), ‘An algorithm for mean curvature motion’, *Interfaces Free Bound.* **6**, 195–218.
- X. Chen (1992), ‘Generation and propagation of interface in reaction diffusion equations’, *J. Differential Equations* **96**, 116–141.
- X. Chen (1994), ‘Spectrum for the Allen–Cahn, Cahn–Hilliard and phase field equations for generic interfaces’, *Comm. Partial Differential Equations* **19**, 1371–1395.
- X. Chen and C. M. Elliott (1994), ‘Asymptotics for a parabolic double obstacle problem’, *Proc. R. Soc. London A* **444**, 429–445.
- X. Chen, C. M. Elliott, A. R. Gardiner and J. J. Zhao (1998), ‘Convergence of numerical solutions to the Allen–Cahn equation’, *Appl. Anal.* **69**, 47–56.
- Y.-G. Chen, Y. Giga and S. Goto (1991), ‘Uniqueness and existence of viscosity solutions of generalized mean curvature flow equations’, *J. Differential Geom.* **33**, 749–786.
- Y.-G. Chen, Y. Giga, Y. T. Hitaka and M. Honma (1994), A stable difference scheme for computing motion of level surfaces by the mean curvature, in *Proceedings of the Global Analysis Research Center Symposium, Seoul, Korea* (D. Kim *et al.*, eds), pp. 1–19.

- D. L. Chopp (1993), ‘Computing minimal surfaces via level set curvature flow’, *J. Comput. Phys.* **106**, 77–91.
- D. L. Chopp and J. A. Sethian (1999), ‘Motion by intrinsic Laplacian of curvature’, *Interfaces Free Bound.* **1**, 107–123.
- U. Clarenz, U. Diewald, G. Dziuk, M. Rumpf and R. Rusu (2004), ‘A finite element method for surface restoration with smooth boundary conditions’, *Computer Aided Geometric Design* **21** (5), 427–445.
- B. D. Coleman, R. S. Falk and M. Moakher (1995), ‘Stability of cylindrical bodies in the theory of surface diffusion’, *Phys. D* **89**, 123–135.
- M. G. Crandall and P.-L. Lions (1996), ‘Convergent difference schemes for nonlinear parabolic equations and mean curvature motion’, *Numer. Math.* **75**, 17–41.
- M. G. Crandall, H. Ishii and P.-L. Lions (1992), ‘User’s guide to viscosity solutions of second order partial differential equations’, *Bull. Amer. Math. Soc.* **27**, 1–67.
- K. Deckelnick (1997), ‘Weak solutions of the curve shortening flow’, *Calc. Var.* **5**, 489–510.
- K. Deckelnick (2000), ‘Error analysis for a difference scheme approximating mean curvature flow’, *Interfaces Free Bound.* **2**, 117–142.
- K. Deckelnick and G. Dziuk (1994), On the approximation of the curve shortening flow, in *Calculus of Variations, Applications and Computations: Pont-à-Mousson, 1994* (C. Bandle, J. Bemelmans, M. Chipot, J. Saint Jean Paulin and I. Shafrir, eds), Pitman Research Notes in Mathematics Series, pp. 100–108.
- K. Deckelnick and G. Dziuk (1995), ‘Convergence of a finite element method for non-parametric mean curvature flow’, *Numer. Math.* **72**, 197–222.
- K. Deckelnick and G. Dziuk (1999), ‘Discrete anisotropic curvature flow of graphs’, *Math. Model. Numer. Anal.* **33**, 1203–1222.
- K. Deckelnick and G. Dziuk (2000), ‘Error estimates for a semi implicit fully discrete finite element scheme for the mean curvature flow of graphs’, *Interfaces Free Bound.* **2**, 341–359.
- K. Deckelnick and G. Dziuk (2001), Convergence of numerical schemes for the approximation of level set solutions to mean curvature flow, in *Numerical Methods for Viscosity Solutions and Applications* (M. Falcone and C. Makridakis, eds), Vol. 59 of *Series Adv. Math. Appl. Sciences*, pp. 77–94.
- K. Deckelnick and G. Dziuk (2002a), ‘A fully discrete numerical scheme for weighted mean curvature flow’, *Numer. Math.* **91**, 423–452.
- K. Deckelnick and G. Dziuk (2002b), A finite element level set method for anisotropic mean curvature flow with space dependent weight, Abschlußband SFB 256, Bonn.
- K. Deckelnick and C. M. Elliott (1998), ‘Finite element error bounds for curve shrinking with prescribed normal contact to a fixed boundary’, *IMA J. Numer. Anal.* **18**, 635–654.
- K. Deckelnick and C. M. Elliott (2004), ‘Uniqueness and error analysis for Hamilton–Jacobi equations with discontinuities’, *Interfaces Free Bound.* **6**, 329–349.

- K. Deckelnick, G. Dziuk and C. M. Elliott (2003a), ‘Error analysis of a semidiscrete numerical scheme for diffusion in axially symmetric surfaces’, *SIAM J. Numer. Anal.* **41**, 2161–2179.
- K. Deckelnick, G. Dziuk and C. M. Elliott (2003b), Fully discrete semi-implicit second order splitting for anisotropic surface diffusion of graphs, Preprint No. 33/2003, Universität Magdeburg, *SIAM J. Numer. Anal.*, to appear.
- K. Deckelnick, C. M. Elliott and V. M. Styles (2001), ‘Numerical diffusion-induced grain boundary motion’, *Interfaces Free Bound.* **3**, 393–414.
- P. de Mottoni and M. Schatzman (1995), ‘Geometric evolution of developed interfaces’, *Trans. Amer. Math. Soc.* **347**, 1533–1589.
- M. Droske and M. Rumpf (2004), ‘A level set formulation for Willmore flow’, *Interfaces Free Bound.* **6**, 361–378.
- G. Dziuk (1988), Finite elements for the Beltrami operator on arbitrary surfaces, in *Partial Differential Equations and Calculus of Variations* (S. Hildebrandt and R. Leis, eds), Vol. 1357 of *Lecture Notes in Mathematics*, Springer, pp. 142–155.
- G. Dziuk (1991), ‘An algorithm for evolutionary surfaces’, *Numer. Math.* **58**, 603–611.
- G. Dziuk (1994), ‘Convergence of a semi-discrete scheme for the curve shortening flow’, *Math. Models Methods Appl. Sci.* **4**, 589–606.
- G. Dziuk (1999a), Numerical schemes for the mean curvature flow of graphs, in *IUTAM Symposium on Variations of Domains and Free-Boundary Problems in Solid Mechanics* (P. Argoul, M. Frémond and Q. S. Nguyen, eds), Kluwer, Dordrecht/Boston/London, pp. 63–70.
- G. Dziuk (1999b), ‘Discrete anisotropic curve shortening flow’, *SIAM J. Numer. Anal.* **36**, 1808–1830.
- G. Dziuk, E. Kuwert and R. Schätzle (2002), ‘Evolution of elastic curves in \mathbb{R}^n : existence and computation’, *SIAM J. Math. Anal.* **33**, 1228–1245.
- K. Ecker (2002) Lectures on regularity for mean curvature flow, Preprint No. 23/2002, Universität Freiburg.
- K. Ecker and G. Huisken (1989), ‘Mean curvature evolution of entire graphs’, *Ann. of Math.* **130**, 453–471.
- C. M. Elliott (1997), Approximation of curvature dependent interface motion, in *The State of the Art in Numerical Analysis* (I. S. Duff et al., ed.), Vol. 63 of *Inst. Math. Appl. Conf. Ser., New Ser.*, Clarendon Press, Oxford, pp. 407–440.
- C. M. Elliott and H. Garcke (1997), ‘Existence results for diffusive surface motion laws’, *Adv. Math. Sci. Appl.* **7**, 467–490.
- C. M. Elliott and A. R. Gardiner (1996), Double obstacle phase field computations of dendritic growth, University of Sussex, CMAIA Research Report 96-15.
- C. M. Elliott and J. R. Ockendon (1982), *Weak and Variational Methods for Moving Boundary Problems*, Pitman, London.
- C. M. Elliott and R. Schätzle (1996), ‘The limit of the anisotropic double-obstacle Allen–Cahn equation’, *Proc. Roy. Soc. Edinburgh* **126**, 1217–1234.
- C. M. Elliott and R. Schätzle (1997), The limit of the fully anisotropic double-obstacle Allen–Cahn equation in the non-smooth case, *SIAM J. Math. Anal.* **28**, 274–303.

- C. M. Elliott and A. M. Stuart (1993), ‘The global dynamics of discrete semilinear parabolic equations’, *SIAM J. Numer. Anal.* **30**, 1622–1663.
- C. M. Elliott and V. M. Styles (2003), ‘Computations of bidirectional grain boundary dynamics in thin metallic films’, *J. Comput. Phys.* **187**, 524–543.
- C. M. Elliott, A. R. Gardiner and T. Kuhn (1996), Generalizes double obstacle phase field approximation of the anisotropic mean curvature flow, University of Sussex, CMAIA Research Report 96-17.
- C. M. Elliott, A. R. Gardiner and R. Schätzle (1998), ‘Crystalline curvature flow of a graph in a variational setting’, *Adv. Math. Sci. Appl.* **8**, 425–460.
- C. M. Elliott, M. Paolini and R. Schätzle (1996), ‘Interface estimates for the fully anisotropic Allen–Cahn equation and anisotropic mean curvature flow’, *Math. Models Methods Appl. Sci.* **6**, 1103–1118.
- J. Escher, U. F. Mayer and G. Simonett (1998), ‘The surface diffusion flow for immersed hypersurfaces’, *SIAM J. Math. Anal.* **29**, 1419–1433.
- L. C. Evans (1993), ‘Convergence of an algorithm for mean curvature motion’, *Indiana Univ. Math. J.* **42**, 533–557.
- L. C. Evans and J. Spruck (1991), ‘Motion of level sets by mean curvature I’, *J. Differential Geom.* **33**, 636–681.
- L. C. Evans and J. Spruck (1992a), ‘Motion of level sets by mean curvature II’, *Trans. Amer. Math. Soc.* **330**, 321–332.
- L. C. Evans and J. Spruck (1992b), ‘Motion of level sets by mean curvature III’, *J. Geom. Anal.* **2**, 121–150.
- L. C. Evans and J. Spruck (1995), ‘Motion of level sets by mean curvature IV’, *J. Geom. Anal.* **5**, 77–114.
- L. C. Evans, H. M. Soner and P. E. Souganidis (1992), ‘Phase transition and generalised motion by mean curvature’, *Comm. Pure Appl. Math.* **45**, 1097–1123.
- X. Feng and A. Prohl (2003), ‘Numerical analysis of the Allen–Cahn equation and approximation for mean curvature flows’, *Numer. Math.* **94**, 33–65.
- F. Fierro, R. Goglione and M. Paolini (1994), ‘Finite element minimization of curvature functionals with anisotropy’, *Calcolo* **3–4**, 191–210.
- M. Fried (1999), Niveauflächen zur Berechnung zweidimensionaler Dendrite, Dissertation Freiburg.
- M. Fried (2004), ‘A level set based finite element algorithm for the simulation of dendritic growth’, *Comput. Vis. Sci.* **7** 97–110.
- M. Gage (1993), ‘Evolving plane curves by curvature in relative geometries’, *Duke Math. J.* **72**, 441–466.
- M. Gage and R. S. Hamilton (1996), ‘The heat equation shrinking convex plane curves’, *J. Differential Geom.* **23** 69–96.
- H. Garcke and V. M. Styles (2004), ‘Bi-directional diffusion induced grain boundary motion with triple junctions’, *Interfaces Free Bound.* **6**, 271–294.
- Y. Giga (2002), Surface evolution equations: a level set method, Hokkaido University Technical Report Series in Mathematics No. 71.
- Y. Giga and K. Ito (1998), ‘On pinching of curves moved by surface diffusion’, *Commun. Appl. Anal.* **2**(3), 393–405.
- D. Gilbarg and N. S. Trudinger (1998), *Elliptic Partial Differential Equations of Second Order*, Grundlehren der mathematischen Wissenschaften, Springer.

- P. M. Girao (1995), ‘Convergence of a crystalline algorithm for the motion of a simple closed convex curve by weighted curvature’, *SIAM J. Numer. Anal.* **32**, 886–899.
- M. A. Grayson (1987), ‘The heat equation shrinks embedded plane curves to round points’, *J. Differential Geom.* **26**, 285–314.
- M. A. Grayson (1989) ‘A short note on the evolution of a surface by its mean curvature’, *Duke Math. J.* **58** (3), 555–558.
- M. E. Gurtin (1993), *Thermomechanics of Evolving Phase Boundaries in the Plane*, Oxford Mathematical Monographs, Oxford University Press.
- C. Herring (1951), Surface diffusion as a motivation for sintering, in *The Physics of Powder Metallurgy* (W. E. Kingston, ed.), McGraw-Hill, New York, pp. 143–179.
- G. Huisken (1984), ‘Flow by mean curvature of convex surfaces into spheres’, *J. Differential Geom.* **20**, 237–266.
- G. Huisken (1989), ‘Non-parametric mean curvature evolution with boundary conditions’, *J. Differential Equations* **77**, 369–378.
- T. Ilmanen (1993), ‘Convergence of the Allen–Cahn equation to Brakke’s motion by mean curvature’, *J. Differential Geom.* **38**, 417–461.
- C. Johnson and V. Thom’ee (1975), ‘Error estimates for a finite element approximation of a minimal surface’, *Math. Comp.* **29**, 343–349.
- M. A. Katsoulakis and A. T. Kho (2001), ‘Stochastic curvature flows: asymptotic derivation, level set formulation and numerical experiments’, *Interfaces Free Bound.* **3**, 265–290.
- M. Kimura (1997), ‘Numerical analysis of moving boundary problems using the boundary tracking method’, *Japan J. Indust. Appl. Math.* **14**, 373–398.
- R. Kornhuber and R. Krause (2003), On multi-grid methods for vector Allen–Cahn equations, in *Domain Decomposition Methods in Science and Engineering* (I. Herrera *et al.*, eds), UNAM, Mexico City, Mexico, pp. 307–314.
- T. Kuhn (1996), Approximation of anisotropic and advected mean curvature flows by phase field models, DPhil thesis, University of Sussex.
- T. Kuhn (1998), ‘Convergence of a fully discrete approximation for advected mean curvature flows’, *IMA J. Numer. Anal.* **18**, 595–634.
- E. Kuwert and R. Schätzle (2004a), ‘The Willmore flow with small initial energy’, *J. Differential Geom.* **57**, 409–441.
- E. Kuwert and R. Schätzle (2004b), ‘Removability of point singularities of Willmore surfaces’, *Ann. of Math.* **159**, 1–43.
- O. A. Ladyzhenskaya, V. A. Solonnikov and N. N. Ural’tseva (1968), *Linear and Quasilinear Equations of Parabolic Type*, AMS, Providence, RI.
- G. Lieberman (1986), ‘The first initial-boundary value problem for quasilinear second order parabolic equations’, *Ann. Scuola Norm. Sup. Pisa* **13**, 347–387.
- G. B. McFadden, A. A. Wheeler, R. J. Braun, S. R. Coriell and R. F. Sekerka (1993), ‘Phase-field models for anisotropic interfaces’, *Phys. Rev. E* **48** (3), 2016–2024.
- U. F. Mayer and G. Simonett (2000), ‘Self-intersections for the surface diffusion and the volume-preserving mean curvature flow’, *Differential Integral Equations* **13**, 1189–1199.

- U. F. Mayer and G. Simonett (2002), ‘A numerical scheme for axi-symmetric solutions of curvature driven free boundary problems, with applications to the Willmore flow’, *Interfaces Free Bound.* **4**, 89–109.
- B. Merriman, J. K. Bence and S. Osher (1994), ‘Motion of multiple junctions: A level set approach’, *J. Comput. Phys.* **112**, 343–363.
- K. Mikula and J. Kacur (1996), ‘Evolution of convex plane curves describing anisotropic motions of phase interfaces’, *SIAM J. Sci. Comput.* **17** (6), 1302–1327.
- K. Mikula and D. Sevcovic (2001), ‘Evolution of plane curves driven by a nonlinear function of curvature and anisotropy’, *SIAM J. Appl. Math.* **61** (5), 1473–1501.
- W. W. Mullins (1957), ‘Theory of thermal grooving’, *J. Appl. Phys.* **28**, 333–339.
- F. A. Nichols and W. W. Mullins (1965), ‘Surface-(interface-) and volume-diffusion contributions to morphological changes driven by capillarity’, *Trans. Metall. Soc., AIME* **233**, 1840–1847.
- R. H. Nochetto and C. Verdi (1996a), ‘Convergence of double obstacle problems to the geometric motions of fronts’, *SIAM J. Math. Anal.* **26**, 1514–1526.
- R. H. Nochetto and C. Verdi (1996b), ‘Combined effect of explicit time-stepping and quadrature for curvature driven flows’, *Numer. Math.* **74**, 105–136.
- R. H. Nochetto and C. Verdi (1997), ‘Convergence past singularities for a fully discrete approximation of curvature driven interfaces’, *SIAM J. Numer. Anal.* **34**, 490–512.
- R. H. Nochetto, M. Paolini and C. Verdi (1993), ‘Sharp error analysis for curvature dependent evolving fronts’, *Math. Models Methods Appl. Sci.* **3**, 771–723.
- R. H. Nochetto, M. Paolini and C. Verdi (1994), ‘Optimal interface error estimates for the mean curvature flow’, *Ann. Scuola Norm. Sup. Pisa Cl. Sci.* **21**, 193–212.
- R. H. Nochetto, M. Paolini and C. Verdi (1996), ‘A dynamic mesh algorithm for curvature dependent evolving interfaces’, *J. Comput. Phys.* **123**, 296–310.
- V. I. Oliker and N. N. Uraltseva (1993), ‘Evolution of nonparametric surfaces with speed depending on curvature II: The mean curvature case’, *Comm. Pure Appl. Math.* **46**, No 1, 97–135.
- S. Osher and R. Fedkiw (2003), *Level Set Methods and Dynamic Implicit Surfaces*, Vol. 153 of *Applied Mathematical Sciences*, Springer.
- S. Osher and J. A. Sethian (1988), ‘Fronts propagating with curvature dependent speed: Algorithms based on Hamilton–Jacobi formulations’, *J. Comput. Phys.* **79**, 12–49.
- M. Paolini (1995), An efficient algorithm for computing anisotropic evolution by mean curvature, in *Proceedings of the International Conference on Curvature Flows and Related Topics held in Levico, Italy, June 27–July 2nd, 1994* (A. Damlamian *et al.*, eds), Vol. 5 of *GAKUTO Int. Ser., Math. Sci. Appl.*, Gakkotosho, Tokyo, pp. 199–213.
- M. Paolini (1997), ‘A quasi-optimal error estimate for a discrete singularly perturbed approximation to the prescribed curvature problem’, *Math. Comp.* **66**, 45–67.
- M. Paolini and C. Verdi (1992), ‘Asymptotic and numerical analysis of the mean curvature flow with a space dependent relaxation parameter’, *Asymptot. Anal.* **5**, 553–574.

- A. Polden (1996), Curves and surfaces of least total curvature and fourth-order flows, PhD dissertation, Universität Tübingen, Germany.
- T. Preußer and M. Rumpf (2000), A level set method for anisotropic geometric diffusion in 3D image processing, Report SFB 256 Bonn, **37**.
- J. Rubinstein, P. Sternberg and J. B. Keller (1989), ‘Fast reaction, slow diffusion and curve shortening’, *SIAM J. Appl. Math.* **49**, 116–133.
- R. Rusu (2001), An algorithm for the elastic flow of surfaces, Preprint Math. Fak. Univ. Freiburg 01-35.
- A. Schmidt (1996), ‘Computation of three dimensional dendrites with finite elements’, *J. Comput. Phys.* **125**, 293–312.
- J. A. Sethian (1990), ‘Numerical algorithms for propagating interfaces: Hamilton–Jacobi equations and conservation laws’, *J. Differential Geom.* **31** (1), 131–161.
- J. A. Sethian (1999), *Level Set Methods and Fast Marching Methods*, Vol. 3 of *Cambridge Monographs on Applied and Computational Mathematics*, Cambridge University Press.
- G. Simonett (2001), ‘The Willmore flow near spheres’, *Differential Integral Equations* **14**, 1005–1014.
- H. M. Soner (1993), ‘Motion of a set by the curvature of its boundary’, *J. Differential Equations* **101**, 313–372.
- J. E. Taylor (1992), ‘Mean curvature and weighted mean curvature’, *Acta Metall. Mater.* **40**, 1475–1485.
- J. E. Taylor, J. W Cahn and C. A. Handwerker (1992), ‘Geometric models of crystal growth’, *Acta Metall. Mater.* **40**, 1443–1474.
- C. Truesdell (1983), ‘The influence of elasticity on analysis: The classical heritage’, *Bull. Amer. Math. Soc. (N.S.)* **9**, 293–310.
- A. Veeser (1999), ‘Error estimates for semi-discrete dendritic growth’, *Interfaces Free Bound.* **1**, 227–254.
- A. Visintin (1996), *Models of Phase Transitions*, Vol. 28 of *Progress in Nonlinear Differential Equations*, Birkhäuser, Boston.
- N. J. Walkington (1996), ‘Algorithms for computing motion by mean curvature’, *SIAM J. Numer. Anal.* **33**, 2215–2238.
- A. A. Wheeler and G. B. McFadden (1996), ‘A ξ -vector formulation of anisotropic phase-field models: 3-D Asymptotics’, *European J. Appl. Math.* **7**, 367–381.
- T. J. Willmore (1993), *Riemannian Geometry*, Clarendon, Oxford.
- E. Yokoyama and R. F. Sekerka (1992), ‘A numerical study of the combined effect of anisotropic surface tension and interface kinetics on pattern formation during the growth of two-dimensional crystals’, *J. Crystal Growth* **125**, 389–403.